TMX 52355

THE STATISTICAL DESCRIPTION OF A SPRAY IN TERMS OF DROP VELOCITY, SIZE AND POSITION

BY

JOBN FREDERICK GROENEWEG

A thesis submitted in partial fullfillment of the requirements for the degree of

DOCTOR OF PHILOSOPHY
(Mechanical Engineering)

at the

UNIVERSITY OF WISCONSIN

1967

ACKNOWLEDGEMENTS

The author wishes to thank the many persons whose efforts have contributed to this investigation. Special mention is due: Professors M. M. El-Wakil, P. S. Myers, and O. A. Uyehara for their guidance and advise; Dr. E. J. Rice for his continued interest and helpful suggestions; and Richard E. Sowls and Dr. Hiroyuki Hiroyasu for their invaluable experimental assistance. The staff of the NASA, Lewis Research Center was particularly helpful with the data reduction and the preparation of the manuscript.

Completion of this work was made possible by generous financial support from the Wisconsin Alumni Research Foundation, the Cummins Engine Foundation, the National Science Foundation, and the National Aeronautics and Space Administration.

ABSTRACT

The problem of statistically describing a spray immediately after formation and during subsequent propagation is investigated both theoretically and experimentally. Particular emphasis is placed on the roles of drop velocity and position in the spray in addition to the usual considerations of drop size.

In order to provide a physical context for the theoretical presentation, observed spray characteristics and single drop behavior are reviewed. The facts that (a) spray formation is a random process which is distributed in space, and (b) each individual drop history is a unique function of its initial conditions and later environment; lead to the hypothesis that immediately after spray formation the droplet variables of velocity, position, and temperature should be considered as statistically distributed along with drop size.

An available adaptation of molecular statistical mechanics to the spray problem is presented and extended to include droplet temperature in addition to size, position, and velocity. Equations of change, developed from the spray transport equation, define mean spray variables. The relationship of the general density function to available spatial and flux size distributions is given, and an assessment of required experimental information is made.

The development of double-exposure, fluorescent photography for the purpose of measuring velocities and sizes of individual drops at selective locations in a spray is described. Data taken on an unconfined spray formed by a swirl atomizer form the basis for construction of bivariate, size-velocity density functions at various radial and axial positions. From the measurement of the sizes and velocities of more than 32,000 drops, both formation and propagation characteristics are given for the ethyl alcohol spray at an injection pressure of 25 psig. Formation behavior at two other pressures, 40 and 55 psig, is included. Bivariate, size-velocity mass densities, their associated single variable distributions, and mean quantities are calculated. Both local variations and one-dimensional forms obtained by integration over a cross section are shown.

Conclusions from the experiments are: (a) drop velocity in a spray is a statistically distributed variable the knowledge of which is equally important to drop size; (b) the form of the bivariate, size-velocity density functions is strongly dependent on position with the key feature determining the variations being the amount of droplet-gas interaction that has occurred; (c) bimodal

density functions are formed during propagation by selective deceleration of drops according to size; and (d) in many cases the differences in the shape and modal characteristics of spatial and flux drop size distributions are large. The implications of these conclusions for the interpretation of spray data, analytical description of spray situations, and design of future experiments are discussed.

TABLE OF CONTENTS

APPENDICES (Continued) Page

LIST OF TABLES

LIST OF FIGURES

LIST OF SYMBOLS

Upper Case Roman

C_D	Drag coefficient for a drop, dimensionless
C_E	Equilibrium vaporization constant, $in.^2/sec$
C_{pf}	Specific heat of vapor, $BTU/(lb_m)(^oR)$
C_{pL}	Specific heat of the liquid, $BTU/(lb_m)(^oR)$
C_T	Threshold constant for drop shattering, dimensionless
D	Drop diameter, microns
D_v	Diffusion coefficient, $in.^2/sec$
F_b	Body force, lb_f
H	Heat transfer coefficient, $BTU/(in.^2)(sec)(^oR)$
$\underline{I}$	Unit tensor
K_{fL}	Mass transfer coefficient, $lb_m/(in.^2)(sec)$
M	Droplet mass, lb_m
$\dot{M}$	Rate of change of droplet mass, lb_m/sec
N	Normalization factor, total number of drops
Nu	Nusselt number for heat transfer, $(HD)/k_m$
Nu'	Nusselt number for mass transfer, $(DpK_{fL})/(D_v\rho_m)$
Pr	Prandtl number, $(\mu_m C_{pm})/k_m$
Re	Reynolds number, $(\rho D\lvert\underline{v} - \underline{u}\rvert)/\mu$
R_f	Gas constant, lb_f in./$(lb_m)(^oR)$
S	Surface, $in.^2$
S_f	Surface area across which the flux of a spray property is measured, $in.^2$
sc	Schmidt number, $\mu_m/D_v\rho_m$
su	Drop deformation number, $(\rho_g \sigma D g_c)/\mu_g^2$

T_g Gas temperature, ^{o}R

T_L Liquid temperature, ^{o}R

T_{LS} Equilibrium or steady-state liquid temperature, ^{o}R

T_m Mean temperature in the gas film surrounding a drop, ^{o}R

V Volume of space, $in.^3$

V_S Sampling volume, $in.^3$

W General weighting function, (Eq. 2.7)

Web Weber number, $(\rho_g |\underline{v} - \underline{u}|^2 D)/(\sigma g_c)$

Lower Case Roman

$\underline{c}$ Molecular velocity, in./sec

e Droplet energy, kinetic + internal, lb_f in./lb_m

f General density function of Γ_i, number of drops/unit Γ_i

f_B Measured density function (Eq. 3.1), number of drops/$(in.^3)(in./sec)(\mu)$

f_F Flux drop size distribution (Eq. 2.25), number of drops/$(in.^2)(sec)(\mu)$

f_k Density function for k^{th} species in a gas mixture, number/(in./sec) $(in.^3)$

f_o Initial value of the spray density function at the surface of formation

f_S Spatial drop size distribution (Eq. 2.24), number of drops/$(in.^3)$(p)

f_T Spray density function integrated over a cross section, (Eq. 4.14), number of drops/(in.)(μ)(in./sec)

g General function, (Eq. 2.9)

g_c force-mass conversion factor

h_{fL}	Latent heat of vaporization, BTU/lb_m
k_m	Mean thermal conductivity in the gas film, $BTU/(in.)(sec)(^oR)$
m	Multiple used to define category limits
n_{ijk}	Number of drops in the i^{th} size, j^{th} axial, velocity, and k^{th} radial velocity categories
n_S	Number of drops per unit volume of space, $no./in.^3$
P	Gas pressure, $lb_f/in.^2$
p_{fL}	Vapor pressure of liquid, $lb_f/in.^2$
p_{fg}	Partial pressure of vaporizing fluid, $lb_f/in.^2$
$\underline{q}$	Heat flux vector, $BTU/(in.^2)(sec)$
r	Radial coordinate, in.
s_f	Surface of formation, $in.^2$
t	Time, sec
t_D	Flash duration of the light source, sec
t_I	Time interval between successive flashes, sec
δt	Time period, sec
$\underline{u}$	Gas velocity, in./sec
$\underline{v}$	Drop velocity, in./sec
$\underline{v}_E$	Mean liquid velocity at the atomizer exit, in./sec
$\underline{v}_S$	Mean velocity of the conical liquid sheet at the atomizer exit, in./sec
$\dot{w}$	Total liquid mass flow rate, lb_m/sec
$\underline{x}$	Position vector, in.
z	Axial coordinate, in.

Script

$\mathcal{A}$	Drop acceleration, $in./sec^2$
$\mathcal{C}$	Peculiar molecular velocity (deviation from mass average), in./sec

$\mathcal{D}$ Rate of change of drop diameter, in./sec

$\mathcal{M}$ Molecular weight

$\mathcal{N}$ Avogadros number

$\mathcal{R}$ Gas constant, lb_f in./(lb_m)(^oR)

$\mathcal{S}$ Source of drops, number/(unit Γ_i)(sec)

$\mathcal{T}$ Rate of change of drop temperature, ^oR/sec

$\mathcal{U}$ Internal energy of gas per unit mass, BTU/lb_m

$\mathcal{V}$ Peculiar drop velocity (deviation from mass average), in./sec

Greek

α Correction factor for unidirectional mass transfer, dimensionless

Γ_i General droplet variable

ϵ Total photographic exposures at a given spray condition

ζ Correction factor for heat transfer, dimensionless

θ Angle in cylindrical coordinates, degrees

κ_Γ Skewness with respect *to* Γ, (Eq. 4.6), dimensionless

λ_Γ Coefficient of variation of Γ, (Eq. 4.5), dimensionless

μ_m Mean viscosity of gas film, lb_m/(in.)(sec)

ν Liquid volume fraction, dimensionless

ξ Dimensionless ratio

$\underline{\underline{\pi}}_f$ Pressure tensor for the gas, lb_f/in.2

$\underline{\underline{\pi}}_s$ Spray analog of the pressure tensor, (Eq. 2.21), lb_f/in.^{2}

ρ_f Fluid density, mass of gas per unit spatial volume, lb_m/in.^{3}

ρ_g	Gas density, mass of gas per unit volume occupied by gas, $lb_m/in.^3$
ρ_L	Liquid density, mass of liquid per unit volume occupied by liquid, $lb_m/in.^3$
ρ_s	Spray density, mass of liquid per unit spatial volume, $lb_m/in.^3$
$\rho_{\Gamma_i \Gamma_j}$	Correlation of Γ_i and Γ_j, (Eq. 4.7), dimensionless
σ	Surface tension, $lb_f/in.$
σ_B	Stefan-Boltzmann constant, $BTU/(in.^2)(sec)(^oR^4)$
σ_Γ	Standard deviation of Γ
$\underline{\underline{\tau}}$	Shear stress tensor, $lb_f/in.^2$
Φ	General spray property, a function of Γ_i
φ	Angle of drop trajectory with the spray axis, degrees
ψ_j	A weighting function of D, $\underline{v}$, and T_L
ω	Rate of change of liquid mass per unit spatial volume, $lb_m/(in.^3)(sec)$

Subscripts

A	Average with respect to drop surface area
f	Gas mixture or vapor of the sprayed liquid
g	Gas
L	Liquid
M	Mass average
M	Mass rate average
m	Mean property in gas film
o	Initial value
r	Component in the r direction

z	component in the z direction

Mathematical Operators and Symbols

D/Dt	substantial derivative
$\nabla_{\underline{x}}$	differential operator $\partial/\partial x_i$, in.$^{-1}$
$\nabla_{\underline{v}}$	differential operator $\partial/\partial v_i$, sec/in.
$\lvert\ \rvert$	magnitude or absolute value
$\langle\ \rangle$	ensemble average
$\underline{\quad}$	underline--vector quantity
$\hat{}$	category mean
$\overline{\quad}$	overbar--time average
$\langle y \lvert x \rangle$	expected value of y given x
Δ	incremental difference

INTRODUCTION TO THE PROBLEM OF SPRAY DESCRIPTION

The frequent practical problem of having a continuous volume of liquid which must be finely distributed throughout a region of space gives rise to the studies of collections of large numbers of liquid droplets called a spray. The resulting theoretical and experimental problems of choosing, relating, and measuring variables which quantitatively describe a spray is the subject of this investigation.

For purposes of discussion the range of spray studies may be divided into two general areas as illustrated in Fig. 1. The first of these, spray formation, is concerned with the processes in which liquid in a reservoir passes through an atomizer and disintegrates to form a spray. The object of studying this phenomenon is to characterize the resulting collection of droplets given the initial conditions of fluid properties, atomizer geometry, energy addition, and properties of the medium in which the spray is formed. A second area, that of spray propagation, involves the prediction and measurement of changes in spray properties due to transfer processes in the two-phase flow downstream. The conceptual boundary separating these two regimes may be called the surface of formation. A quantitative description of the spray at this interface is the end point of formation studies and the initial condition for propagation studies. The method of describing the spray at the surface of formation and some aspects of its subsequent

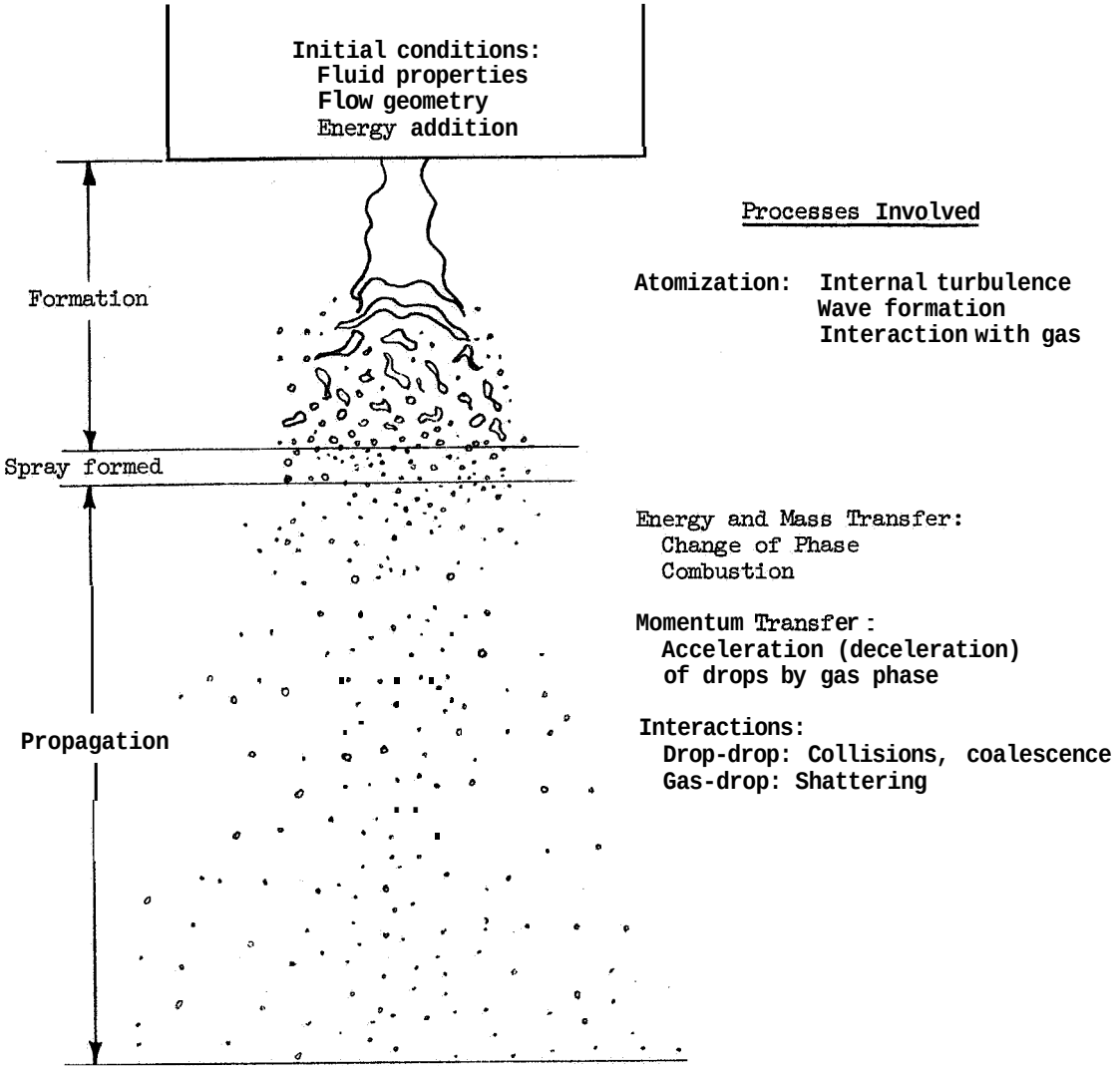

Fig. 1. - Formation - Propagation Classification of Spray Studies.

propagation will receive most of the emphasis in the discussion which fallows.

In the hundreds of spray studies which have been conducted over the past century (Refs. 1, 2), droplet size has received the most emphasis as the key variable in spray description. Since the atomization process is random (See discussion in Chapter I) and large numbers of different sized droplets are formed, a statistical treatment in terms of a size distribution and associated means of the distribution is used. While large numbers of drop size distributions have been measured, very little progress has been made toward their theoretical prediction from initial conditions. Ambiguities and contradictions, which are common within the body of size data, are most often blamed on experimental difficulties in size measurement. Perhaps equal sources of the confusion stem from the common failures to fully specify the conditions under which the data were taken or to place the experimental effort within some sort of conceptual framework, such as the formation-propagation scheme just discussed.

In spite of these shortcomings, empirically correlated spray data have contributed in several areas. Notable examples are the fields of combustible mixture formation from liquid fuels (spray combustion, Ref. 3) and chemical process studies (spray drying, Ref. 4). A particularly useful combustion application is the calculation of

rocket combustion chamber lengths and efficiencies based on a spray vaporization model (Ref. 5).

But solutions to many problems of interest require more detailed spray data and more sophisticated spray theories. For example, treatment of the unsteady spray processes occurring in a diesel engine (Ref. 6) is restricted by the nature of existing spray descriptions; and the problem of avoiding rocket combustion instability (Ref. 7) makes a closer examination off spatial patterns af spray propagation necessary. Consequently, a reevaluation of spray data and theory is indicated so that complex situations such as these may be more satisfactorily handled.

It should be noted that many features of the spray propagation processes are common to other two-phase, gas-particle flows. One example of current interest is the description of the flow of burning metal particles through the chamber of a solid-fueled rocket motor (Ref. 8). Here, also, the basic system considered is a collection of a large number of particles which interact with a gaseous medium (or with each other) by undergoing acceleration and change of phase. Thus, clarification of the variables describing a spray should find wider application.

As indicated above, the droplet size (mass) is the variable which has received the most attention. Another dynamic variable necessary to describe particle motion, droplet velocity (momentum), has been largely neglected. Some measurements of drop velocity have been made (Refs. 9,

10, 11, 12), but velocity has not been purposely treated as a random variable on an equal statistical basis with drop size. Instead, data have been interpreted on the supposition that drops of a given size all move with the same velocity at a given location. This assumption was not made in the development of a spray theory based on an adaptation of statistical mechanics (Ref. 13). However, applications of the theory (Ref. 14) have reverted to old assumptions, i.e., all droplets have the same velocity or a single size has a single velocity. Such simplifications for the sake of mathematical convenience or lack of experimental information tend to nullify the potential for further understanding offered by the general statistical formulation.

In order to clarify the role of drop velocity as a spray variable, measurements of velocity and size were made at various locations in a spray and the data were analyzed in terms of a general statistical mechanical model. Specific goals were: (1) to assess the physical justification for treating velocity as a random variable in a manner similar to drop size; and (2) to determine the implications of such a model for (a) interpretation of previous size measurements, (b) the design of future experiments, and (c) the analytical simulation of spray situations. The difficulties in measuring sizes and velocities add the large number of measurements required precluded extensive variations in experimental parameters aimed at obtaining general correlations. Rather, the experiment was exploratory in nature

with the goal of establishing quantitatively the character of a particular spray situation.

Chapter I begins by summarizing the observed physical conditions that a model must describe and the theoretical implications of these experimental facts. Against this background, the adaptation of molecular statistical mechanics to sprays (Ref. 13) is presented and discussed in Chapter II. The experimental methods used to measure size-velocity distributions are explained in Chapter III along with data reduction methods. Chapter IV presents the measured distributions and associated means and regression curves which illustrate the comprehensive character of the statistical model. Finally, in Chapter V, the conclusions regarding the role of droplet velocity in spray description are summarized.

Chapter I

A PHYSICAL DESCRIPTION OF THE SPRAY SITUATION

Before launching into the description of a detailed model of spray behavior, it is appropriate to review observed spray conditions and consider the implications they have for theoretical analysis. An overall examination of a spray and its formation characteristics is made. The objectives are to define the physical context within which a spray theory applies and to establish some general goals of the theory. A set of spray variables is chosen and samples of more detailed spray measurements are presented to demonstrate the need for a statistical treatment. Next, the behavior of single droplets moving in environments similar to those found in sprays is reviewed. This type of information, which must be built into a statistical spray model, is illustrated by calculated histories for conditions similar to those existing in the sprays where measurements were made. Finally, the characteristics of a spray model demanded by the physical observations are summarized.

A, Experimental Observations and Their Theoretical Implications.

The details of spray formation may only be seen with the aid of high speed photography, i.e., exposure times short compared to the time required for the liquid masses to move distances equal to their dimensions of interest. Since many of the droplets formed are small ($10\mu \approx 4\times10^{-4}$ in.), maximum velocities of 10^6 to 10^7 diameters per second occur. Consequently, photographic methods must be pushed to their technical limits to resolve the details of spray events in space and time.

1. Flow Regimes in the Spray Situation

Figure 2 is a photograph of the atomization conditions produced by a swirl atomizer. It is a specific example of the conditions described schematically in Fig. 1. The picture, which is a cross sectional view in a thin plane passing through the spray axis, was taken by a double-exposure, fluorescent method which will be described in Chapter III. Features common to all atomizers which form liquid sheets are shown. The wave structure on the surface of the hollow liquid cone

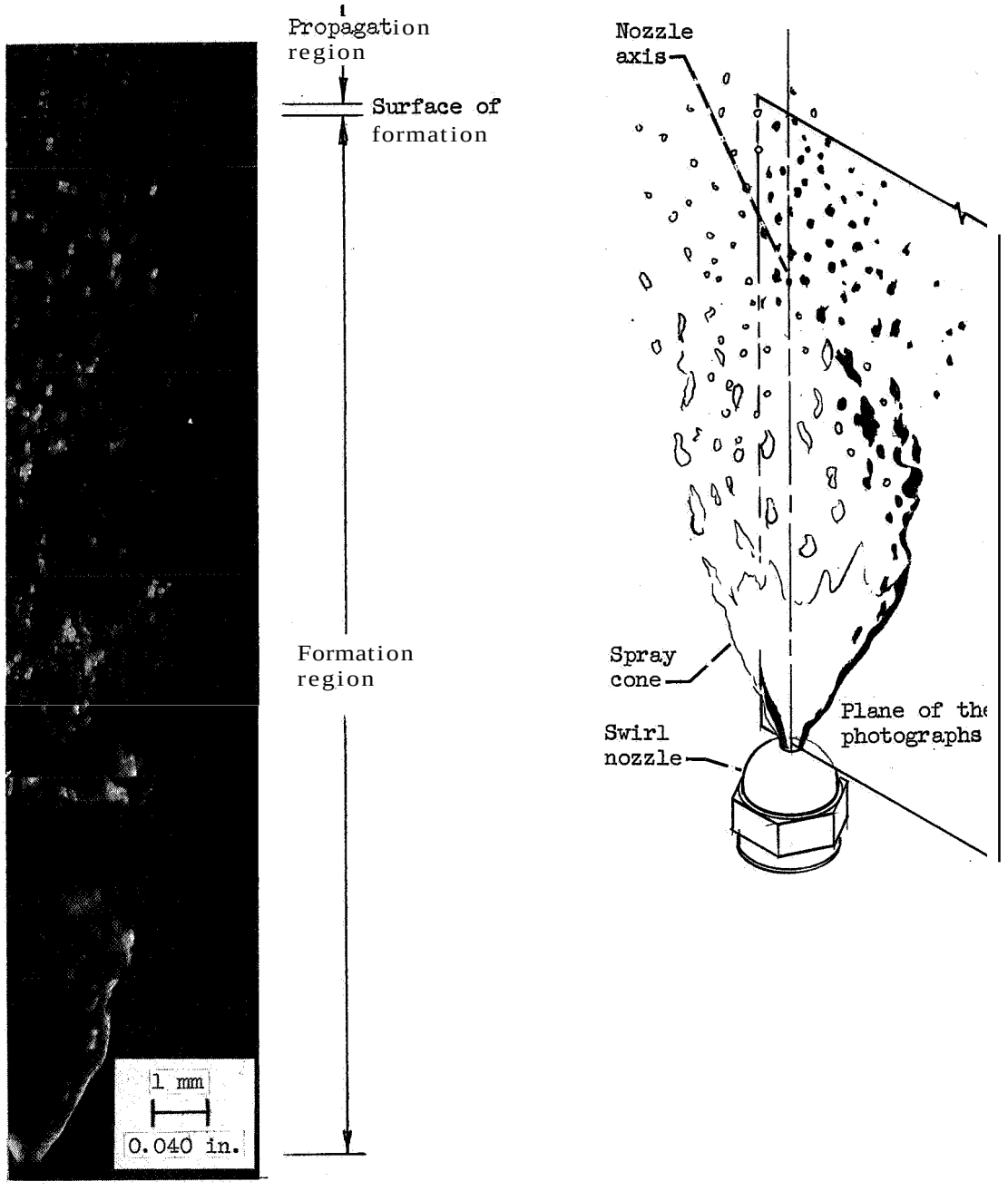

Fig. 2. - Specific example of spray formation (composite double exposure fluorescent photograph).

is clearly visible. Wave amplitude grows with distance downstream until the sheet tears into ligaments. The intermittent tearing produces groups of ligaments which break into clusters of globules and finally form drops. The identity of the droplet "waves" is then destroyed by drag mechanisms acting during downstream propagation. While wave formation plays a less obvious role in the case of atomizers not producing thin liquid sheets, the gross behavior in terms of disturbance growth, ligamentation and drop formation is similar.*

Several features of the atomization conditions shown in Fig. 2 illustrate the physical interpretation of the terms "spray" and "surface of formation" used in the introduction. Implicit in the definition of a spray as a collection of liquid droplets is the assumption that a droplet is approximately spherical, or that one characteristic dimension of the droplet is sufficient to describe its mass and dynamic behavior. In practical terms this means that at some downstream distance where spray formation is considered to be complete, the occurance of highly aspherical globules such as dumbbell shapes is rare. The term "surface of formation" refers to the locus of downstream distances where this condition is first satisified. For convenience the surface of formation is indicated as a plane in Fig. 2.

*See Refs. 3 and 15 where observations of atomization processes are summarized.

In this context, description of details within the formation zone where liquid masses having highly irregular shapes exist, is outside the realm of spray theory. In many applications this limitation is minimized. Practical atomizers are usually operated at flow rates and energy inputs such that the breakup length, the dimension characterizing the formation space, is small in comparison to the length of the entire spray path studied. If, on the other hand, processes such as vaporization or combustion occur in the formation zone at rates which are a substantial fraction of the liquid Tlow rate; the applicability of spray theory to the overall flow process will be limited. In that case boundary conditions at the surface of formation must be obtained from a more general theory of liquid mass removal and dispersion (as yet nonexistant) which can describe greatly distorted liquid globules and ligaments.

Within these limitations, the goals of spray theory may be stated as follows: (a) to choose the variables and type of functional relationship necessary to quantitatively describe a spray at the surface of formation (the description problem); (b) to predict the functional relationship from a knowledge of injection parameters (the formation problem); (c) given this initial functional relationship, to develop equations which describe the change in the function downstream (the propagation problem).

The choice of variables to be considered is relatively straight forward. A complete dynamic description of particle motion involves a knowledge of momentum and position of a particle at any time. Thus, drop diameter D, velocity $\underline{v}$, and position $\underline{x}$ are obvious choices.

Most sprays of interest exist in a gaseous medium characterized by a density ρ_g, pressure p, temperature T_g and velocity $\underline{u}$.* This means a spray problem is inherently a two-phase, mixture problem. With energy exchange occurring between liquid and gas, a measure of droplet internal energy is required. The droplet temperature T_L, is usually sufficient. Insight into the type of function relating these variables in a spray is gained by considering more detailed experimental observations.

2. Random Nature of Spray Processes.

Photographs such as Fig. 2 taken at other times while carefully holding spray parameters** constant are similar in character but different in detail. In particular, if the value of some spray property is continuously monitored

*In many instances, more than one chemical species is present in the gas and/or the liquid phases. Variables specifying chemical composition must then be included.

**Spray parameters are all quantities under the control of the operator (experimenter) in a spray situation. Examples of such quantities which may be known and varied at will are liquid flow rate, initial fluid properties, and geometries of the nozzle and the containing vessel.

within a small spatial volume of the spray, a result such as that shown in Fig. 3 is obtained. The spray property Φ which is a function of the droplet variables Γ_i undergoes random fluctuations about its mean $\bar{\Phi}$, in a manner analogous to velocity fluctuations in turbulent flow. The physical meaning of random in this case is as follows: Although all spray parameters are controlled in the same known manner, successively measured histories of Φ are never the same (Ref. 16). The randomness is a result of the inability of the operator to control the details of each drop formation process. Practically speaking a statistical treatment is required when $\bar{\Phi}$ alone cannot quantitatively* describe the spray to the desired accuracy. The fact that $\bar{\Phi}(t)$ is not a constant in Fig. 3 implies that: (a) some spray parameters were systematically changed during the measurement or (b) particular fixed values of the parameters resulted in some sort of resonant phenomena in the spray system. In either case, overall (large scale) unsteady variations in mean spray properties are produced.

Although continuous time histories of spray properties have rarely been measured and reported, two available

*The "coefficient of variation" (intensity of turbulence) given by $\sigma_\Phi/\bar{\Phi}$ is one indication of the degree of randomness. The value of this ratio for which random effects become operationally significant is obviously relative to the degree of detail sought.

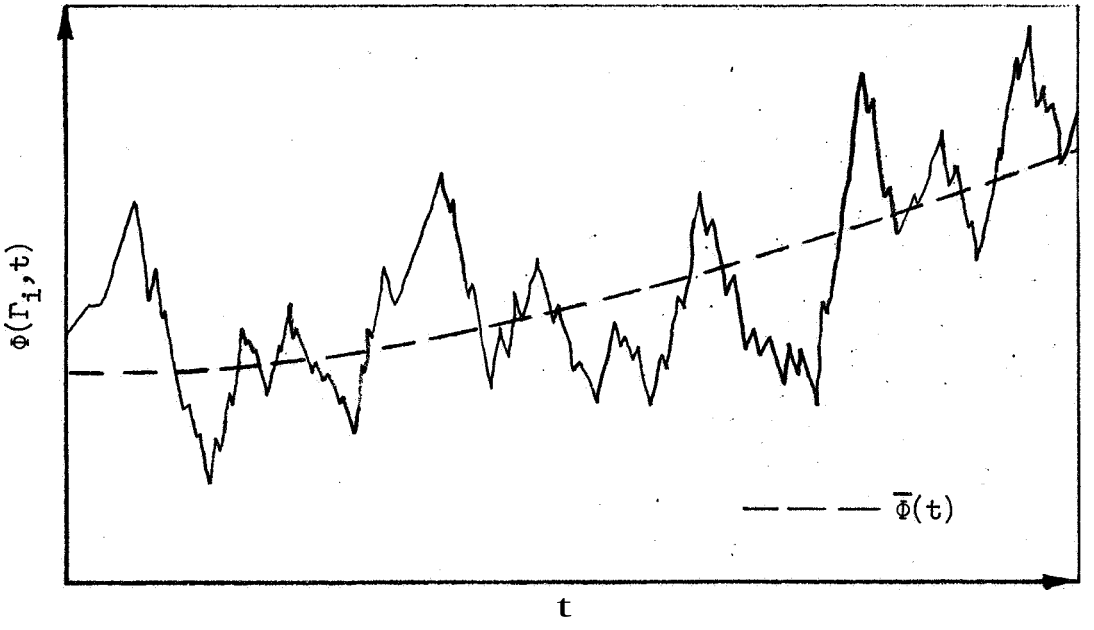

$\Phi(\Gamma_i,t)$ is a property of the spray defined per unit of the spray variables Γ_i at a time t. e.g., If $\Gamma_i = \underline{x}$, $\Phi(\underline{x},t)$ is the number of drops per unit volume.

Approximate operational definitions of the mean $\overline{\Phi}$ and standard deviation σ_Φ:

$$\overline{\Phi} = \frac{1}{\delta t}\int_{t'-\frac{\delta t}{2}}^{t'+\frac{\delta t}{2}} \Phi(\Gamma_i,t)\, dt$$

$$\sigma_\Phi^2 = \frac{1}{\delta t}\int_{t'-\frac{\delta t}{2}}^{t'+\frac{\delta t}{2}} [\Phi - \overline{\Phi}]^2\, dt$$

Where: δt is long compared to the most rapid fluctuations in Φ but short compared to changes in spray parameters or periods of resonant oscillation. In general Φ and σ_Φ may be functions of t' and δt.

Fig. 3. - Schematic Result of Continuous Spray Sampling.

examples are shown in Fig. 4. The measurements were performed on sprays formed by impinging jets with injection parameters held constant (steady-state). In the first case (Ref. 17) a light beam was passed through the spray and the transmitted portion was monitored by a phototube. The resulting signal (Fig. 4(a)) which is proportional to the intensity of the unobstructed beam is a very rough measure of the amount (projected area) of liquid occupying the lighted volume. More quantative data were obtained (Ref. 18) by using a photographic technique, which approximated continuous sampling for the larger drops, to measure spatial densities in specified size ranges (Fig. 4(b)). Whether the records appear to vary in a continuous or discrete manner depends on the definition of the particular spray property and the way in which it was measured. The "noisy" patterns characteristic of random processes are apparent in these records.

Rather than continuous time histories of spray properties, most of the detailed spray data available consist of various forms of drop size distributions. A common method of estimating a size distribution is to instantaneously sample the spray photographically with no attempt to obtain a continuous sample as in Fig. 4(b). An example of this type of data (Ref. 19) is given in Fig. 5 where the spray density (the mass of liquid per unit spatial volume per unit diameter) is plotted as a function of drop size and position in the spray. Spray parameters were

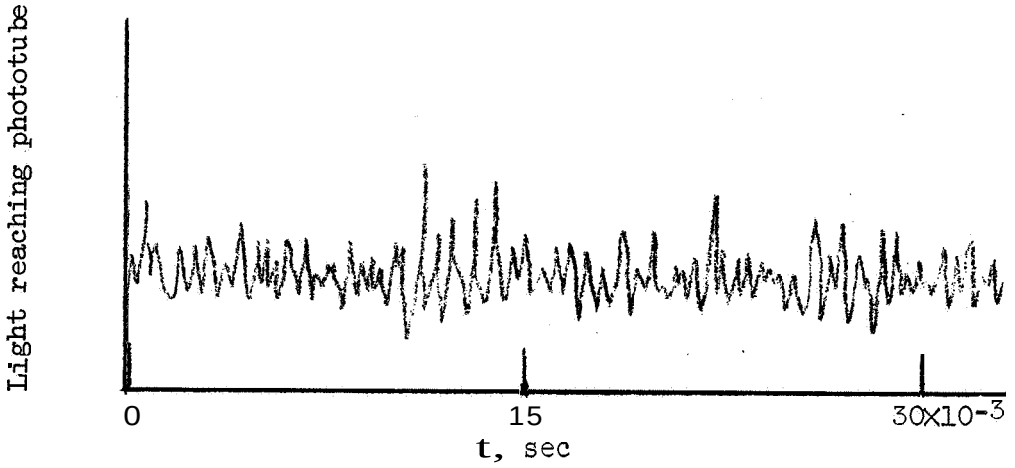

(a) Phototube Output Obtained when Liquid Obstructs a Light Beam Passing Through a Spray Formed by Impinging Jets (Ref. 17).

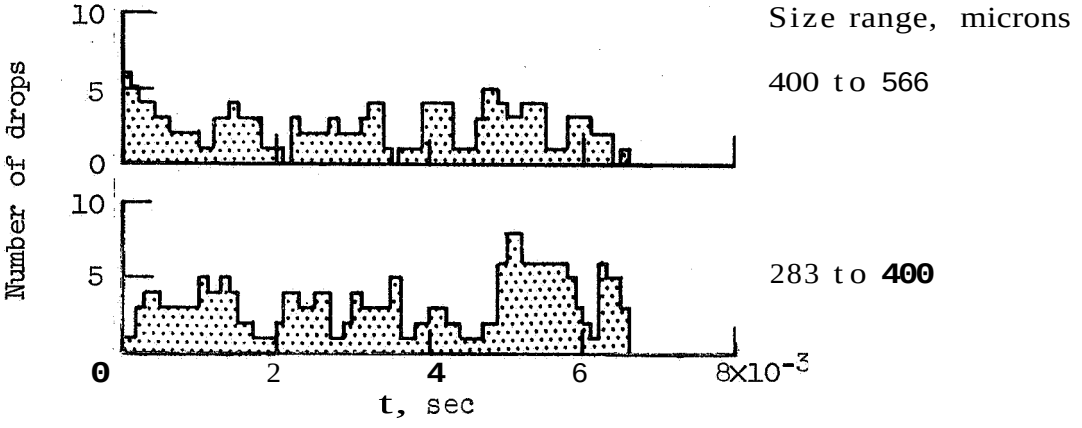

(b) Number of Drops in a Fixed Size Range and Spatial Volume as a Function of Time (Ref. 18).

Fig. 4. - Examples of Measured Time Histories of Spray Properties.

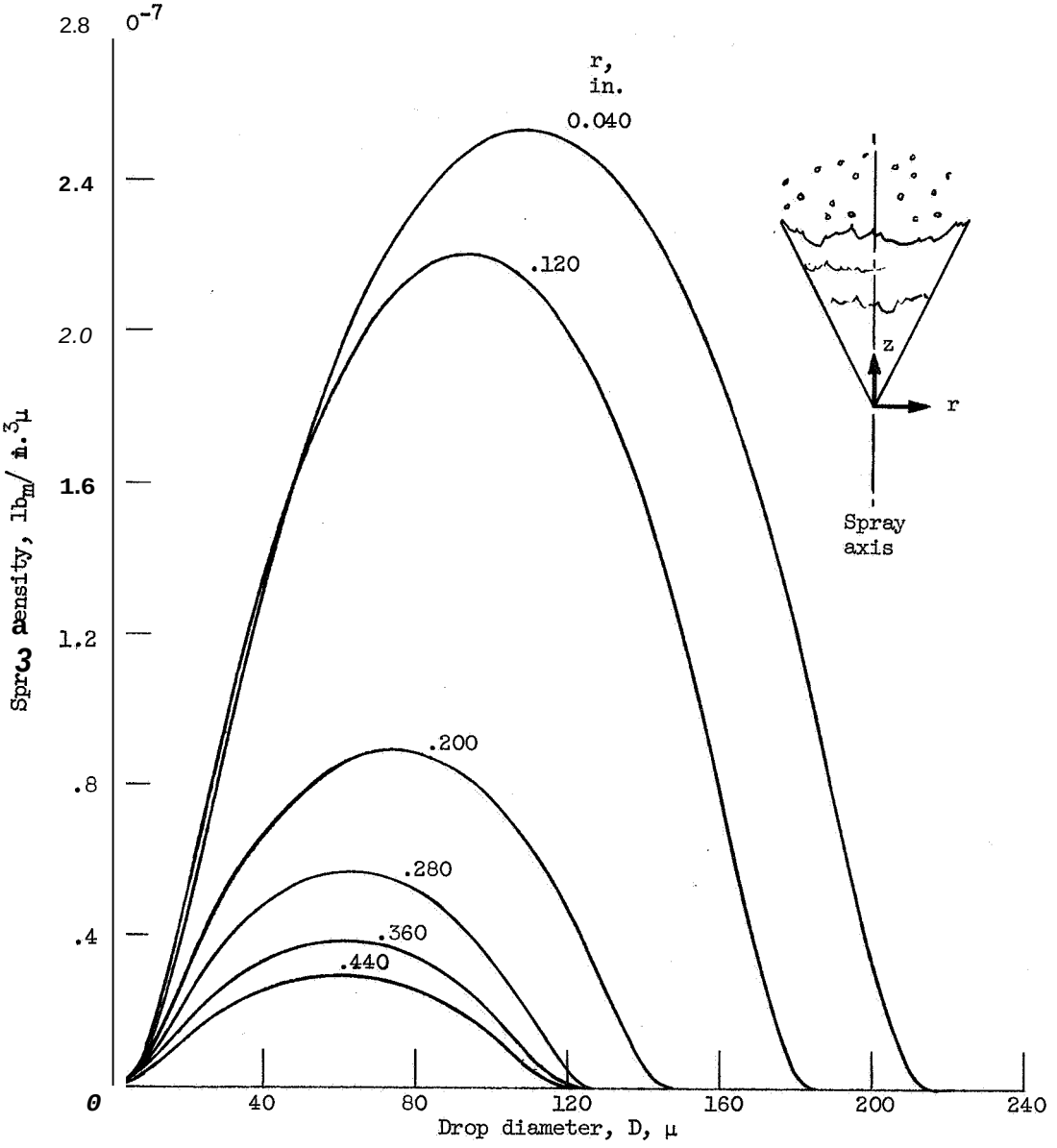

Fig. 5. - Spray Density Distributions as a Function of Drop Size and Position in a Spray Formed by a Swirl Nozzle. (Data from the Correlation in Ref. 19.) Constant Downstream Distance z = 1.25 in.

held constant (steady-state injection) and instantaneous photographs of droplets in a known spatial volume were taken at random intervals in time. Categorized data from many photographs were weighted by the droplet mass and correlated as shown.

This type of spray measurement may be regarded as sampling at instants of time from a large collection of records such as that of Fig. 3.* The collection of all possible records is called the ensemble and will be discussed in more detail in Chapter 11. In sampling from the ensemble the operation shifts from one of fixing spray variables Γ_i and measuring time variations to fixing times and counting frequencies of occurrance of the various Γ_i. In the case of Fig. 5 the Γ_i were specifically the size D and position $\underline{x}$ which are random variables taking on the particular values in their range of definition with varying frequencies.

A question remains as to how the other two droplet variables, $\underline{v}$ and T_L, should be treated. Experimental evidence just reviewed indicates that the spray formation processes are distributed in space, are random in nature, and result in a droplet population randomly distributed with respect to size and location. Such observations

*For a steady-state condition there is no beginning or end for a record and thus no fixed time references are available.

strongly suggest that droplet velocities at the surface of formation should be regarded as randomly distributed about a mean which is not necessarily the mean injection velocity. A theoretical formulation which treats v in this manner, and experimental data which support such a treatment are of primary concern in the discussions presented in later chapters. The lack of an experimental technique to measure individual droplet temperatures in a spray prevented a similar investigation of T_L.

As far as the variables describing the gas phase are concerned, limiting the consideration to dilute sprays allows the gas to be described by local mean values of the properties. The liquid volume fraction $\forall$, which is the ratio of volume occupied by the liquid to the volume occupied by the mixture of liquid plus gas, is a measure of spatial dilutemess. It may be used to characterize the degree droplet-droplet interactions as well as droplet-gas interactions. Small volume fractions imply that statistical fluctuations induced in the gas properties by the fluctuating droplet population can be ignored.

Because of the experimental difficulites involved, no direct measurements of local gas Properties within the spray were made. An attempt was made to infer local gas velocity from drop velocity measurements. The maximum values of $\forall$ measured in this investigation were about 10^{-2}.

B. Summary of Single Droplet Behavior

A statistical mechanical formalism which relates the random behavior of the droplet variables D, $\underline{x}$, $\underline{v}$, and, possibly T_L, in a spray logically includes expressions for rates of change of these variables as determined from the dynamics of a single drop. Thus, the ability to apply such a collective description depends to a large extent on the degree to which individual drop processes are understood.

The single droplet processes considered here are limited to droplet-gas interactions, specifically: vaporization, drag, and heat transfer effects. The extreme droplet-gas interactions resulting in drop shattering (secondary atomization, Refs. 20, 21, 22) involve statistical populations of the droplet's fragments whose properties remain largely unexplored (Ref. 23). Results of experimental and theoretical study of droplet-droplet interactions such as trajectory modifying encounters or collisions resulting in splitting or coalescense are largely qualitative or difficult to apply (Refs. 24, 25, 26). For a dilute spray, droplet-droplet interaction effects are small compared to the droplet-gas effects.

The development summarized below (Ref. 27) is based on empirical correlations for mass, momentum, and heat transfer to a drop moving in a gas stream. Details regarding fluid properties, steady-state temperatures, and equilibrium vaporization constants are given in Appendix A.

1. Governing Equations

Macroscopic balances applied to a single liquid drop yield the following three equations:

Mass Balance:

$$\frac{dM}{dt} = - \frac{\pi D D_v}{R_f T_m} p_{fL} \alpha Nu' \qquad (1.1)$$

where:

M = droplet mass

D_v = diffusion coefficient

p_{fL} = vapor pressure of liquid at temperature T_L

R_f = gas constant for vaporized liquid

T_m = mean temperature in the gas film

p = static pressure of gas

$\alpha = \frac{p}{p_{fL}} \ln\left(\frac{p}{p - p_{fL}}\right)$ a factor expressing unidirectional mass transfer, $\alpha \geq 1$.

Nu = Nusselt number for mass transfer

The system described by Eq. (1.1) is a liquid drop vaporizing in an infinite gaseous medium where the concentration of the vapor is zero at large distances from the liquid-gas interface.

Momentum Balance:

$$M \frac{d\underline{v}}{dt} = - \rho_g C_D \frac{\pi D^2}{8} (\underline{v} - \underline{u}) |\underline{v} - \underline{u}| + F_b \qquad (1.2)$$

where:

ρ_g = gas density

C_D = drag coefficient

F_b = body forces such as gravity

Forces due to gradients in gas pressure (Ref. 28) and the possibility of vapor leaving the drop at other than drop velocity (Ref. 29) have been neglected.

Energy Balance:

$$MC_{pL}\frac{dT_L}{dt} = \pi D k_m (T_g - T_L)\zeta Nu + h_{fL}\frac{dM}{dt} \qquad (1.3)$$

Using the assumption of infinite conductivity of the liquid, Eq. (1.3) states that internal energy changes due to heat transfer from the gas to the liquid plus the latent heat necessary to sustain the current mass transfer rate.

where:

C_{pL} = specific heat of the liquid

k_m = mean thermal conductivity in the gas film

ζ = correction factor to account for heat used to superheat the diffusing vapor, $0 \leq \zeta \leq 1$.

$$= \frac{\xi}{e^{\xi} - 1} \quad \text{and} \quad \xi = C_{pf} p_{fL} \frac{D_v \alpha Nu'}{R_f T_m k_m Nu}$$

Nu = Nusselt number for heat transfer

h_{fL} = latent heat of vaporization

Empirical correlations must be used for Nu', C_D, and Nu. The following are samples of available equations.

Mass Transfer: Ranz-Marshall (Ref. 30)

$$Nu' = 2 + 0.6\, Sc^{1/3} Re_m^{1/2} \qquad (1.4)$$

where:

$$Nu' = \frac{DpK_{fL}}{D_v \rho_m}$$

K_{fL} = mass transfer coefficient

ρ_m = mean density in gas film

$P_m R_m T_m$

Sc = Schmidt number = $\frac{\mu_m}{\rho_m D_v}$, μ_m = mean viscosity in gas film

Re_m = mean Reynolds number = $\frac{\rho_m D |\underline{v} - \underline{u}|}{\mu_m}$

A similar expression was obtained (Ref. 31) when the effects of droplet shape were considered.

Momentum Transfer:. Drag

A variety of empirical drag data have been obtained under conditions ranging from a single solid sphere in steady motion to an accelerating, vaporizing, collection of droplets in turbulent flow (Refs. 19, 32). 'Equations for drag coefficients covering a range to a maximum of $Re \approx 10^3$ are given in Table I, and are plotted in Fig. 6 for comparison with the standard solid sphere curve. Values of Re_g existing in the sprays sampled in this study were less than 100.

Heat Transfer: - Ranz-Marshall (Ref. 30)

$$'Nu = 2 + 0.6\ Pr^{1/3} Re_m^{1/2} \qquad (1.7)$$

This is the heat transfer analog of Eq. '(1.4),

where:

Pr = Prandtl number = $\frac{C_{pm}\mu_m}{k_m}$

TABLE I. - DRAG EXPRESSIONS USED IN CALCULATIONS

C_D equation for: $Re_g = \frac{\rho_g \lvert \underline{v} - \underline{u} \rvert D}{\mu_g}$	$\frac{24}{Re_g}$ (1.5a)	$\frac{27}{Re_g^{0.84}}$ (1.5b)	$0.271\, Re_g^{0.217}$ (1.5c)	$\frac{24}{Re_g}\left(1+\sqrt{1.11\times10^{-2}Re_g}\right)^2 \left(\sqrt{1+\delta}+\sqrt{\delta}\right)$ where $\delta = 3.75\times10^{-5}\frac{Re_g^3}{Su}$ (1.6)
Source	Stokes Law	Ingebo Ref. 35	Rabin et al. (Ref. 36,37)	Approximate fit to curves of Hughes (Ref. 38)
Conditions	Creeping flow	Accelerating groups of solid spheres and drops	Shock tube data for single drops deforming to disk shapes	Deforming drops with δ a measure of deviation from the standard solid sphere curve. Where: $Su = \frac{g_c \sigma \rho_g D}{\mu_g^2} = \frac{Re_g^2}{Web}$ $Web = \frac{\rho_g \lvert \underline{v} - \underline{u} \rvert^2 D}{\sigma g_c}$ σ = surface tension
Range of use	$Re_g < 0.5$	$0.5 \leq Re_g \leq 78$	$Re_g > 78$	$0.5 \leq Re_g \leq 200$

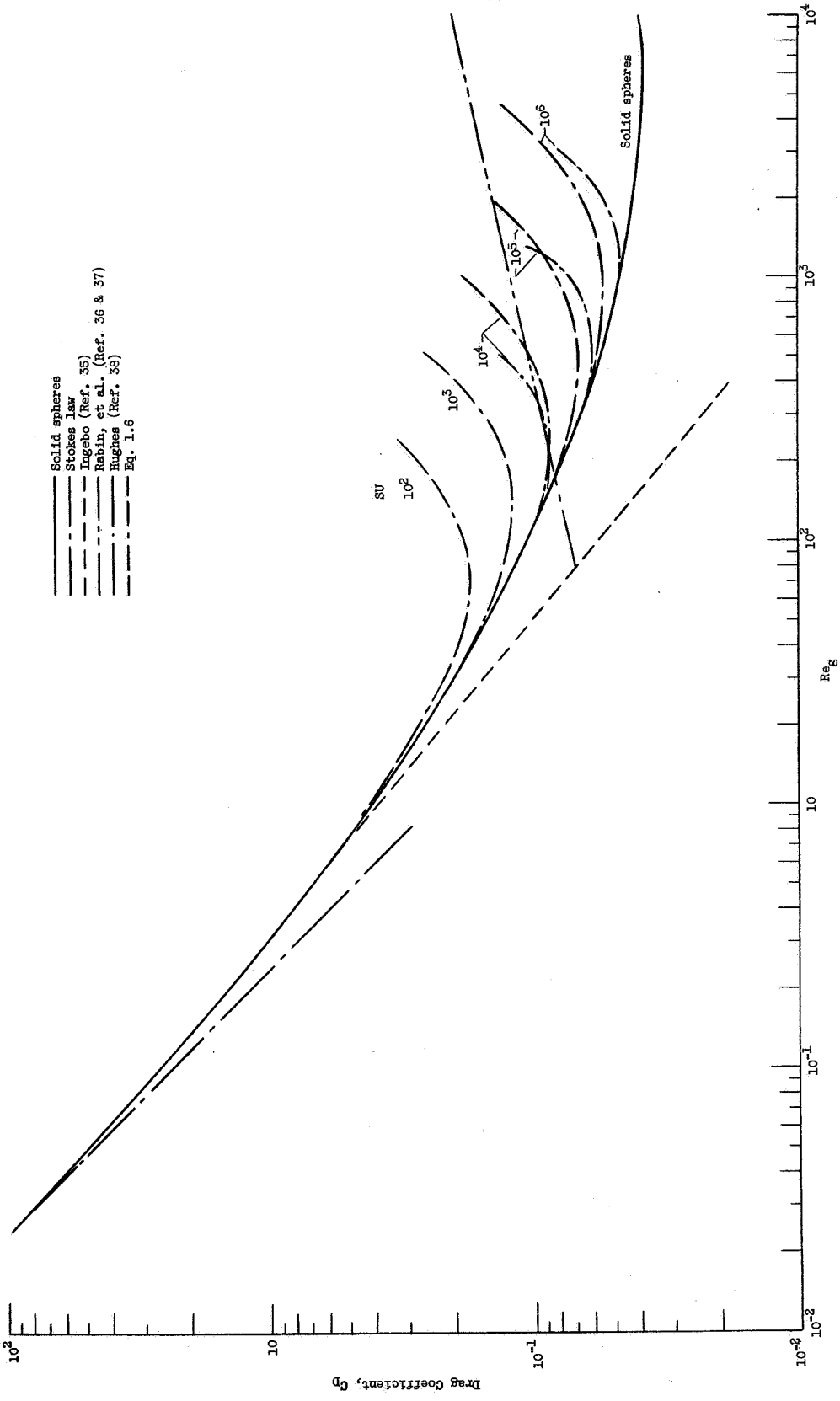

Fig. 6. - Drag Coefficients for Spheres and Drops.

C_{pm} = mean specific heat in gas film

$Nu = \frac{HD}{k_m}$

H = heat transfer coefficient

Several important restrictions on Eqs. (1.4 to 1.7) should be noted in order to assess the validity of their application. The Ranz-Marshall equations were obtained under steady-state conditions but are applied at successive instants of time to calculate unsteady droplet histories (Refs. 5, 6). This quasi-steady treatment is supported by limited experimental tests (Refs. 33, 34). Two specific limitations imposed by experimental technique were that initial drop sizes less than about 500μ and relative velocities greater than about 230 in./sec could not be obtained. Differences between measured and calculated histories increased as drop size and molecular weight of the vaporizing liquid decreased.

In contrast to the processes of heat and mass transfer, more drag data have been obtained under unsteady conditions and samples of such expressions are given in Table I. The shortcoming here is that the multiplicity of factors such as deformation, acceleration, vaporization, and gas turbulence are not easily separated experimentally] and direct measurements of single droplet trajectories and associated velocities relative to the gas (Ref. 39) are rare. The quantitative effects of gas turbulence levels on all three transport processes

(Ref. 40(e)) need more experimental investigation in order to explicitly incorporate turbulence effects in the empirical equations.*

2. Droplet Histories.

Simultaneous solution of the three nonlinear ordinary differential Eqs. (1.1) to (1.3) yields mass, velocity, and temperature histories for a droplet. Usually, variation of fluid thermodynamic and transport properties with temperature cannot be ignored. In addition to this complication, the correlations use averages of the fluid properties across the variable composition in the gas film surrounding the drop, and the factors α and ζ further complicate the coupling. As a result a numerical solution is required.

In order to illustrate the character of single droplet histories and provide a point of comparison with the experimental spray conditions, numerical solutions for ethyl alcohol droplets injected into air at atmospheric pressure were obtained. Variations of droplet mass, velocity, and temperature as a function of distance traveled are given in Fig. 7 for all initial conditions held constant except drop diameter. The calculations were stopped when the mass fraction vaporized reached 0.95. Figure 7(a) emphasizes the fact that due to the cubic relation between

*For an extensive review of gas–particle flow see Refs. 40a to 40f.

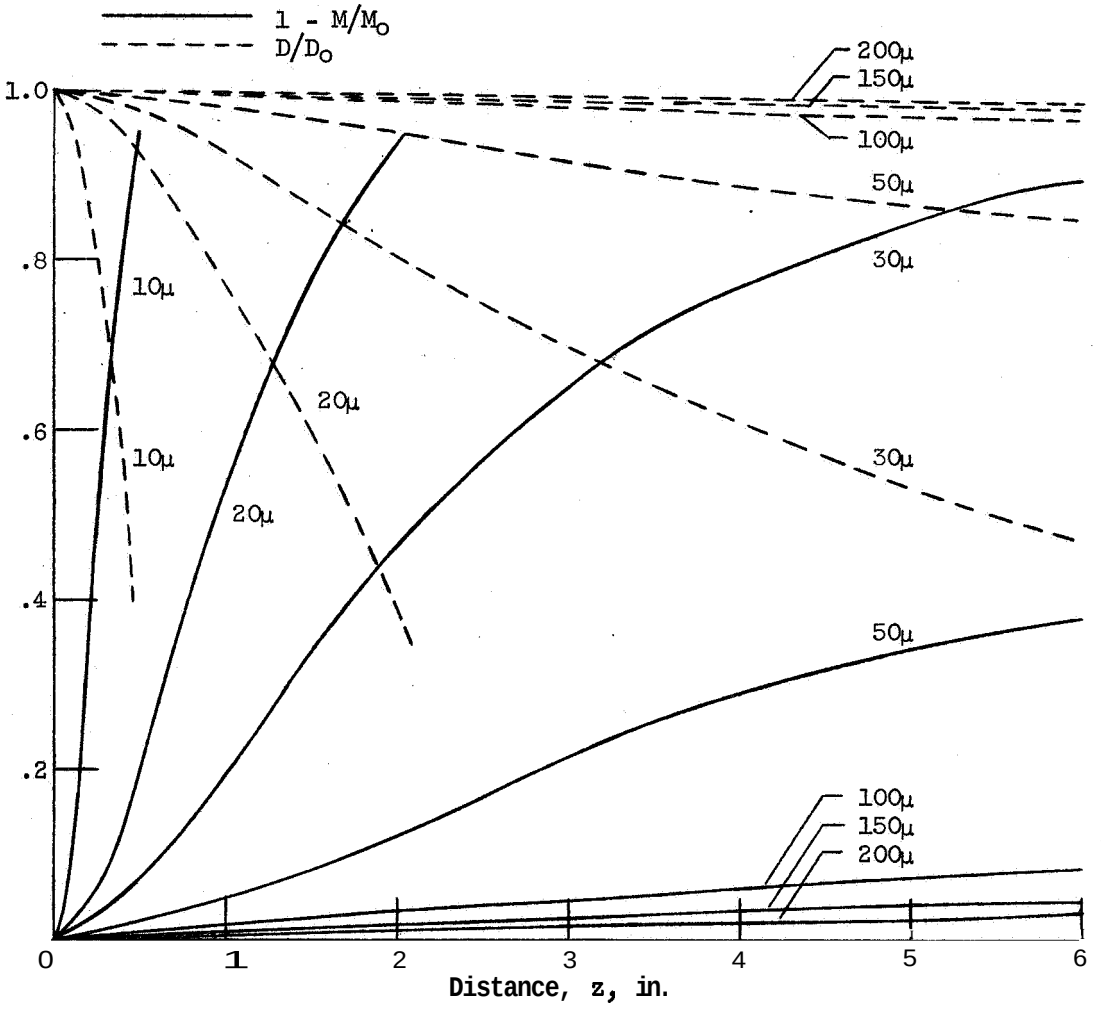

(a) Mass Fraction Vaporized and Diameter Ratio.

Fig. 7. - Calculated Histories for Ethyl **Alcohol Droplets Injected into** Air **at Atmospheric Pressure (Drop Size as the Parameter). Conditions:** T_g = 535° **R,** u_z = 2.44 z^2 - z + 25, T_{LO} = 535° **R, Drag Eqs. 1.5a & 1.6,** v_{zo} = 540 **in./sec.**

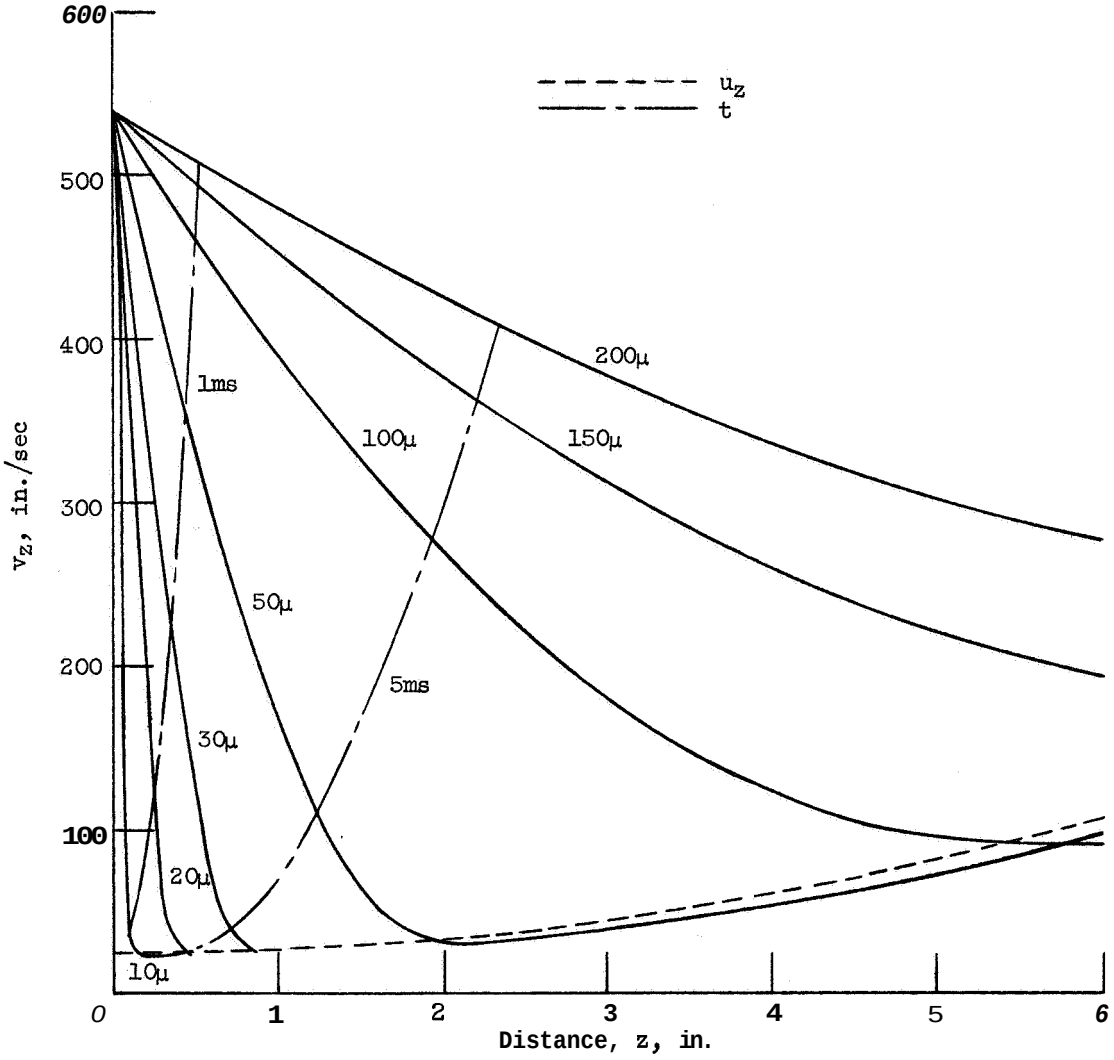

(b) Drop Velocity.

Fig. 7. - Continued.

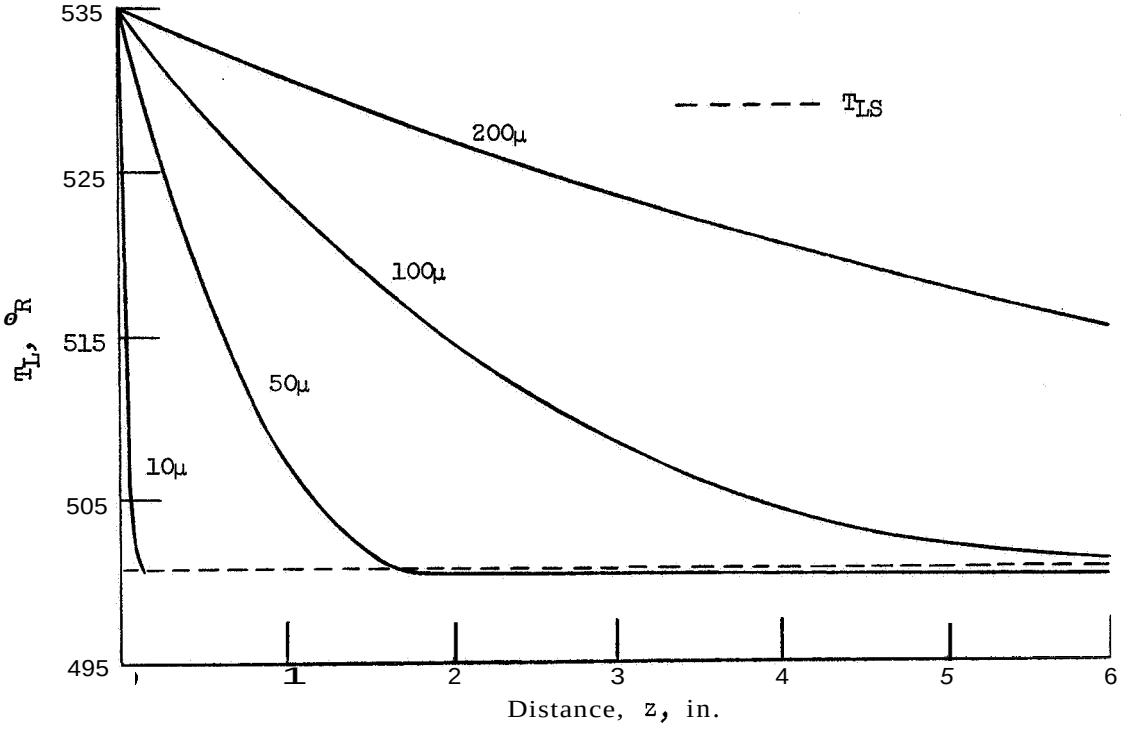

(c) Droplet Temperature.

Fig. 7. - Concluded.

diameter and volume (mass), small changes in diameter are equivalent to much larger changes in volume. This situation has obvious experimental ramifications when sizes are measured and masses computed, i.e., errors are cubed. The drag expression used outside the Stokes Law range was Eq. (1.6) which provides for drag coefficient increases from the solid sphere curve as the distortion parameter Su increases. Air velocity as a function of distance was chosen equal to the exhaust fan velocity which existed in the experiment.* Since u_z changed slowly with z in this example, droplets decelerated to air velocity and then followed closely with only small overshoot and lag for larger drops (Fig. 7(b)). Two curves of constant travel times of 1 and 5 milliseconds have been superimposed on the family of curves to give an added indication of relative penetration as a function of size. Velocity - distance curves calculated for solid spheres of the same initial size show negligible deviation from the vaporizing case. This is due to the fact that, under these initial conditions and gas environment, the smaller sized drops whose faster changing size would be expected to effect the trajectories reach and "lock in" with air velocity so quickly that no deviations are allowed. Droplet temperature which was initially equal to the gas

*This is not the behavior of gas velocity inside the spray due to entrainment as discussed in Chapter IV.

temperature decreases to an approximately constant value, T_{LS}, (called the steady-state or wet-bulb temperature) as shown in Fig. 7(c). An expression for T_{LS} is obtained from Eqs. (1.1) and (1.3) by setting $dT_L/dt = 0$:

$$T_{LS} = T_g - \frac{h_{fL}}{C_{pf}} (e^{\xi} - 1) \qquad (i.8)$$

Since ξ shows only a weak dependence on D and $\underline{v}$ through the ratio Nu'/Nu, and this dependence decreases as Re increases; T_{LS} can be considered to be only a function of fluid properties.*

The consequences of considering variable droplet temperature were investigated. Mass histories for drops started at the steady-state temperature are compared with the unsteady computations in Fig. 8. Differences are largely due to the fact that the vapor pressure of ethyl alcohol increases by a factor of 3.5 over the temperature range 500° to 535° R.

Sensitivity of the trajectories to the drag expressions used are shown in Fig. 9. Differences between the pairs of curves for the same size reflect the behavior of the C_D against Re (proportional to size) curves shown in Fig. 6.

Another set of conditions which occur frequently in practice lead to the type of histories shown schematically in Fig. 10. Here gas temperature and velocity are greater

*See Appendix A for temperature dependent alcohol properties and steady-state temperature computation.

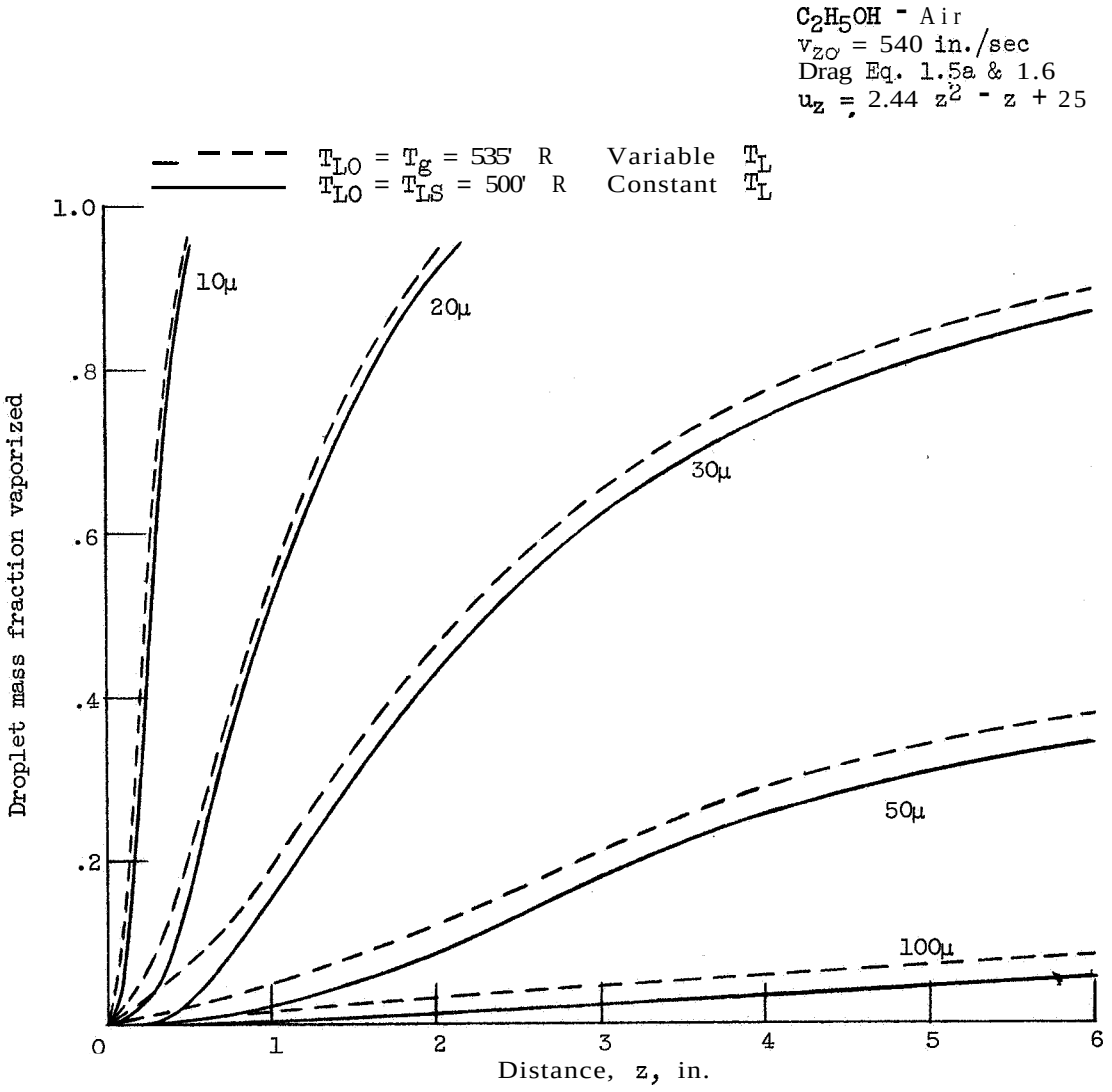

Fig. 8. - Comparison of **Mass** Histories for Variable Droplet Temperature to Fixed Steady-state Case.

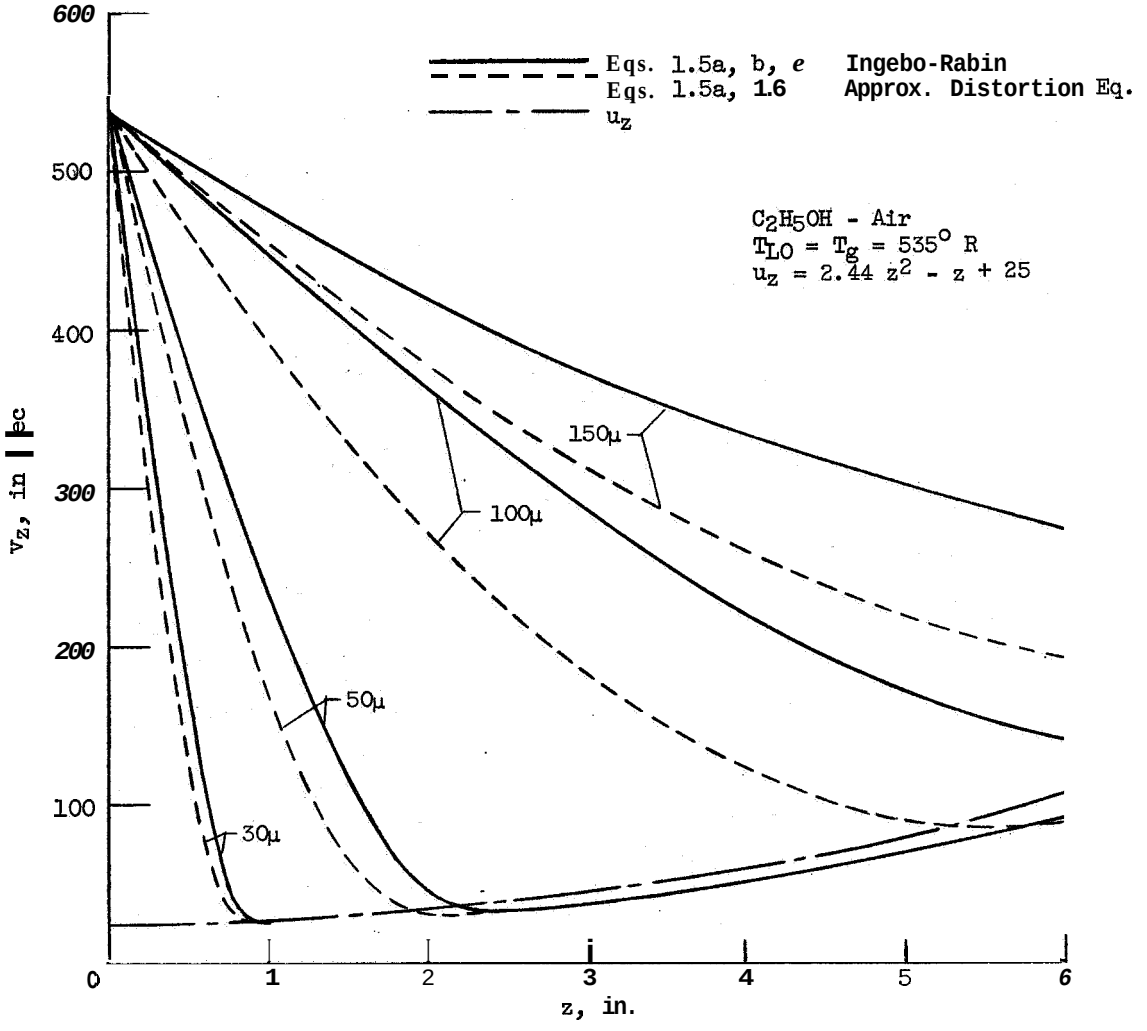

Fig. 9. - Comparison of Droplet Trajectories for Two Drag Expressions.

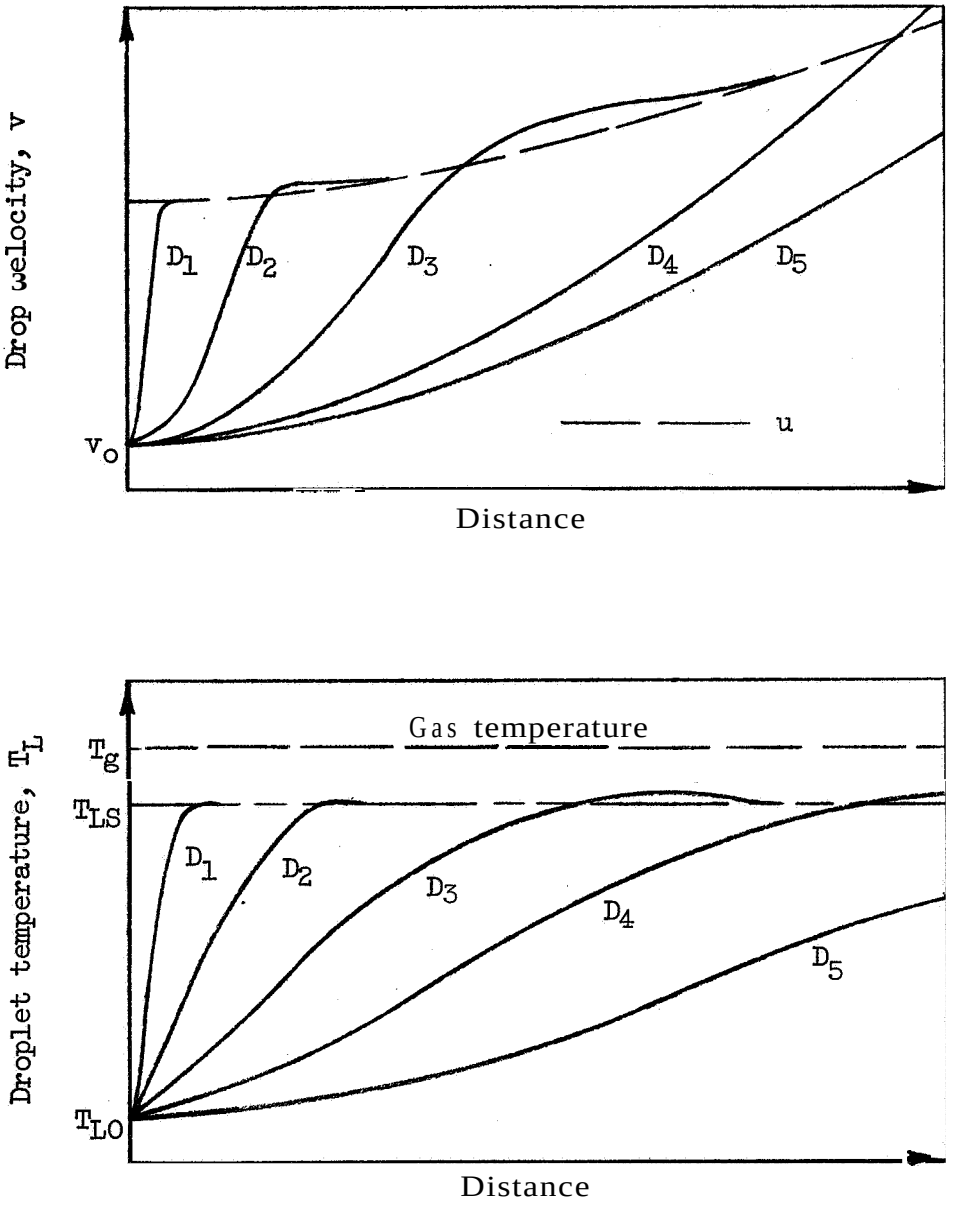

Fig. 10. - Schematic Droplet Histories for: $T_{LO} < T_g$ and $v_o < u$. $D_1 < D_2 < D_3 < D_4 < D_5$.

than initial drop values and thus droplets heat up and accelerate.

Within the framework just outlined, single droplet behavior is given by three functional relations for rates of change of mass, momentum, and energy. In terms of D, $\underline{v}$, and T_L the rate equations may be considered as functions of the following arguements:

$$\mathcal{D} \equiv \frac{dD}{dt} = \mathcal{D}(D, \underline{v}, \underline{x}, T_L, \underline{u}, p, T_g)^* \tag{1.9a}$$

$$\underline{\mathcal{A}} \equiv \frac{d\underline{v}}{dt} = \underline{\mathcal{A}}(D, \underline{v}, \underline{x}, T_L, \underline{u}, p, T_g) \tag{1.9b}$$

$$\mathcal{T} \equiv \frac{dT_L}{dt} = \mathcal{T}(D, \underline{v}, \underline{x}, T_L, \underline{u}, p, T_g) \tag{1.9c}$$

The quantities p_{fL}, $\underline{v} - \underline{u}$, and $T_g - T_L$ drive the droplet toward equilibrium with the gas whose extent is considered so great that gas properties are not appreciably modified by the droplet transport processes. The equilibrium condition approached is one where $\underline{v} \approx \underline{u}$ and $T_g - T_{LS}$ is a constant.** Smaller size means that the magnitudes of the rates are greater as shown by a tabulation of their diameter dependence (see Table 11). Thus

---

* Note that $\frac{dM}{dt} = \rho_L \frac{\pi D^2}{2} \frac{dD}{dt}$ and other fluid thermodynamic and transport properties might be included as arguments of the functions.

** An equilibrium size for a drop exists only if a saturation condition is considered, i.e., $p_{fL} = p_{fg}$ where p_{fg} is the partial pressure of the vaporizing fluid far from the drop. In the above model for a single drop in an infinite medium, $p_{fg} = 0$.

TABLE II. - DEPENDENCE OF THE RATES $\mathcal{D}, \underline{\mathcal{A}}, \mathcal{T}$ ON D FROM EQUATIONS (1.1) TO (1.7)*

Rate	Diameter dependence	Special cases
$\mathcal{D}$ Size change	$-\frac{C_1 + C_2 D^{1/2}}{D}$	$C_2 = 0$ for stagnant case of $\lvert \underline{v} - \underline{u} \rvert = 0$
$\underline{\mathcal{A}}$ Acceleration	$-\frac{C_3}{D^{n+1}}$	$n = 1$ Stokes Law $0 < n < 1$ approximate solid sphere behavior $-1 \leq n \leq 0$ distorting drops sign of $\underline{\mathcal{A}}$ given by $\underline{v} - \underline{u}$
$\mathcal{T}$ Temperature change	$\pm \frac{C_4}{D}\left[(C_5 - C_7) + (C_6 - C_8)D^{1/2}\right]$	(a) $-C_4$ if $T_g < T_L$ $\mathcal{T}$ is - (b) $+C_4$ if $T_g > T_L$ and $\mathcal{T}$ is - for $T_L > T_{LS}$ + for $T_L < T_{LS}$

*The C's are functions of fluid properties with C_2, C_3, C_7, C_8 also functions of relative velocity.

small drops quickly reach velocity and temperature equilibrium with the gas; while larger droplets respond more slowly, may overshoot due to thermal or mechanical inertia, and may never closely approach equilibrium especially when large gradients in T_g and u exist.

Against this physical background, several characteristics which a spray model should possess may be summarized. A statistical mechanics treating droplet variables as random is required due to the complex and uncontrolled behavior of the drop formation processes. With single droplet behavior incorporated as a basis, the statistics must account for the situation where the initial values x_o, D_o, $\underline{v}_o$, and perhaps T_{Lo} for the drops are statistically distributed at the surface of formation. Coupling effects in the flow of the gas-droplet mixture must be considered even for dilute sprays, and the fact that statistical variations in gas properties and drop-drop interactions increase with liquid concentrations must be realized.

Chapter II

STATISTICAL MECHANICS OF A SPRAY

A statistical mechanics for sprays has been formulated (Refs. 13, 14, 41) by directly adapting the concepts and methodology of classical molecular statistical mechanics (Ref. 42). As is true of the classical model, the spray adaptation offers many physical insights through the consideration of extensive detail. These conceptual advantages are gained at the price of great practical difficulties in attempts to apply the theory to realistic situations.

The structure of the theory as outlined in this chapter generally follows the previous development (Refs. 13, 14) but specifically differs in the following ways. Physical meanings and relations of equations to experimental observations receive considerable emphasis; and terms involving droplet internal energy as a random variable are included. This later addition to the theory remains to be experimentally justified

and clarified. Comparisons of the molecular condition with the spray situation are made which point out basic physical differences in spite of formal similarities in the analytic descriptions. Their purpose is to serve as a guide for further interplay between the parent microscopic theory and its macroscopic offspring.

The presentation begins with a discussion of the spray density function f as one answer to the problem of spray description. Next, a basis for spray propagation theory is offered in the transport equation for f. From this equation conservation equations for liquid, gas, and mixture are obtained and mean spray quantities are defined. Finally, two general approaches to application of the theory are presented and assessed in terms of existing and required experimental information.

A. The Density Function f

Consider a function $f(\Gamma_i, t)$ which has the following mathematical and physical interpretation. The variables Γ_i are randomly distributed, and, for the case of sprays, are chosen as those necessary to describe the condition of a droplet. As discussed previ-

ously reasonable choices for the Γ_i are size D,* position $\underline{x}$, velocity $\underline{v}$, and temperature T_L. The time t is a parameter. The function f has characteristics of both a physical density with units number of drops per unit Γ_i, and a probability density since it represents the probable number of drops in the range $d\Gamma_i$ about Γ_i at a time t. It is not a probability density function in the strict mathematical sense because the normalization has not been carried out:

$$N = \int f(\Gamma_i, t)\, d\Gamma_i \qquad (2.1)$$

where the integral is over the entire range of each Γ_i. The normalization factor N which is the total number of particles represented by f at a time t must be determined by physical restraints on the spray system under

*More general choices of the Γ_i would be droplet mass, momentum and enthalpy since these would allow liquid density dependence on temperature (volumetric expansion effects) and specific heat variations with temperature to be included. However, the choices used above are those variables which were experimentally measured (with the exception of T_L). Also, since the mass is variable, it is convenient to separate mass and velocity into two terms rather than use the product.

consideration. Specifically, the restraints take the form of limitations on the range of one or more of the $\dot{\Gamma}_i$ (for example, $\underline{x}$ may be restricted to a finite range to define the volume of the system considered); and specification of the value of some function of f and $\dot{\Gamma}_i$ in terms of spray parameters (for example, an average value of the liquid flow rate at the boundary of the system). Of course, a probability density function, $f' = f/N$, may be used but a complete physical description includes an explicit specification of N or its equavelent in terms of system parameters.*

The statistical nature of f may be explored by considering a collection of sample functions composed of individual histories similar to the one introduced in Fig. 3. Such a collection is shown in Fig. 11. The jth sample function $\Phi^{(j)}(\Gamma_i + \Delta\Gamma_i, t)$ is defined as the number of drops in the range of variables Γ_i to $\Gamma_i + \Delta\Gamma_i$ at a time t. The collection of all possible sample functions obtained under identical conditions is called the ensemble or sample space. The specification of identical conditions means that all spray parameters were controlled in the same manner throughout each history and the same variable range Γ_i to $\Gamma_i + \Delta\Gamma_i$ was considered. A

---

*The situation is analogous to Planck's Law for the energy distribution of black body radiation as a function of wavelength with temperature as a parameter. The normalization factor in this case is the total energy radiated at all wavelengths ($\sigma_B T^4$) and must be included if the distribution is normalized.

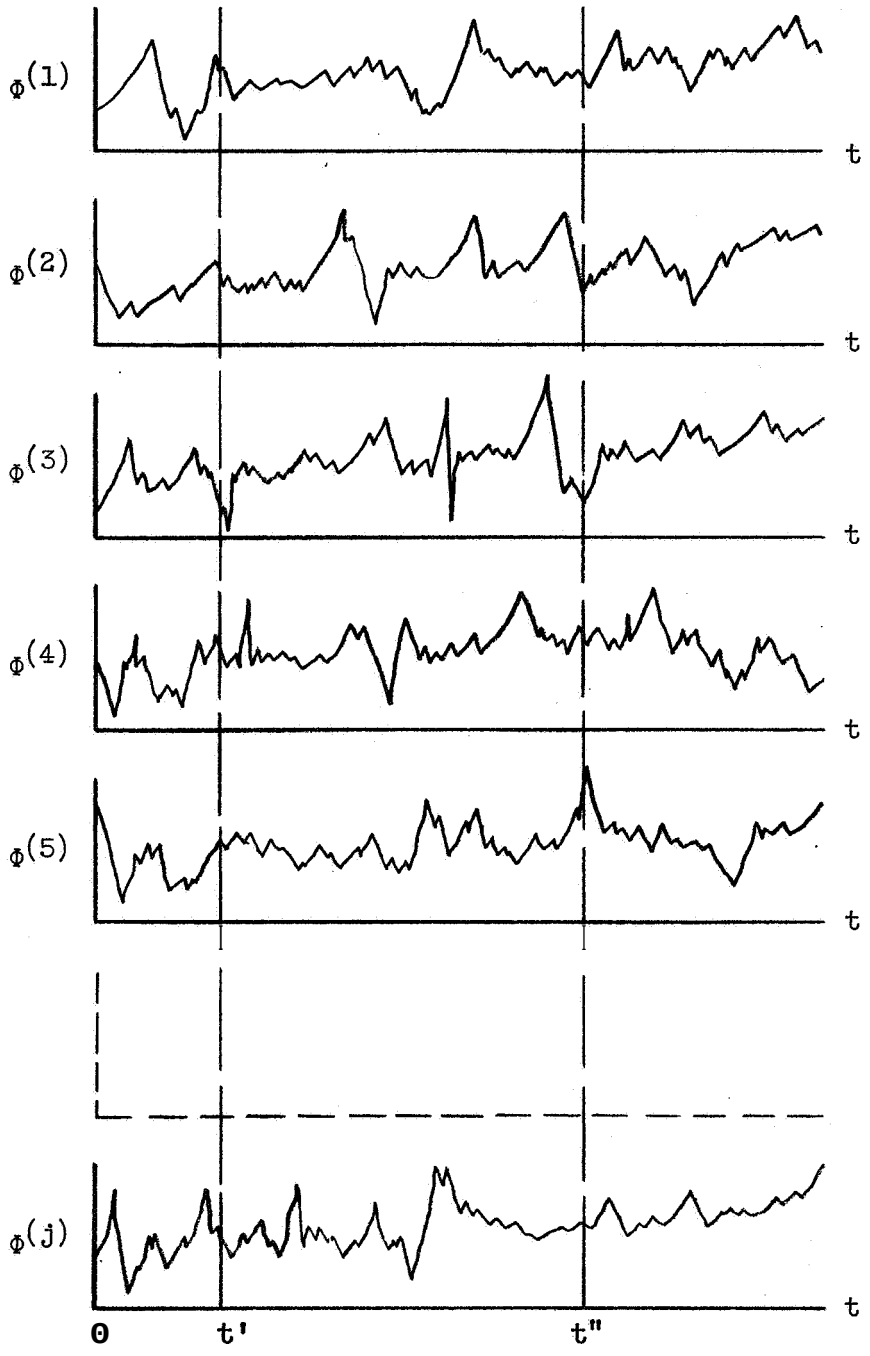

Fig. 11. - Schematic Representation of a Group of Sample Functions $\#(j)(\Gamma_i + \Delta\Gamma_i, t)$ which together Form a Portion of the Ensemble

definition of the density function f for the ensemble may be given in terms of a limiting process performed on a sum over the ensemble at a given time t':

$$f(\Gamma_i,t') \equiv \lim_{j\to\infty} \lim_{\Delta\Gamma_i\to 0} \frac{1}{j\Delta\Gamma_i} \sum \Phi^{(j)}(\Gamma_i + \Delta\Gamma_i,t') \quad (2.2)$$

In the particular case when f is independent of time, the random process which f describes is said to be stationary.* Averages (also called moments or expected values) of a function $g(\Gamma_i,t)$ over the ensemble are defined by:

$$\langle g(\Gamma_i,t)\rangle = \frac{\int g(\Gamma_i,t)f(\Gamma_i,t)\,d\Gamma_i}{\int f(\Gamma_i,t)\,d\Gamma_i} \quad (2.3)$$

where the integrals are over the entire range of each Γ_i. The brackets $\langle\,\rangle$ are used to distinguish the ensemble average from a time average denoted by an overbar $\bar{\ }$. For a stationary process the ensemble averages are independent of time.

Higher order joint density functions may be formed by considering the distribution of sets of spray variables $\Gamma_i(1)$, $\Gamma_i(2)$, ... $\Gamma_i(N)$ at times t_1, t_2, ... t_N. In particular the second order density

*A stationary condition implies that spray parameters were held constant to achieve a steady state. However, holding spray parameters constant does not necessarily mean that the random process is stationary since a system resonance may occur.

$f^{(2)}(\Gamma_i^{(1)},\Gamma_i^{(2)},t_1,t_2)$ represents the probable number of drops in the range $d\Gamma_i^{(1)}$ about $\Gamma_i^{(1)}$ at t_1 and in the range $d\Gamma_i^{(2)}$ about $\Gamma_i^{(2)}$ at t_2. Such a density would become significant physically if a spray process depended strongly on the joint distribution of pairs of Γ_i. When dilute sprays are considered, drop-drop interaction effects are assumed small and further considerations are limited to the first order density $f(\Gamma_i,t)$ with the superscript (1) omitted. From an experimental point of view, formidable difficulties are encountered in even estimating f which is a multivariate density in $i + 1$ variables.

Various time averages defined along any member $\Phi(j)$ of the ensemble may be defined in a manner similar to that given in Fig. 3. However, precise definition of averaging times for nonstationary processes is a very delicate matter. For stationary random processes the theoretical analysis of continuous time series has been developed in considerable detail for application in fields such as communication (Ref. 43) and random vibration (Ref. 16). However, present spray sampling capabilities are largely limited to instantaneous sampling or long term averaging. As a result the application of time series theory to sprays must await the development of experimental methods for measuring continuous time histories of spray properties.

The density function f is a conceptual answer to the problem of how to describe a spray in terms of droplet

variables. The manner in which f changes due to changes in the Γ_i will now be considered.

B. The Transport Equation: A Continuity Equation for f

An equation of change for $f(\Gamma_i,t)$ may be written in the form of a generalized continuity equation:

$$\frac{\partial f}{\partial t} + \frac{\partial}{\partial \Gamma_i}(\dot{\Gamma}_i f) = \mathcal{S} \qquad (2.4)$$

where $\mathcal{S}$ represents a source or sink term for' f; number of drops/unit Γ_i/unit time,

$\dot{\Gamma}_i \equiv \frac{d\Gamma_i}{dt}$ The total time derivative giving the rate of change of Γ_i for a droplet.

Equation (2.4) results from an accounting of possible changes in f within a region of the multidimensional space defined by the variables Γ_i (see Appendix B.1).*

For the particular choice of droplet variables and notation summarized in Table 111, the specific form of the equation of change for the droplet density function $f(D,\underline{x},\underline{v},T_L,t)$ is:

$$\frac{\partial f}{\partial t} + \frac{\partial}{\partial D}(\dot{D}f) + \nabla_{\underline{x}} \cdot (\underline{v}f) + \nabla_{\underline{v}} \cdot (\underline{a}f) + \frac{\partial}{\partial T_L}(\dot{T}f) = \mathcal{S}$$

(i.) (ii.) (iii.) (iv.) (v.) (vi.)

(2.5)

* If the associations of f with a density ρ, Γ_i with a coordinate $\underline{x}$, $\partial/\partial\Gamma_i$ with an operator $\partial/\partial x_i = \nabla_x$, and $\dot{\Gamma}_i$ with a velocity; $\dot{\underline{x}} = \underline{v}$ are made by analogy; the equation takes on the appearance of the usual continuity equation in fluid dynamics:
$\frac{\partial \rho}{\partial t} + \nabla_{\underline{x}} \cdot \rho\underline{v} = \mathcal{S}$.

TABLE III. - SUMMARY OF NOTATION FOR DROPLET VARIABLES D, $\underline{x}$, $\underline{v}$, T_L IN TERMS OF GENERAL Γ_i

i	Γ_i	$\dot{\Gamma}_i$ *	$\frac{\partial}{\partial \Gamma_i}$
1	D size	$\mathcal{D} \equiv \frac{dD}{dt}$	$\frac{\partial}{\partial D}$
2,3,4	$\underline{x}$ position vector	$\underline{v} \equiv \frac{d\underline{x}}{dt}$	$\frac{\partial}{\partial \underline{x}} \equiv \nabla_{\underline{x}}$
5,6,7	$\underline{v}$ velocity vector	$\underline{\mathcal{A}} \equiv \frac{d\underline{v}}{dt}$	$\frac{\partial}{\partial \underline{v}} \equiv \nabla_{\underline{v}}$
8	T_L temperature	$\mathcal{J} \equiv \frac{dT_L}{dt}$	$\frac{\partial}{\partial T_L}$

*Rates given by equations for single droplet transport processes occurring with the gas.

This is the spray analog of the Boltzmann Equation employed in molecular statistical mechanics. However, additional terms appear in the spray equation due to the interactions of the droplets with the surrounding gas - a situation which has no counterpart in the molecular model. The separate terms of Eq. (2.5) account for changes in $f(D, \underline{x}, \underline{v}, T_L, t)$ due to:

i. Explicit time variation

ii. Change of size (mass) due to vaporization. Note that a spray is a mixture of an infinite number of "species," i.e., sizes of drops.

iii. & iv. Mechanics of droplet motion. Note that the acceleration $\mathcal{A}$ is velocity dependent so that $\nabla_{\underline{v}} \cdot \underline{\mathcal{A}} \neq 0$; but since $\underline{v}$ and $\underline{x}$ are treated as independent variables, $\nabla_{\underline{x}} \cdot \underline{v} = 0$, and term iii can be written $\underline{v} \cdot \nabla_{\underline{x}} f$.

v. Change in droplet temperature (enthalpy) due to heat and mass transfer.

vi. Sources or sinks of droplets other than vaporization such as collisions, shattering, and condensation.

This continuity equation for f applies to the liquid drops (or in general any particle phase) only, but the rate expressions $\mathcal{D}$, $\underline{\mathcal{A}}$, and $\mathcal{T}$ couple the particle motion to the gas motion (see Eq. (1.9)). With the restriction that large scale statistical fluctuations in

the gas motion do not occur (as discussed in Chapter I), the usual equations of change for gas flow in terms of mean gas properties apply with the addition of source terms arising from droplet-gas interactions. Thus, a theoretical basis for spray propagation studies is established.

C. Equations of Change and Associated Mean Quantities

The fact that variations of spray properties in time and space are often the primary concern in practical problems leads to the application of an averaging procedure to Eq. (2.5) in order to obtain equations of change for average spray properties which are only a function of $\underline{x}$ and t. Detailed information about the statistital variation of D, $\underline{v}$ and T_L is thus sacrificed in the hope of finding solutions in terms of the average quantities and experimental methods of measuring the averages directly. From a mathematical point of view each term of Eq. (2.5) can be multiplied by any function $\psi_j(D,\underline{v},T_L)$ and integrated over the entire range of these three variables to obtain marginal densities and ensemble averages. The term marginal indicates that the integration over at least one of the variables, in this case the position variable $\underline{x}$, is not carried out.

When these operations are carried out on Eq. (2.5) (see Appendix B.2 for details) the following equation of change for ψ_j results:

$$\frac{\partial}{\partial t}\iiint \psi_j f \, dD \, d\underline{v} \, dT_L + \nabla_{\underline{x}} \cdot \iiint \psi_j \underline{v} f \, dD \, d\underline{v} \, dT_L$$

(i.) (ii.)

$$-\iiint \mathscr{D} f \frac{\partial \psi_j}{\partial D} \, dD \, d\underline{v} \, dT_L - \iiint \underline{\mathscr{A}} f \cdot \nabla_{\underline{v}} \psi_j \, dD \, d\underline{v} \, dT_L$$

(iii.) (iv.)

$$-\iiint \mathscr{T} f \frac{\partial \psi_j}{\partial T_L} \, dD \, d\underline{v} \, dT_L = \iiint \mathscr{S} \psi_j \, dD \, d\underline{v} \, dT_L$$

(v.) (vi.) (2.6)

The significance of each term is as follows:

i. the rate of change of the spatial density of ψ_j

ii. the divergence of the flux of ψ_j; a "convective" term

Terms due to transfer of ψ_j between phases:

iii. mass transfer, e.g., vaporization

iv. momentum transfer, e.g., aerodynamic drag

v. energy transfer, e.g., heat transfer and vaporization

vi. rate of creation of ψ_j per unit spatial volume.

If the weighting functions ψ_j are chosen to be the droplet mass, momentum and energy; equations of change for these three quantities result. Table IV summarizes these specific functions of D, $\underline{v}$, and T_L and their derivatives. The integrals which result from substitution of the expressions from Table IV into Eq. (2.6) are given in Table V along with a condensed notation. The notation was

TABLE IV. - WEIGHTING FUNCTIONS $\psi_j(D,\underline{v},T_L)$ AND DERIVATIVES USED TO OBTAIN EQUATIONS OF CHANGE FOR DROPS

j	ψ_j	Droplet property	$\partial\psi_j/\partial D$	$\nabla_{\underline{v}}\psi_j$	$\partial\psi_j/\partial T_L$
1	$\rho_L \frac{\pi D^3}{6} \equiv M$	Mass	$\rho_L \frac{\pi D^2}{2}$	0	0
2	$\rho_L \frac{\pi D^3}{6} \underline{v} \equiv M\underline{v}$	Momentum	$\rho_L \frac{\pi D^2}{2} \underline{v}$	$M\underline{\underline{I}}$ since $\nabla_{\underline{v}} \underline{v} = \underline{\underline{I}}$	0
3	$\rho_L \frac{\pi D^3}{6} \left(\frac{v^2}{2} + C_{p_L} T_L\right) \equiv Me$	Energy (Kinetic + internal)	$\rho_L \frac{\pi D^2}{2} \left(\frac{v^2}{2} + C_{p_L} T_L\right)$	$M\underline{v}$ since $\nabla_{\underline{v}} \frac{v^2}{2} = \underline{v}$	$M \frac{\partial}{\partial T_L} (C_{p_L} T_{GI})$

Note: $v^2 = \underline{v}\cdot\underline{v}$; $h_L = C_{p_L} T_L$; $C_p \approx C_v$ for liquid

TABLE V. - AVERAGE QUANTITIES APPEARING IN THE EQUATIONS OF CHANGE FOR THE DROPS

(a) Densities and Fluxes

Quantity, ψ_j	Spatial density of ψ_j $\iiint \psi_j f \, dD \, d\underline{v} \, dT_L$ ψ_j/unit spatial volume	Flux of ψ_j $\iiint \psi_j \underline{v} f \, dD \, d\underline{v} \, dT_L$ ψ_j/unit area · time
Mass, M	$\iiint \rho_L \frac{\pi D^3}{6} f \, dD \, d\underline{v} \, dT_L$ $= \rho_s$	$\iiint \rho_L \frac{\pi D^3}{6} \underline{v} f \, dD \, d\underline{v} \, dT_L$ $= \rho_s \langle \underline{v} \rangle_M$
Momentum, $M\underline{v}$	$\iiint \rho_L \frac{\pi D^3}{6} \underline{v} f \, dD \, d\underline{v} \, dT_L$ $= \rho_s \langle \underline{v} \rangle_M$	$\iiint \rho_L \frac{\pi D^3}{6} \underline{v}\underline{v} f \, dD \, d\underline{v} \, dT_L$ $= \rho_s \langle \underline{v}\underline{v} \rangle_M$
Energy, Me	$\iiint \rho_L \frac{\pi D^3}{6} \left(\frac{v^2}{2} + C_{p_L} T_L \right) f \, dD \, d\underline{v} \, dT_L$ $= \rho_s \left\langle \frac{v^2}{2} + C_{p_L} T_L \right\rangle_M$	$\iiint \rho_L \frac{\pi D^3}{6} \left(\frac{v^2}{2} + C_{p_L} T_L \right) \underline{v} f \, dD \, d\underline{v} \, dT_L$ $= \rho_s \left\langle \left(\frac{v^2}{2} + C_{p_L} T_L \right) \underline{v} \right\rangle_M$

TABLE V. - C oludɐɒ AVERAGE QUANTITIES APPEARING IN THE EQUATIONS OF CHANGE FOR THE DROPS

(b) Source Terms

Quantity, ψ_j	Source terms arising from transport of ψ_j between phases ψ_j created/unit spatial volume · time		
	$\iiint \mathscr{D} f \frac{\partial \psi_j}{\partial D} \, dD \, d\underline{v} \, dT_L$ Mass transfer	$\iiint \underline{\mathscr{A}} f \cdot \nabla_{\underline{v}} \psi_j \, dD \, d\underline{v} \, dT_L$ Momentum transfer	$\iiint \mathscr{T} f \frac{\partial}{\partial T_L} \psi_j \, dD \, d\underline{v} \, dT_L$ Energy transfer
Mass, M	$\iiint \rho_L \frac{\pi D^2}{2} \mathscr{D} f \, dD \, d\underline{v} \, dT_L$ $= \omega$	----------	----------
Momentum, $M\underline{v}$	$\iiint \rho_L \frac{\pi D^2}{2} \mathscr{D} \underline{v} f \, dD \, d\underline{v} \, dT_L$ $= \omega \langle \underline{v} \rangle_M$	$\iiint \rho_L \frac{\pi D^3}{6} \underline{\mathscr{A}} f \, dD \, d\underline{v} \, dT_L$ $= \rho_s \langle \underline{\mathscr{A}} \rangle_M$	----------
Energy, Me	$\iiint \rho_L \frac{\pi D^2}{2} \mathscr{D} \left(\frac{v^2}{2} + C_{p_L} T_L \right) f \, dD \, d\underline{v} \, dT_L$ $= \omega \left\langle \frac{v^2}{2} + C_{p_L} T_L \right\rangle_M$	$\iiint \rho_L \frac{\pi D^3}{6} (\underline{\mathscr{A}} \cdot \underline{v}) f \, dD \, d\underline{v} \, dT_L$ $= \rho_s \langle \underline{\mathscr{A}} \cdot \underline{v} \rangle_M$	$\iiint \rho_L \frac{\pi D^3}{6} C_{p_L} \mathscr{T} f \, dD \, d\underline{v} \, dT_L$ $= \rho_s \langle C_{p_L} \mathscr{T} \rangle_M$

chosen to emphasize the analogy between the droplet and the gas dynamic equations of change. Bracketed quantities are weighted ensemble averages with the weighting factor indicated by the subscript. They are defined for any functions $g(\Gamma_i,t)$ and $W(\Gamma_i)$ by a generalized form of Eq. (2.3):

$$\langle g(\Gamma_i,t)\rangle_W = \frac{\int W(\Gamma_i)g(\Gamma_i,t)f(\Gamma_i,t)d\Gamma_i}{\int W(\Gamma_i)f(\Gamma_i,t)d\Gamma_i} \tag{2.7}$$

The specific weighting functions used in Table V are droplet mass, $M = \rho_L \pi D^3/6$, and rate of change of mass, $M = \rho_L \pi D^2 \dot{D}/2$. For example, the mass average velocity $\langle \underline{v} \rangle_M$ is given by:

$$\langle \underline{v} \rangle_M = \frac{\iiint M\underline{v}f \; dD \; d\underline{v} \; dT_L}{\iiint Mf \; dD \; d\underline{v} \; dT_L} = \frac{\iiint M\underline{v}f \; dD \; d\underline{v} \; dT_L}{\rho_s} \tag{2.8}$$

It is customary in spray studies to define various mean diameters (Ref. 44):

$$(D_{rs})^{r-s} = \frac{\iiint D^r f \; dD \; d\underline{v} \; dT_L}{\iiint D^s f \; dD \; d\underline{v} \; dT_L} \tag{2.9}$$

The exponents r and s are often chosen arbitrarily or by largely qualitative arguements. However, the mean quantities defined in Table V on physical grounds provide a rational choice of mean diameters depending on the term considered. For example, the powers of diameter of interest for the transport terms are influenced by the

dependence of $\mathcal{D}$, $\mathcal{A}$ and $\mathcal{T}$ on D. Also since $\underline{v}$ and T_L have been included in the theory on an equal basis with D, means in terms of D alone provide a very limited description of the spray. A generalized form of Eq. (2.9) with a weighting function W may be defined for one of the drop variables Γ_i.

$$\left(\Gamma_{i\ rs}\right)_W^{r-s} = \frac{\iiint W \Gamma_{if}^{r}\, d\Gamma_i}{\iiint W \Gamma_{if}^{s}\, d\Gamma_i} \tag{2.10}$$

For s = 0, Eq. (2.10) reduces to a special case of Eq. (2.7). In general the weighted ensemble average given by Eq. (2.7) provides a set of mean quantities having more direct physical interpretation.

The source term appearing on the right of Eq. (2.6) cannot be treated in more detail without specifying a process such as collisions or shattering. If droplet collisions are considered and the ψ_j chosen are summational invariants of an encounter, the source integral is equal to zero (Ref. 41). Summational invariants are droplet properties which are conserved in a collision; i.e., the sum of the ψ_j for drops before the encounter equals the sum of the ψ_j for the droplets existing after the encounter. The droplet mass, momentum, and energy as defined in Table IV are conserved in a collision only if vaporization, drag and internal dissipation in the liquid are negligible during the collision and surface energy, $\pi D^2\sigma$, is fncluded along with the kinetic and internal

forms. The source term involving $\mathcal{L}$ will not be included in the discussion which follows. This means that the equations presented are valid for $\mathcal{L} = 0$ or when ψ_j are summational invariants for the process considered.

The resulting equations of change for the droplets are:

continuity

$$\frac{\partial \rho_s}{\partial t} + \nabla_{\underline{x}} \cdot \rho_s \langle \underline{v} \rangle_M = \omega \tag{2.11}$$

momentum

$$\frac{\partial}{\partial t} \rho_s \langle \underline{v} \rangle_M + \nabla_{\underline{x}} \cdot \rho_s \langle \underline{v}\, \underline{v} \rangle_M = \omega \langle \underline{v} \rangle_{\dot{M}} + \rho_s \langle \underline{\mathcal{A}} \rangle_M \tag{2.12}$$

energy

$$\frac{\partial}{\partial t} \rho_s \left\langle \frac{v^2}{2} + C_{pL} T_L \right\rangle_M + \nabla_{\underline{x}} \cdot \rho_s \left\langle \left(\frac{v^2}{2} + C_{pL} T_L \right) \underline{v} \right\rangle_M$$

$$= \omega \left\langle \frac{v^2}{2} + C_{pL} T_L \right\rangle_{\dot{M}} + \rho_s \langle \underline{\mathcal{A}} \cdot \underline{v} \rangle_M + \rho_s \langle C_{pL} \mathcal{T} \rangle_M \tag{2.13}*$$

Corresponding equations of change for the gas phase are:

continuity

$$\frac{\partial \rho_f}{\partial t} + \nabla_{\underline{x}} \cdot \rho_f \underline{u} = -\omega \tag{2.14}$$

momentum

$$\frac{\partial}{\partial t} (\rho_f \underline{u}) + \nabla_{\underline{x}} \cdot (\rho_f \underline{u}\, \underline{u} + \underline{\underline{\pi}}_f) = -\omega \langle \underline{v} \rangle_{\dot{M}} - \rho_s \langle \underline{\mathcal{A}} \rangle_M \tag{2.15}$$

---

*See Appendix C.l for an alternate form of the terms $\omega \left\langle \frac{v^2}{2} + C_{pL} T_L \right\rangle_{\dot{M}}$ and $\rho_s \langle C_p \mathcal{T} \rangle_M$.

energy

$$\frac{\partial}{\partial t}\rho_f\left(\frac{u^2}{2}+\mathcal{U}\right)+\nabla_{\underline{x}}\cdot\left[\rho_f\underline{u}\left(\frac{u^2}{2}+\mathcal{U}\right)-\underline{q}-\underline{\underline{\pi}}_f\cdot\underline{u}\right]$$

$$=-\omega\left\langle\frac{v^2}{2}+C_{pL}T_L\right\rangle_{\dot{M}}-\rho_s\langle\underline{\mathcal{A}}\cdot\underline{v}\rangle_M-\rho_s\langle C_{pL}\mathcal{T}\rangle_M \qquad (2.16)$$

where:

ρ_f = density of the gas-vapor mixture, mass of gas per unit spatial volume (gas + Liquid). This is distinguished from ρ_g which is the mass of gas per unit volume occupied by gas.

$$\rho_f=\rho_g\left(1-\frac{\rho_s}{\rho_L}\right)=\rho_g(1-\nu) \qquad (2.17)$$

As the spray becomes more dilute: $\nu \to 0$ and

$\rho_f \to \rho_g$

$\mathcal{U}$ = internal energy of the gas per unit mass

$\underline{q}$ = heat flux vector for heat transfer other than that going to the drops

$\underline{\underline{\tau}}$ = shear stress tensor

$\underline{\underline{I}}$ = unit tensor

$\underline{\underline{\pi}}_f = p\underline{\underline{I}} + \underline{\underline{\tau}}$, the pressure tensor for the gas phase

Drop-gas interaction terms appear on the right sides of the equations with the difference in sign between the two sets reflecting the fact that a quantity lost by one phase represents a gain in the other phase. If corresponding equations for liquid and gas are summed, interaction terms cancel and the following equations result for the two-phase mixture.

continuity

$$\frac{\partial}{\partial t}(\rho_s + \rho_f) + \nabla_{\underline{x}} \cdot (\rho_s \langle \underline{v} \rangle_M + \rho_f \underline{u}) = 0 \qquad (2.18)$$

momentum

$$\frac{\partial}{\partial t}(\rho_s \langle \underline{v} \rangle_M + \rho_f \underline{u}) + \nabla_{\underline{x}} \cdot (\rho_s \langle \underline{v}\,\underline{v} \rangle_M + \rho_f \underline{u}\,\underline{u} + \underline{\underline{\pi}}_f) = 0 \qquad (2.19)$$

energy

$$\frac{\partial}{\partial t}\left[\rho_s \left\langle \frac{v^2}{2} + C_{pL} T_L \right\rangle_M + \rho_f \left(\frac{u^2}{2} + \mathcal{U}\right)\right]$$

$$= -\nabla_{\underline{x}} \cdot \left[\rho_s \left\langle \left(\frac{v^2}{2} + C_{pL} T_L\right) \underline{v} \right\rangle_M + \rho_f \left(\frac{u^2}{2} + \mathcal{U}\right) \underline{u} - \underline{q} - \underline{\underline{\pi}}_f \cdot \underline{u}\right] \qquad (2.20)$$

Analogous notation for the liquid and gas phase quantities was not used in the above equations. Rather, a conventional continuum mechanics notation was used for the gas to emphasize the standard form of the gas dynamic terms. For example, the gas velocity $\underline{u}$ is by definition a mass average velocity which is the gas phase counterpart of $\langle \underline{v} \rangle_M$. It is obtained in molecular statistical mechanics by an operation analogous to Eq. (2.7) for sprays. The terms involving $\mathcal{U}$, $\underline{\underline{\pi}}_f$, and $\underline{q}$ represent deviations from the mass average behavior (see Appendix C.2)

Substantial forms of the spray equations may be obtained by using the continuity Eq. (2.11) and the definition of the derivative following the mass average motion:

$$\frac{D}{Dt} \equiv \frac{\partial}{\partial t} + \langle \underline{v} \rangle_M \cdot \nabla_{\underline{x}}$$

The substantial forms of Eqs. (2.8) to (2.10) are:

$$\frac{D}{Dt}\rho_s = -\rho_s(\nabla_{\underline{x}} \cdot \langle \underline{v} \rangle_M) + \omega \tag{2.11a}$$

$$\rho_s \frac{D}{Dt}\langle \underline{v} \rangle_M = -\nabla_{\underline{x}} \cdot \rho_s(\langle \underline{v}\,\underline{v} \rangle_M - \langle \underline{v} \rangle_M \langle \underline{v} \rangle_M) + \omega(\langle \underline{v} \rangle_{\dot{M}} - \langle \underline{v} \rangle_M) + \rho_s \langle \underline{A} \rangle_M \tag{2.12a}$$

$$\rho_s \frac{D}{Dt}\left\langle \frac{v^2}{2} + C_{pL}T_L \right\rangle_M = -\nabla_{\underline{x}} \cdot \rho_s \left[\left\langle \left(\frac{v^2}{2} + C_{pL}T_L \right) \underline{v} \right\rangle_M - \langle \underline{v} \rangle_M \left\langle \frac{v^2}{2} + C_{pL}T_L \right\rangle_M \right] + \omega \left[\left\langle \frac{v^2}{2} + C_{pL}T_L \right\rangle_{\dot{M}} - \left\langle \frac{v^2}{2} + C_{pL}T_L \right\rangle_M \right] + \rho_s \langle \underline{v} \cdot \underline{A} \rangle_M \tag{2.13a}$$

The terms on the right hand sides represent deviations from the mass average motion. For example, a tensor $\underline{\underline{\pi}}_s$ for the spray may be defined in analogy with $\underline{\underline{\pi}}_f$ for the gas as:

$$\underline{\underline{\pi}}_s \equiv \rho_s(\langle \underline{v}\,\underline{v} \rangle_M - \langle \underline{v} \rangle_M \langle \underline{v} \rangle_M) \tag{2.21}$$

From a statistical point of view, $\underline{\underline{\pi}}_s$ is a mass weighted variance-covariance matrix in terms of the drop velocity components. Note that vaporization term such as:

$$\underline{\Omega} \equiv \omega(\langle \underline{v} \rangle_{\dot{M}} - \langle \underline{v} \rangle_M) \tag{2.22}$$

depend on the difference between the averages obtained by weighting with the rate of change of droplet mass and the mass, respectively.

Despite the formal similarities between the equations and methods of droplet and molecular statistical mechanics, several basic physical differences exist. Some of

these are summarized in Table **VI.** The lack of absolute reference conditions describing a spray equilibrium state deprives the spray formulation of the degree of generality possessed by the molecular model.

The spray equations may be manipulated into many other forms analgous to gas dynamic counterparts such as overall "macroscopic" balances (Ref. 45). Equations of change for other quantities such as droplet 'numbers may be obtained from the transport Eq. (2.5) by using alternate weighting function8 ψ_j and intergrating over other combinations of the variables D, $\underline{v}$, and T_L. The utility of all this manipulation hinges on the association of the various terms with measurable quantities.

D. Relationship of the Statistical Model to Practical Situations

The key quantity in the statistical model just presented is obviously the density function f. Given f, all the average densities and fluxes of liquid mass, momentum, and energy may be calculated. With the added information of the state of the gas and expressions for the transport rates $\mathscr{D}$, $\underline{\mathscr{A}}$, and $\mathscr{T}$, all the gas-liquid interaction terms may be evaluated. This is simply a way of saying that a consistent and comprehensive theory has been formulated based on f. Some approaches to the application of the theory and its relationship to existing spray measurements will **now** be considered.

TABLE VI. - COMPARISON OF PHYSICAL FEATURES OF SPRAY AND MOLECULAR SYSTEMS

Characteristic	Spray	Gas molecules
Composition	Inherently an open system with a continuous range of sizes ("kinds" of droplets) in varying concentrations due to phase changes, sources, and fluxes at the boundaries.	Closed system often considered with the number of particles fixed absolutely by Avogadro's number. For an open system a discrete number of species are considered.
Equilibrium state	Nonequilibrium case with mass, momentum, and energy transport is most common. Limiting form of f for a particular case is determined by gas flow conditions and thus no universal "equation of state" has been found.	Equilibrium is often closely approached (at least locally) with the form of f given by the Boltzmann distribution. Thus, an equation of state exists and approaches ideal gas behavior in many cases.
Dynamics of particles	Drop-gas interactions are strong with collision dynamics often of secondary importance. The forces (e.g., drag) are velocity dependent.	Collision dynamics are dominant. Forces are velocity independent; and thus, are derived from a potential.
Observable quantities	Instantaneous dynamic state is observable; for example, individual drops can be photographed and their position, size, and velocity obtained at a time t.	Direct instantaneous measurement of the dynamic state is not possible. In practice the molecules are too numerous and too small, and an uncertainty principle exists. Thermodynamic properties are averages over <u>times</u> which are long compared to changes in dynamic state.

The most thorough scheme of application to the propagation problem is as follows. Given the density function $f(D, \underline{v}, \underline{x}_o, T_L, t)$ and the state of the gas ($p_o, \rho_{fo}, T_{go}, \underline{u}_o$ and composition) at the surface of formation $\underline{x} = \underline{x}_o$; compute $f(D, \underline{v}, \underline{x}, T_L, t)$ at all downstream positions using the spray transport Eq. (2.5) and the gas dynamic equations of change (Eqs. (2.14) to (2.16)) which include the droplet-gas interaction terms. Known injection parameters are built into f_o to fix the normalization constant. For example:

$$\dot{w}(t) = \iiiint \rho_L \frac{\pi D^3}{6} \underline{v} f_o \, dD \, d\underline{v} \, dT_L \, ds_f \qquad (2.23)$$

where

$\dot{w}(t)$ = mass flow rake of liquid at any time t

ds_f = indicates an integral over the surface of formation

The construction of a solution to the four, coupled partial differential equations is very difficult in practice and requires simplifications such as one-dimensionality to arrive at manageable forms to which iterative techniques may be applied.

Aside from mathematical difficulties, the chief impediment to applications is the lack of information about f_o. No theory of formation is available to predict f_o from a knowledge of injection parameters. Measured and correlated data are generally limited to two special

density functions which are explicitly functions of D and $\underline{x}$. The first type, usually called a "volume" or "spatial drop size distribution"* is given in terms of f as:

$$f_S(D,\underline{x},t) = \iint f(D,\underline{x},\underline{v},T_L,t)d\underline{v}\ dT_L \qquad (2.24)$$

The second type, called a "temporal" or "flux distribution" is given by:

$$\underline{f}_F(D,\underline{x},t) = \iint \underline{v}f(D,\underline{x},\underline{v},T_L,t)d\underline{v}\ dT_L \qquad (2.25)$$

For a stationary process f is independent of time and, consequently, so are f_S and $\underline{f}_F$. Table VII compares the ways in which f_S and $\underline{f}_F$ are obtained experimentally and their physical interpretations. Note that the collection method described for measuring $\underline{f}_F$ is limited to steady sprays **while** Eq. (2.25) defines $\underline{f}_F$ in the unsteady case as well.

Even when the cases considered are limited to stationary random processes (steady sprays), questions remain as to the equivalence of $\underline{f}_F$ measured as a direct, experimental average over time and $\underline{f}_F$ found by integrating over the ensemble (Eq. (2.25)). A stationary random process for which time averages are equal to ensemble averages

---

*"Density" is a more precise term to use with "distribution" reserved for the cummulative form of f. However, the common practice is to use distribution for both cases.

TABLE VII. - METHODS OF MEASUREMENT AND PHYSICAL SIGNIFICANCE OF SIZE DISTRIBUTIONS f_S AND f_F

	Spatial distribution f_S	Flux distribution f_F*
Units	$\frac{\text{Number of drops}}{\text{Unit spatial volume} \cdot \text{unit size}}$ at a time t	$\frac{\text{Number of drops}}{\text{Unit area} \cdot \text{unit time}}$ averaged over a time t_A
Schematic experimental configuration	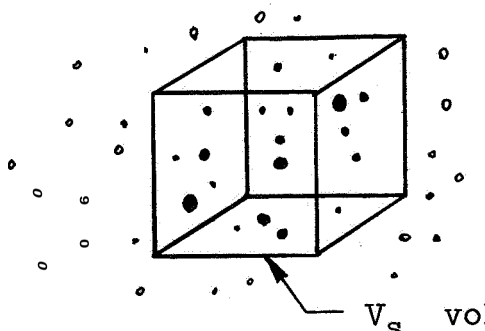	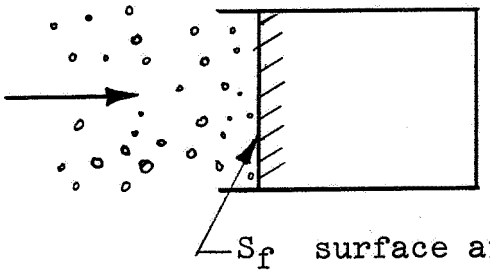
Estimated from categorized size measurements on:	A collection of instantaneous photographs of drops in a known spatial volume V_s	Drops collected as they cross a surface S_F of known area over a period of time t_A.
Estimates improve as:	Number of pictures becomes large; category size ΔD and V_s become small. (See Eq. (2.2))	Averaging time t_A becomes long; ΔD and S_F become small

*Only the steady-state case is described

is termed ergodic. Due to the extreme theoretical difficulties involved in trying to establish necessary conditions for a process to be ergodic (Ref. 46), the condition is usually assumed in practice. The validity of the assumption may then be tested directly if enough accurate data are available or indirectly in a gross sense by the predictive success of the theory. Since direct measurements may be made on a spray to estimate the ensemble density function, the ergodic problem is less acute for sprays than for the molecular case, where the theory is developed entirely in terms of the ensemble but observable quantities are necessarily time averages.

Both f_S and f_F are marginal densities in the sense that $\underline{v}$ and T_L dependence are integrated out mathematically and disregarded experimentally. Thus additional information about $\underline{v}$ and T_L must be provided or assumed in order to calculate transport processes occurring between the gas and liquid. A common practice is to take the initial values of $\underline{v}$ and T_L to be single-valued and equal to the values at the injector: $\underline{v}_E$ and T_{LE} (Ref. 5). The expression for f_o then takes the form:

$$f_o = f_{So}(D,\underline{x}_o,t)\delta(v - v_E)\delta(T_L - T_{LE}) \qquad (2.26)$$

where the delta functions are defined for any variable y as:

$$\delta(y - y_o) = \infty \qquad \text{if } y = y_o$$
$$= 0 \qquad \text{otherwise}$$

$$\text{and} \qquad \int_{-\infty}^{\infty} \delta(y - y_o)dy = 1$$

Physically this means that the actual formation region is ignored as though the spray formed instantaneously at the injector face, and that a drop of given size has unique values of $\underline{v}$ and T_L at any downstream position. Available data for $\underline{f}_F$ and f_S are often ambiguous as to the position dependence, seldom were taken at locations approximating the surface of formation, and are often used interchangeably as though they were equivalent.

The average (expected value) of any function $g(\Gamma_i')$ for a given value of the spray variable Γ_j is defined for $i \neq j$ as:

$$\langle g(\Gamma_i') \,|\, \Gamma_j \rangle = \frac{\int g(\Gamma_i') f(\Gamma_i, t) d\Gamma_i}{\int f(\Gamma_i, t) d\Gamma_i} \qquad (2.27)$$

A particular case of interest is the expected value of velocity at a given size as a function of D and $\underline{x}$ given by:

$$\langle \underline{v} | D \rangle = \frac{\iint \underline{v} f(D, \underline{v}, \underline{x}, T_L, t) d\underline{v}\, dT_L}{\iint f(D, \underline{v}, \underline{x}, T_L, t) d\underline{v}\, dT_L} = \frac{\underline{f}_F}{f_S} \qquad (2.28)^*$$

It has been estimated experimentally by averaging measured

---

* In statistical terminology, this is the regression curve of $\underline{v}$ on D.

velocities of particular sized drops (Refs. 10, 11, and 12), but was not interpreted as being derived from a density function f which contained $\underline{v}$ as a randomly distributed variable. The amount of scatter in the data is probably an indication of statistical fluctuations in the small samples in addition to normal measurement errors. From Eq. (2.28) it is seen that for a stationary ergodic process, $\langle \underline{v} | D \rangle$ is given by the ratio of the distributions as measured by the methods in Table VII.

An alternate approach to the propagation problem is to use the equations of change for average spray variables, Eqs. (2.11) to (2.13), instead of the spray transport Eq. (2.5). The aim is to avoid having to specify and handle all the detailed information associated with f while still providing a useful quantitative description. Initial values of variables such as ρ_s, $\langle \underline{v} \rangle_M$ and $\langle T_L \rangle_M$ along with some drop size information (analgous to specification of gas phase composition) must be specified as initial conditions at the surface of formation.

The success of this approach depends to a large extent on the ability to predict or measure the average spray variables directly without reference to statistical distribution functions. Overall average flow is given by injection rate $\dot{w}$; and local values of mass flux, $\rho_s \langle \underline{v} \rangle_M$, may be obtained by collection tubes (Ref. 47). But other quantities such as ρ_s and $\left\langle \frac{\underline{v}^2}{2} \right\rangle_M$ are difficult to

measure without resorting to detailed photographic measurements on individual drops. When working with average quantities, terms due to deviations from average behavior are often ignored. Ror example, terms due to deviations from $\langle \underline{v} \rangle_M$ are ruled out by assuming $\langle \underline{v}\ \underline{v} \rangle_M = \langle \underline{v} \rangle_M \langle \underline{v} \rangle_M$ and $\left\langle \frac{v^2}{2}\ \underline{v} \right\rangle_M = \langle \underline{v} \rangle_M \left\langle \frac{v^2}{2} \right\rangle_M$ analogous to inviscid and adiabatic assumptions in gas flow. The drop-gas interaction terms such as ω, $\langle \underline{\mathcal{A}} \rangle_M$ and $\langle C_D \mathcal{A} \rangle_M$ are particularly troublesome since the appropriate mean drop size to be used for each depends on the variation of $\mathcal{D}$, $\mathcal{A}$, and $\mathcal{N}$ with D. Existing experimental methods for directly measuring mean sizes are limited in number and uncertain as to the exact diameter weighting (Ref. 48).

In view of limited information available on f or f_o and the key role they play in spray description, the remainder of this paper will deal with experimental measurements of size-velocity density functions as a function position in a spray.

Chapter III

EXPERIMENTAL MEASUREMENT OF THE SPRAY DENSITY FUNCTION

Although a statistical mechanical theory of a spray based on the density function may be precisely formulated, the application and verification of the theory requires the experimental measurement of specific values of f, and such measurements involve uncertainties. Two different types of uncertainties arise. The first type, common to all experiments, results from the practical limits of measurement resolution and accuracy; e.g., the spatial and time resolution limits mentioned in Chapter I in connection with photographic observations. The second type arises from the random nature of the physical processes considered and the resulting statistical character of the quantities of interest. Even if individual droplet properties such as size or velocity are measured with gegligible error, the spray density function f may only be estimated since f is defined

by a limit over all possible samples as the range of the variables considered becomes vanishingly small (Eq. (2.2)).

Formulation of the theory is exact because complete information about the spray is assumed in the definition of f. Application of the theory is approximate because experimental information about a spray is always incomplete. The quantitative value of the theory lies in the possibility of predicting the manner in which a spray progagates given a local value of f which has been estimated within an acceptable band of uncertainty by a limited number of measurements.

As the amount of information contained in f is increased by increasing the number of droplet variables considered as arguments, the number of measurements required to estimate f increases for a given level of uncertainty. Nine variables were considered in Chapter II: size, three components each of position and velocity, temperature and time. For experimental purposes, this number had to be reduced to two or three if meaningful estimations were to be made with available resources. The emphasis was on the treatment of droplet velocity on an equal statistical basis with drop size.

To begin, the scope of the measurements is discussed in terms of the form of f measured, the overall features of the spray system considered, and the sampling scheme employed. Next, the double-exposure fluorescent technique which was used is described. Finally, the specific data acquisition and reduction methods employed are given.

A. The Scope of the Measurements

The particular form of the density function measured was restricted to the variables D, $\underline{v}$, and $\underline{x}$. Droplet temperature was not measured, i.e., the observations "integrated" over T_L. Injection parameters were held constant so that a steady-state spray condition (stationary random process) could be assumed. In terms of the general f, the measured density f_B is:

$$f_B(D,\underline{v},\underline{x}') = \int f(D,\underline{v},\underline{x}',T_L,t)dT_L \qquad (3.1)$$

where $\underline{x}'$ indicates that the functions are evaluated at a particular position in the spray, $\underline{x} = \underline{x}'$. Symmetry was assumed about the spray axis, and only two components of position and velocity were considered - in cylindrical coordinates: r, z, v_r, and v_z. Any v_θ was normal to the film plane and could not be measured.

An unconfined spray was formed by a swirl atomizer injecting into room temperature air at atmospheric pressure. Ethyl alcohol was the fluid used, and the only parameter varied during the course of the investigation was injection pressure. The objective was to measure local values of f_B over a cross section at different downstream distances, the first of which was located near the surface of formation.

The method of estimating f_B was to choose a small sample volume located about a position $\underline{x}'$ in the spray, and measure the sizes and velocities of all droplets in the volume at several instants in time. Since the spray process was assumed to be stationary, the particular sampling times chosen were arbitrary.* The collection of samples formed a portion of the ensemble from which the density f_B was estimated.

Implementation of this method required a sampling technique which had high spatial resolution but did not disturb the spray. The ease of data reduction was also an important consideration since the uncertainty of the estimation was reduced as the number of samples was increased. However, a competing criterion was that the droplet properties be measured as directly as possible so

*If the spray was actually unsteady due, for example, to a resonant oscillation in the formation process; the collection of samples taken at random intervals in time would constitute a time average over the ensemble.

that measurement uncertainties were not further compounded by an involved data reduction analysis to obtain **D** and $\underline{v}$. As a compromise; double-exposure fluorescent photography was used to measure sizes and velocities. This technique had the advantages of leaving the spray undisturbed while providing direct, local values of droplet variables; but the thousands of film measurements required made the data reduction process very lengthy and tedious.

B. The Double-Exposure Fluorescent Technique

The fluorescent technique of photographing droplets in a spray was originally developed (Refs. 49 and 50) and applied (Ref. 19) as a single exposure method for measuring the sizes of the drops in a small spatial volume at any instant. From a collection of such photographic samples, local values of the spatial drop size distribution f_S were obtained (Fig. 5 is a sample of the correlated results). In the present study a precisely controlled double-exposure capability was added to provide a measure of drop velocity as well as size so that f_B could be estimated.

The key feature of the technique is the addition of a fluorescent dye* to the liquid being sprayed. Upon

*The dye concentration is small, typically 0.5% by weight, so that the change in liquid properties is negligible (Ref. 50).

excitation by an intense source, the dye absorbs in ope wavelength band and emits in another making each drop a radiator which exposes the film. The light source is not directed into the camera. Rather, a shaped beam perpendicular to the camera axis is used to selectively light the region of the spray under study. Only drops within the camers's depth of field* are lighted and caused to fluoresce. The portion of the lighted region viewed by the camera constitutes the sampling volume.

Fluorescent photography has a definite advantage over: back-lighting methods when multiple exposures are used. Each droplet image consists of an exposed spot on an unexposed background, and each exposure is recorded independently of the others. This is not the case in back-lighting methods where all film areas are exposed except those corresponding to the current position of the drops. Thus, the second and any succeeding flashes light previously unexposed areas and attempt to record images in previously exposed areas. The result is a reduction in image definition due to reduced contrast.

A pictorial view of the experimental arrangement which was used is given in Fig. 12. The axes of the spray, camera, and lighting system were mutually perpendicular. Liquid containing the fluorescent dye was

*"Depth of field" as used here, is defined as the distance along the camera axis over which the smallest droplets considered (10μ) are sharply focused at the film plane.

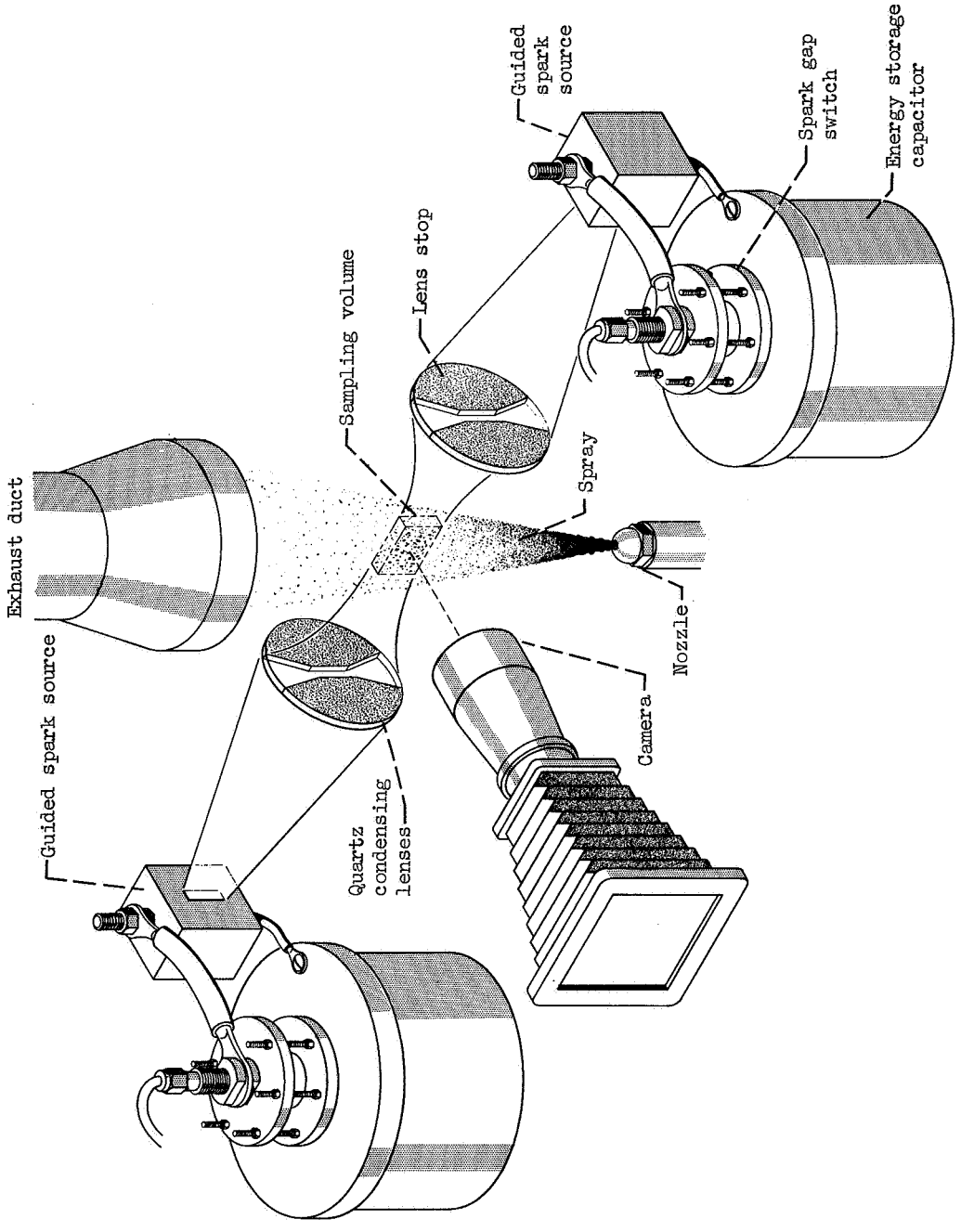

Fig. 12. - Experimental arrangement for double-exposure fluorescent photography.

injected vertically from a swirl atomizer, passed through the region where sampling occurred, and was collected and removed from the room by an exhaust system. Identical lighting systems consisting of constricted spark gaps and quartz condensing lenses having specially shaped aperture stops were located on either side of the camera axis. When either gap was fired the condenser lenses focused and shaped the beam to light the same volume in the spray. The firing sequence of the two sources was controlled to produce two flashes separated by a known time interval. Each drop within the sampling volume viewed by the camera successively fluoresced and was recorded on the film. The position of the camera and lighting system was fixed *to* maintain alignment, and the nozzle was positioned so that the spray could be sampled at various axial and radial locations.

Table VIII summarizes the specifications and operating conditions for the various elements of the sampling system. The performance requirements of the individual components were strongly interrelated by considerations of light economics - getting enough fluorescent radiation *to* the film *to* record distinct, measurable images. Details regarding the development of the lighting and camera systems, the fluorescent dye characteristics, and the alignment and focusing procedures are available elsewhere (Refs. 19, 49). The discussion of the hardware which follows emphasizes the double-exposure capability

TABLE VIII. - SAMPLING SYSTEM SPECIFICATIONS AND OPERATING CONDITIONS

Light Sources: Guided Air Sparks
- Maximum energy - 80 joules; 0.1 μf charged to 40 KV
- Flash duration (half peak) - 1.5 - 2.0 μs
- Delay between flashes - continuously variable; nominal values used 9.5 - 74 μs

Sampling Volume: Thin Slab Parallel to the Spray Axis
- Size - 0.160 × 0.160 × 0.008 inches
- Formed by - two 6-inch, f/1.2 plano-parabolic, fused-quartz condensing lenses

Fluorescent Dye: Uranin (Fluorescein)
- Concentration - 5 grams/liter in 95% Ethyl Alcohol
- Spectral characteristics - absorption peaks at 2500 and 4900 Å; emission peak at 5300 Å.

Camera: Two Lens Relay System
- Objective lens - f/3.5, 6 in. Wollensak Raptar operated at f/5.6
- Reimaging lens - f/2.0, 58mm Zeiss Biotar
- Overall magnification - 25
- Size resolution - 10μ ± 10% (static calibration, ref. 49)
- Working distance - 6 inches
- Depth of field for 10μ objects - ≈220μ

Film: Kodak Royal - X Pan, 4×5 sheets, ASA 1200
- Development - 12 minutes in DK-60a continuous agitation followed by Monckhoven's intensifier

since this was the major extension of the fluorescent technique which was accomplished in this investigation.

The dimensions of the sampling volume which was intensely lighted were fixed at 0.160 x 0.160 in. (the camera's field of view) x 0.008 in. thick (slightly less than the camera's depth of field). A thin, vertical "sheet" of light having these dimensions had to be formed; and the appropriate source geometry was a line. Since available flash tubes, having suitable dimensions, were unable to withstand repeated discharges at energy loadings of at least 10 joules, the less efficient, but more rugged guided air spark was used (Ref. 19).

The construction details of this source are shown in Fig. 13. The discharge occurred in a 0.032 x 0.125 x 0.750 in. slot milled in a teflon block. In addition to guiding the discharge to assure a repeatable path, the slot constricted the spark channel to incregse the current flux and thus the intensity. As the teflon gradually eroded, the intensity decreased and the block had to be replaced after 200 to 300 flashes. Micalex slits in front of the teflon block provided a dimensionally stable line source 0.032 in. wide and 0.650 in. long which was uneffected by the enlargement of the slot. The slits were relieved from the surface of the teflon and were supported by a cover plate so that they would withstand the shock wave produced by the discharge.

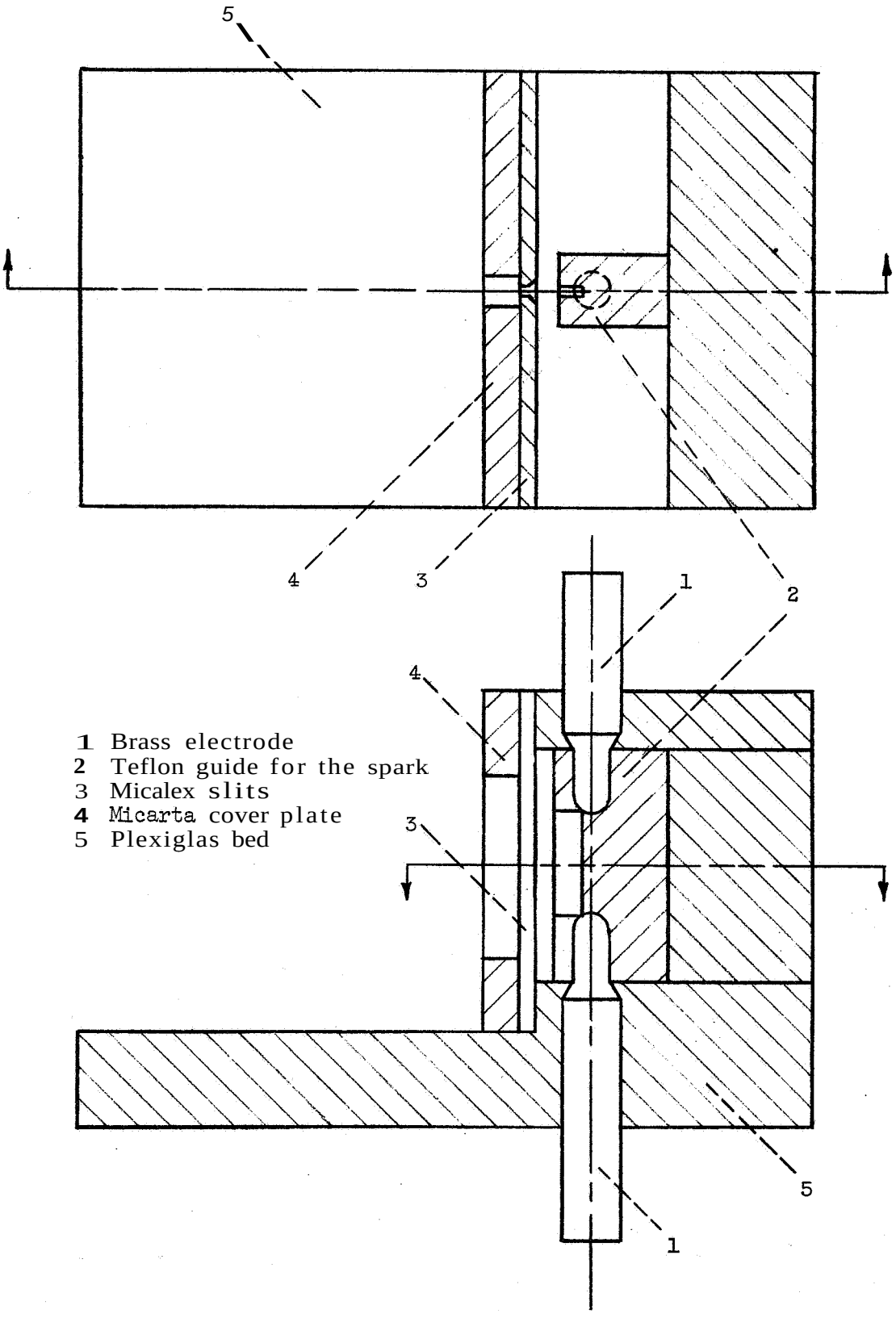

Fig. 13. - Guided **spark source.**

The formation of a constant width light sheet having sharply defined intensity cutoff at the edges can only be approximately accomplished in practice when an incoherent source and conventional lenses are used. Sheet definition can be improved only at the cost of intensity reduction. Two plano-parabolic, fused-quartz* condensing lenses were used to form an image of the source in the spray with a **4X** reduction in size. The plane surfaces were adjacent to increase axial spherical aberration, and a specially shaped aperture stop (Ref. 19) was inserted between the lenses to block portions which would otherwise focus extraneous radiation at the edge of the sheet. In this way, a sheet was produced which had an approximately constant thickness of 0.008 in. over the required distance of 0.160 in.**

Two time intervals were considered in the temporal control of the lighting sequence. They are the duration of a single flash, t_D, and the interval between successive flashes, t_I. Ideal criteria for choosing time intervals are summarized in Fig. 14. Droplet displacements, Ax,

*Ultraviolet transmission was required since the dye absorbed in that spectral region.

**See Appendix D for a discussion of the possibility of using a laser light source to overcome the difficulties associated with the light sheet formation.

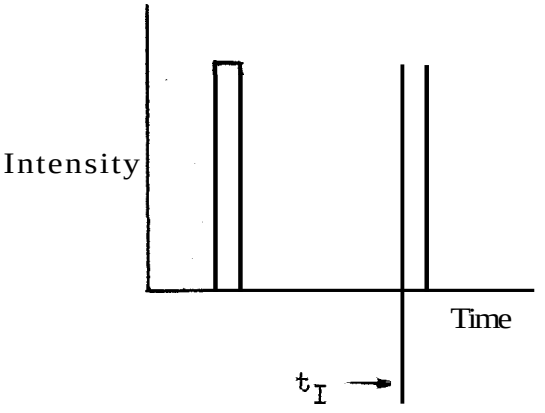

Lighting Sequence

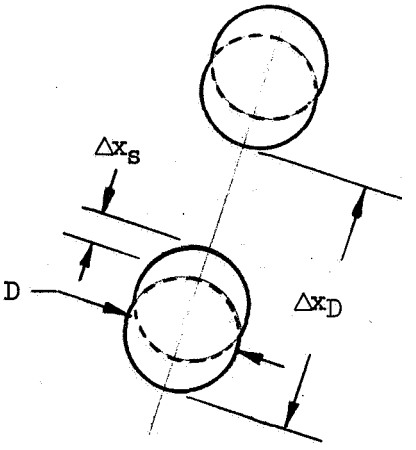

Image Structure

Time interval	Chosen such that	Limiting value determined by:
Flash duration t_D	$\Delta x_s/D < 0.1$ drop moves less than 0.1 of its diameter during exposure	Smallest drops with highest velocities
Flash interval t_I	$\Delta x_D/D > 1$ successive images of the same drop do not overlap	Largest drops with lowest velocities

Fig. 14. - Ideal Timing Criteria for Double Exposure Photography.

are referenced to drop size. Exposure time should be short enough to make motion blur negligible and flash interval long enough to separate the two images. Figure 15 gives numerical values of relative displacement rates as a function of size and velocity. For the range of sizes and liquid sheet velocities considered in the experiments, the ideal criteria indicate that a flash duration of less than 0.1 μs and a minimum interval of approximately 10μs are desirable.

Flash tubes and spark gaps with energy Inputs of 10 to 100 joules per pulse have minimum durations of the order of 1μs. Rather than being rectangular in shape, the intensity pulses have a rapid rise followed by a much slower exponential decay as shown in Fig. 16(a). The resulting appearance of the images of drops which move an appreciable fraction of their diameter during exposure is shown in Fig. 16(b). In this situation droplet shape is not observable. A spherical shape must be assumed and the width of the streak taken as a measure of the size. Since the intensity rise is rapid, one edge of each image is sharp; and displacement can be measured. The problem of motion blur in this case is that the available fluorescent intensity is distributed over the area of the streak with an attendant decrease in image density. Feasibility tests in which a laser was used to light the drops are described in Appendix D. The results indicated

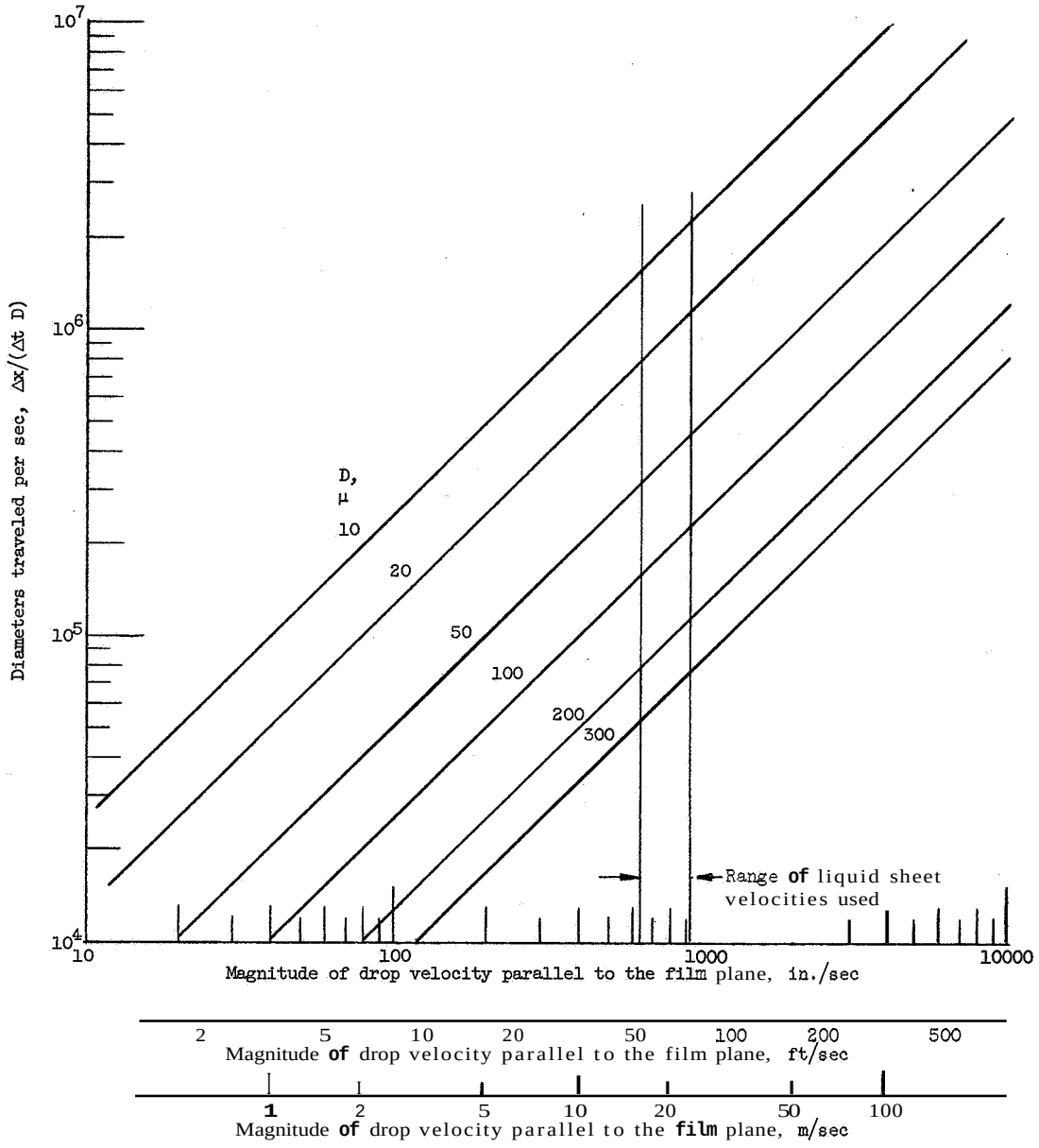

Fig. 15. - Relative Displacement Rates as a Function **of** Drop Size and Velocity.

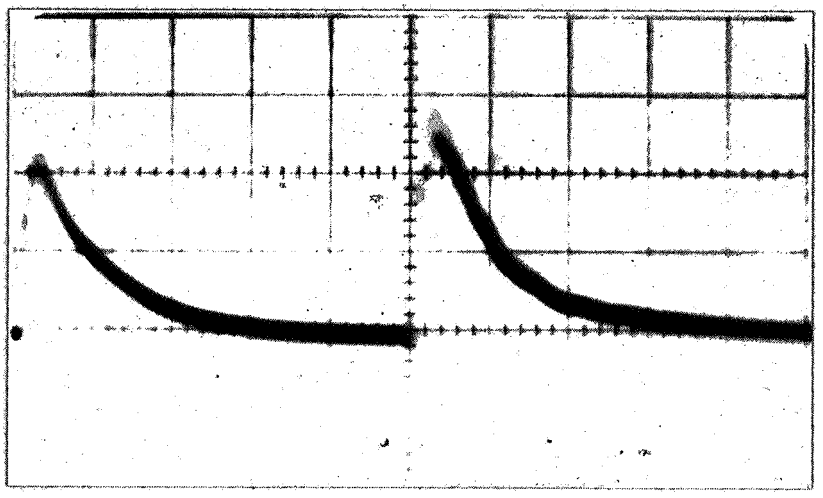

(a) Typical Intensity-Time Trace. 2μs/division

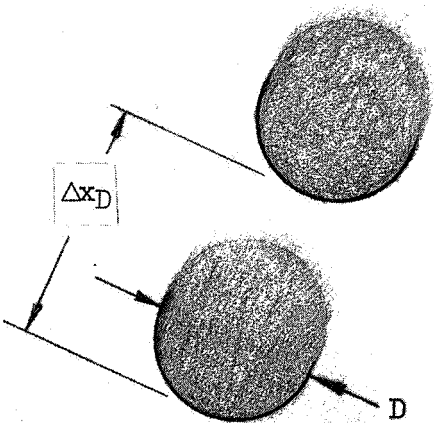

(b) Image Characteristic for Small, Fast Drops.

Fig. 16. - Actual Source **and** Image Characteristics.

that the use of such a source would greatly extend the range of drop velocities that could be successfully photographed.

Since the alignment and focusing af the camera to superimpose the depth of field on the lighted volume was a delicate and critical operation, it would have been desirable to use one source to produce both flashes. A development effort to accomplish this was unsuccessful due to the magnitude of the pulse energies involved and the requirement of a 10μs interval (see Appendix E). Thus, two identical lighting systems were used to independently produce the two pulses.

A block diagram of the apparatus for controlling and monitoring the interval between flashes is shown in Fig. 17. The firing sequence was initiated by manually activating trigger generator I to fire source I whose output was monitored by a vacuum phototube. The output from the phototube triggered the sweep of the oscilloscope which had an internal delay circuit. At the end of a preset delay period measured from the initiation of the sweep an output pulse was generated. The delayed pulse was amplified and applied to trigger generator II to fire source II whose output was also monitored by the phototube. The delay period was continuously adjustable, and the flash interval was measured from the intensity-time trace (see Fig. 16(a)). At a given delay setting the flash interval was constant to within $\pm$0.2 μs.

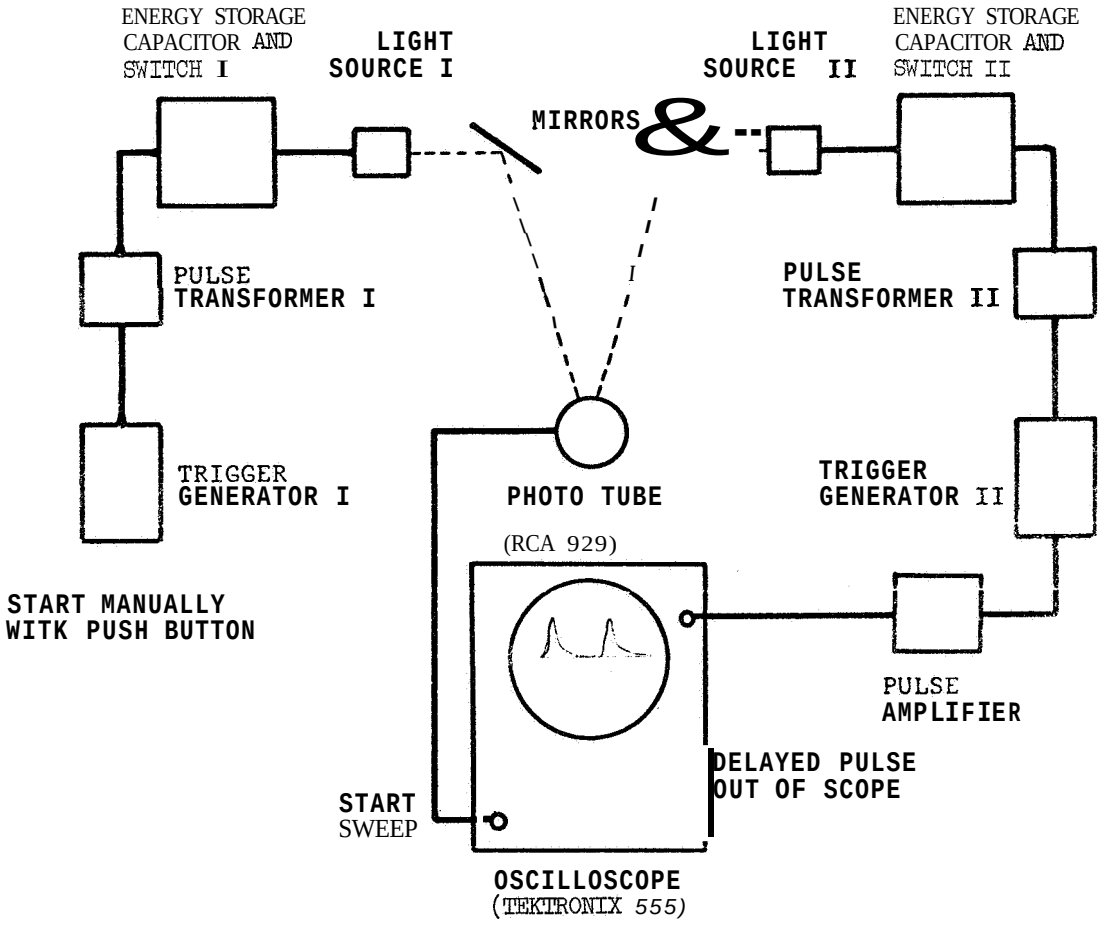

Figure 17. - Block diagram of the light source control and monitoring apparatus.

The specific events which occurred during the firing of either source may be followed by referring to the circuit diagram in Fig. 18. By either applying a +20 volt input pulse or manually closing the switch S_2, the thyration was fired to discharge the capacitor C_3 through the primary of the pulse transformer. A positive 15 kV was generated at the secondary and applied to the trigger electrode of the spark gap switch. The low inductance, coaxial capacitor C_1 was charged to -40 kV. When S_1 fired, the source gap G_1 was overvolted and broke down dumping the energy stored in C_1. In order to minimize the discharge duration, the circuit inductance was kept small by using short lead lengths and the coaxial capacitor design,

A cross sectional view of the spark gap switch which was mounted directly on the capacitor structure is shown in Fig. 19. The hollow electrode containing the coaxial trigger was held at ground potential while the solid electrode was at -40 kV when the capacitor was charged. Thus, the +15 kV trigger pulse was very effective in producing a rapid breakdown. The gap was pressurized with dry nitrogen to provide a controlled inert atomosphere having repeatable discharge characteristics. Changing pressure also provided a simple means of continuously changing breakdown voltage without having to change the gap spacing. When one source was fired, the large magnetic fields produced induced transients in the circuitry of

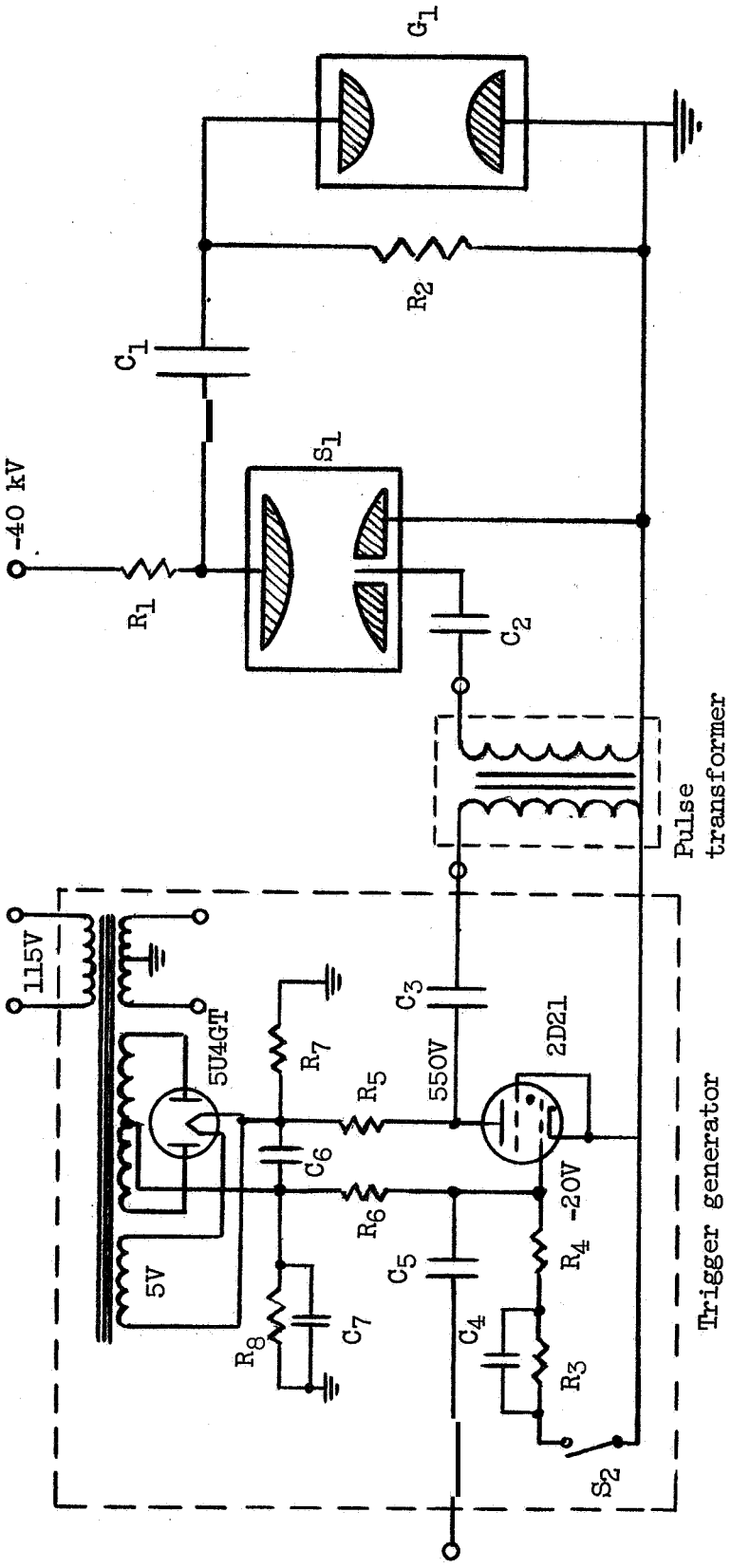

R_1 = 10 M
R_2 = 1 M
C_1 = 0.1μf, 40 kV
C_2 = 500pf
G_1 = Guided spark source
S_1 = Pressurized spark gap switch

C_3 = 1.0
C_4 = 0.02
C_5 = 0.01
C_6 = 16
C_7 = 50

R_3, R_5 = 1 M
R_4 = 22 K
R_6 = 100 K
R_7 = 270 K
R_8 = 2700

Fig. 18. - Spark Source Control Circuit.

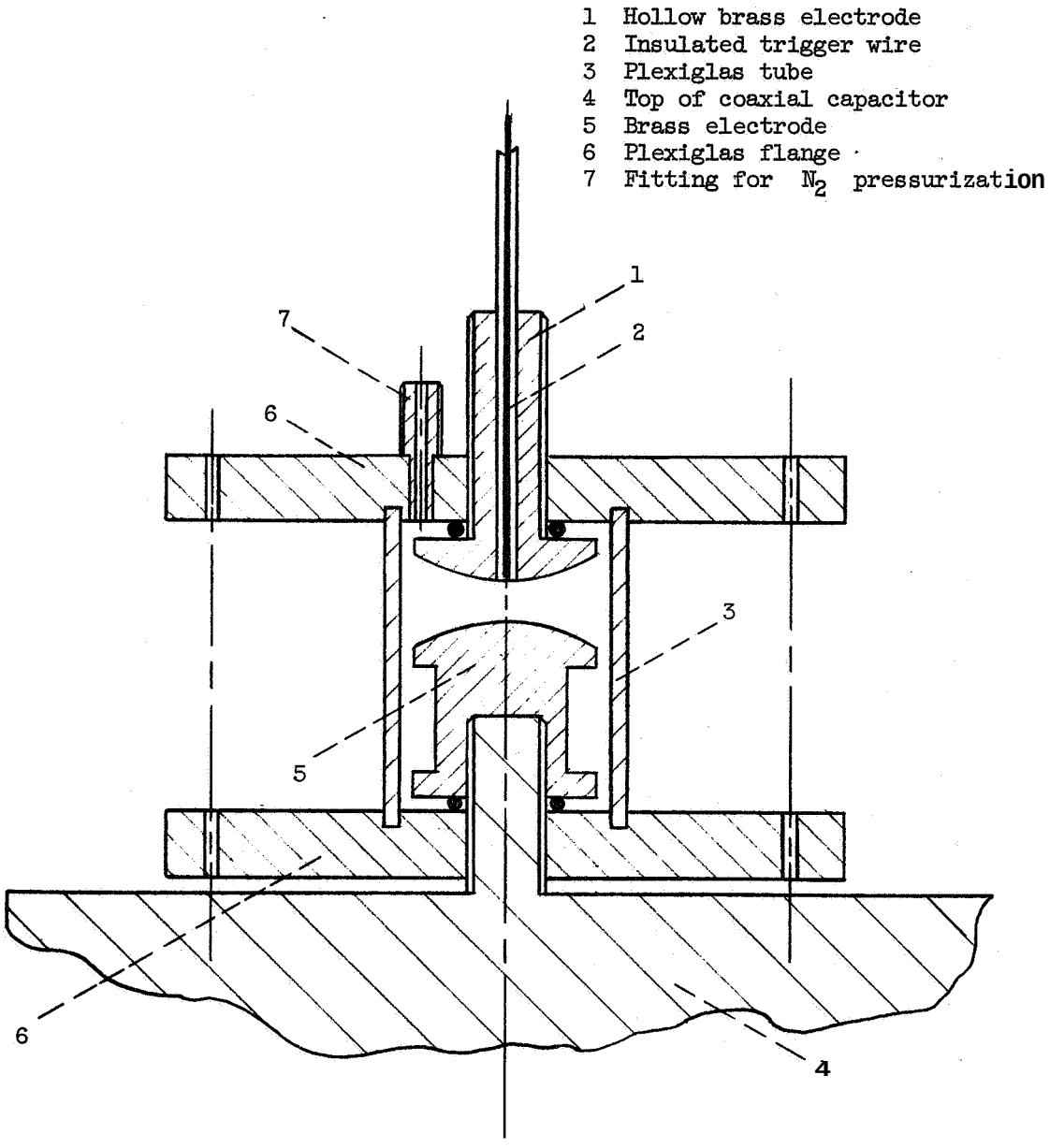

Fig. 19. - Pressurized Spark Gap Switch.

the other source which tended to cause a premature discharge. Such erratic behavior was prevented by maintaining a higher pressure on the switch gap of the source to be fired second.

Upon excitation by the spark source the fluorescent dye absorbed in the ultraviolet and blue, and emitted in the green* in less than 10^{-8} sec. A two lens camera system was used to record the images at a magnification of 25X. The characteristics of the objective lens determined the working distance and light gathering capacity of the system while performing a small magnification. The major portion of the magnification was provided by the reimaging lens which collected all the light gathered by the objective. Although the fastest negative film available was used, the intensification process was required to increase image contrast for the sake of easier readout.

C. Data Acquisition: Conditions and Procedure

The ethyl alcohol containing fluorescein was pressurized with dry nitrogen and injected at room temperature. Flow rate was measured by weighing the supply tank, and pressure was measured immediately upstream of the nozzle. The swirl atomizer which was nominally rated at 0.75 gallon/hour at 100 psig for fuel oil had a minimum orifice diameter of 0.009 in. Since the orifice does not

*See Fig. D2 of Appendix D for the spectral characteristics.

run full but has an air core, double-exposure photographs were taken to determine the mean velocity of the liquid cone as it emerged. Figure 20 shows a series of such photographs, and the measured sheet velocities and flow rates are shown in Fig. 21. The spray cone angle at the orifice was determined by the divergent section in the nozzle orifice, and remained essentially constant at 68° over the range of pressures from 25 to 100 psig.

In order to determine the effect of the exhaust fan on the spray motion, average air velocities due to the fan alone were measured with a hot wire anemometer. The data are plotted in Fig. 22, which shows that the Pan velocity was nearly constant and less than 24 in./sec over the range of axial distances where spray measurements were made. This variation of air velocity with distance was used in the illustrative single drop calculations presented in Chapter I.

Figure 23 illustrates the sampling positions which were used. Each numbered sampling station corresponds to the field viewed by the camera and was recorded on 4 by 5 sheet film. After the zero position was established by viewing the nozzle through the camera, the nozzle was moved to other positions by a traversing mechanism consisting of three perpendicular micrometer screws equipped with dial indicators. Table IX summarizes the conditions which were photographed and analyzed.

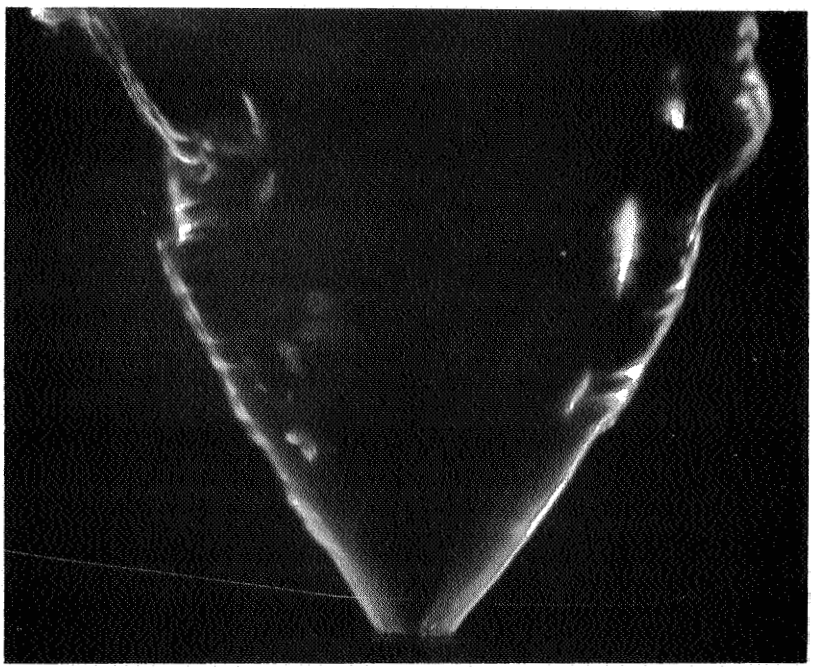

Δp = 25 psi

Δp = 40 psi

Fig. 20. - Double exposure photographs of the spray cone for a range of injection pressures. t_I = 10 μs (25X).

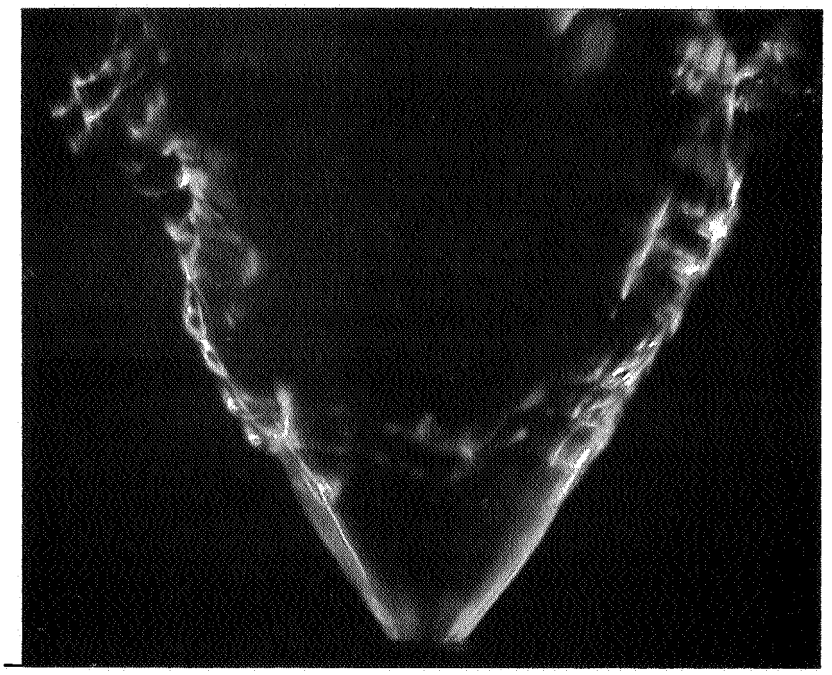

Δp = 55 psi

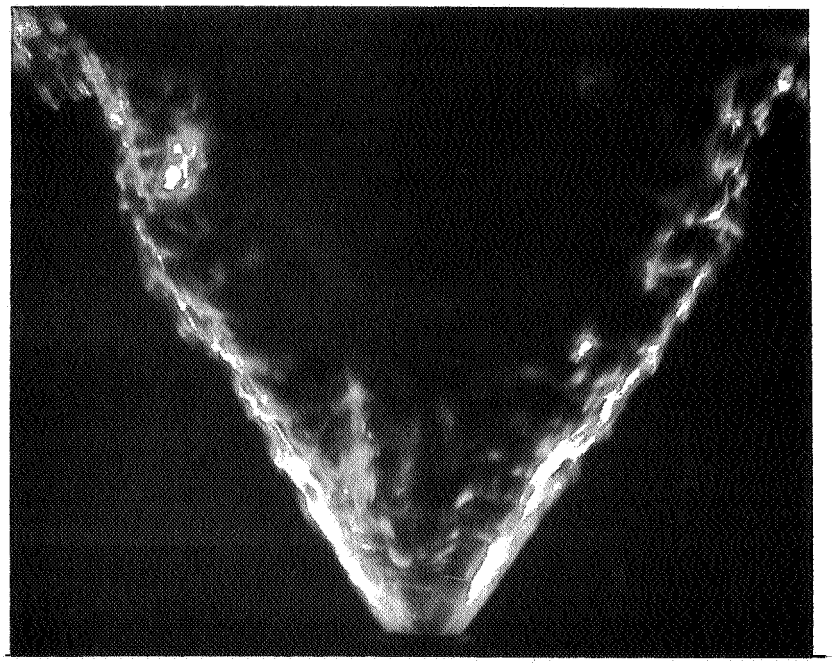

Δp = 100 psi

Fig. 20. – Concluded.

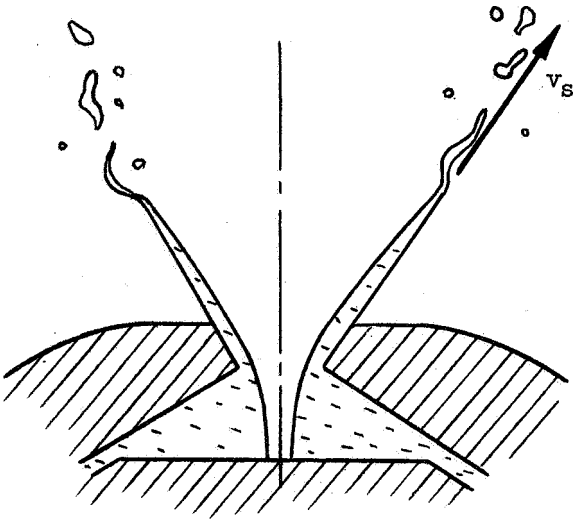

Cross **Section of the Orifice**

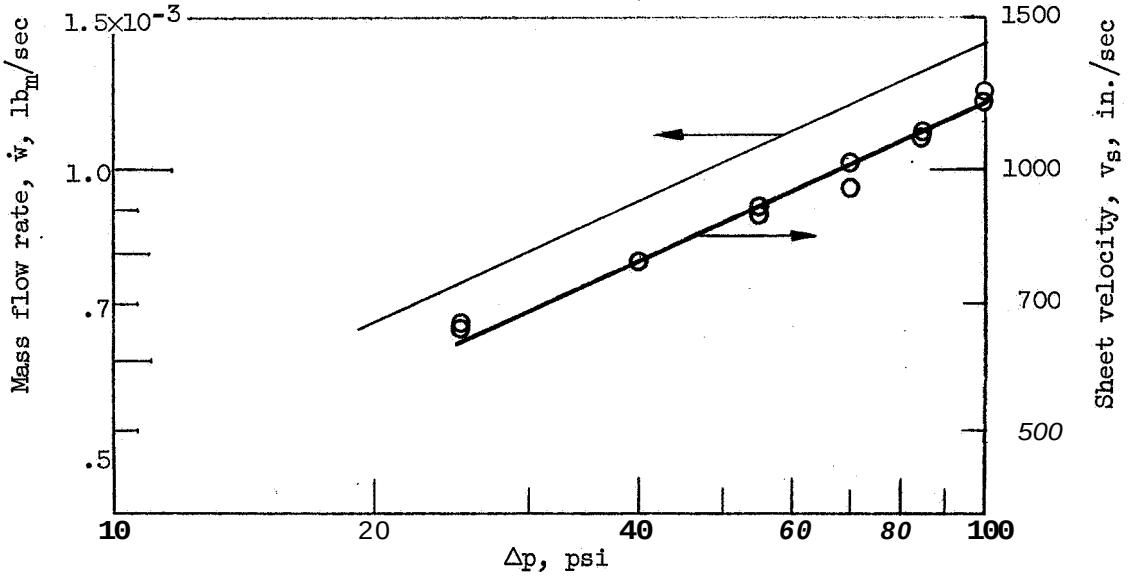

Fig. 21. - Flow Characteristics of the Swirl Atomizer.

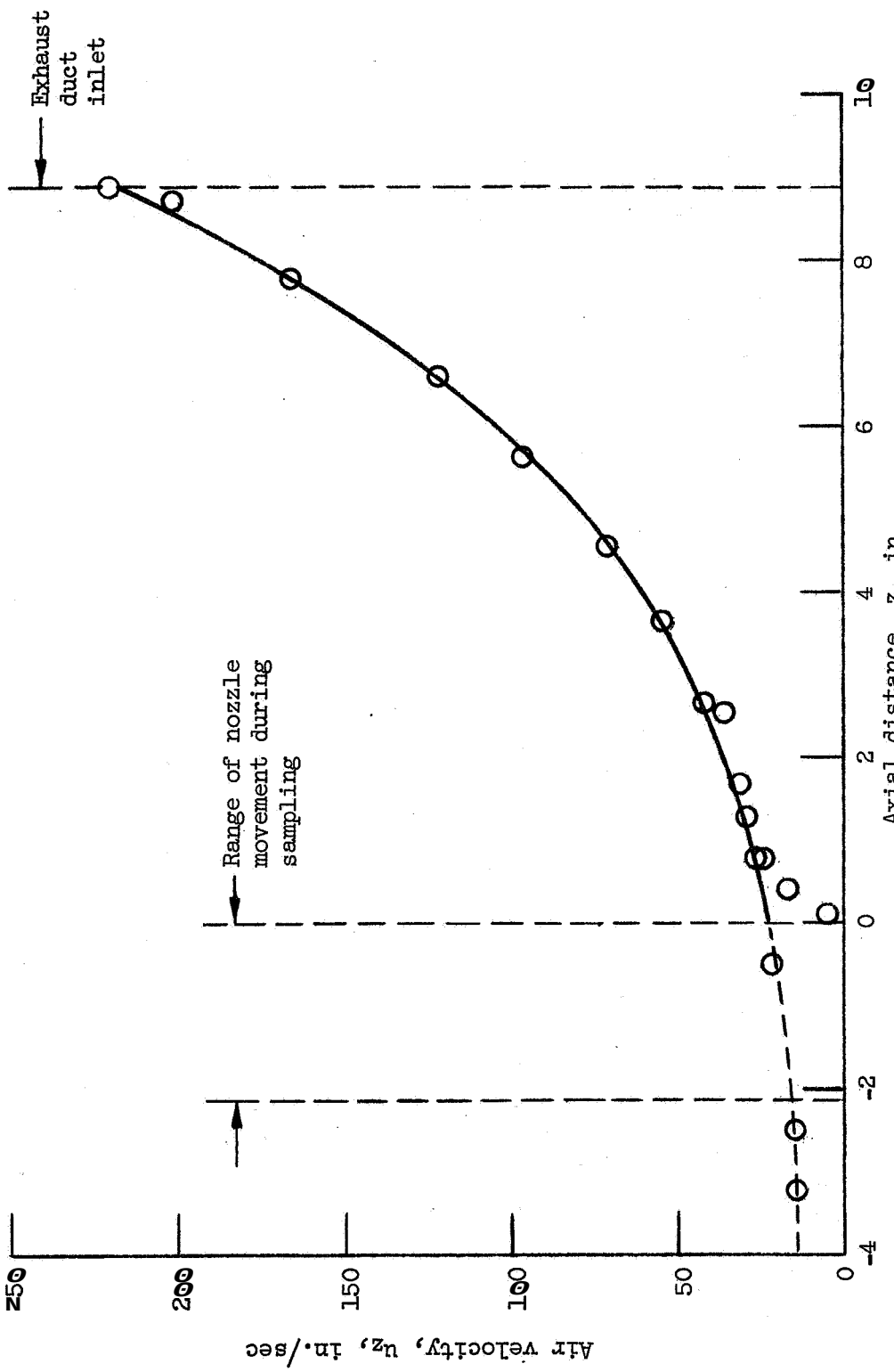

Fig. 22. - Mean Air Velocity Induced by the Exhaust System.

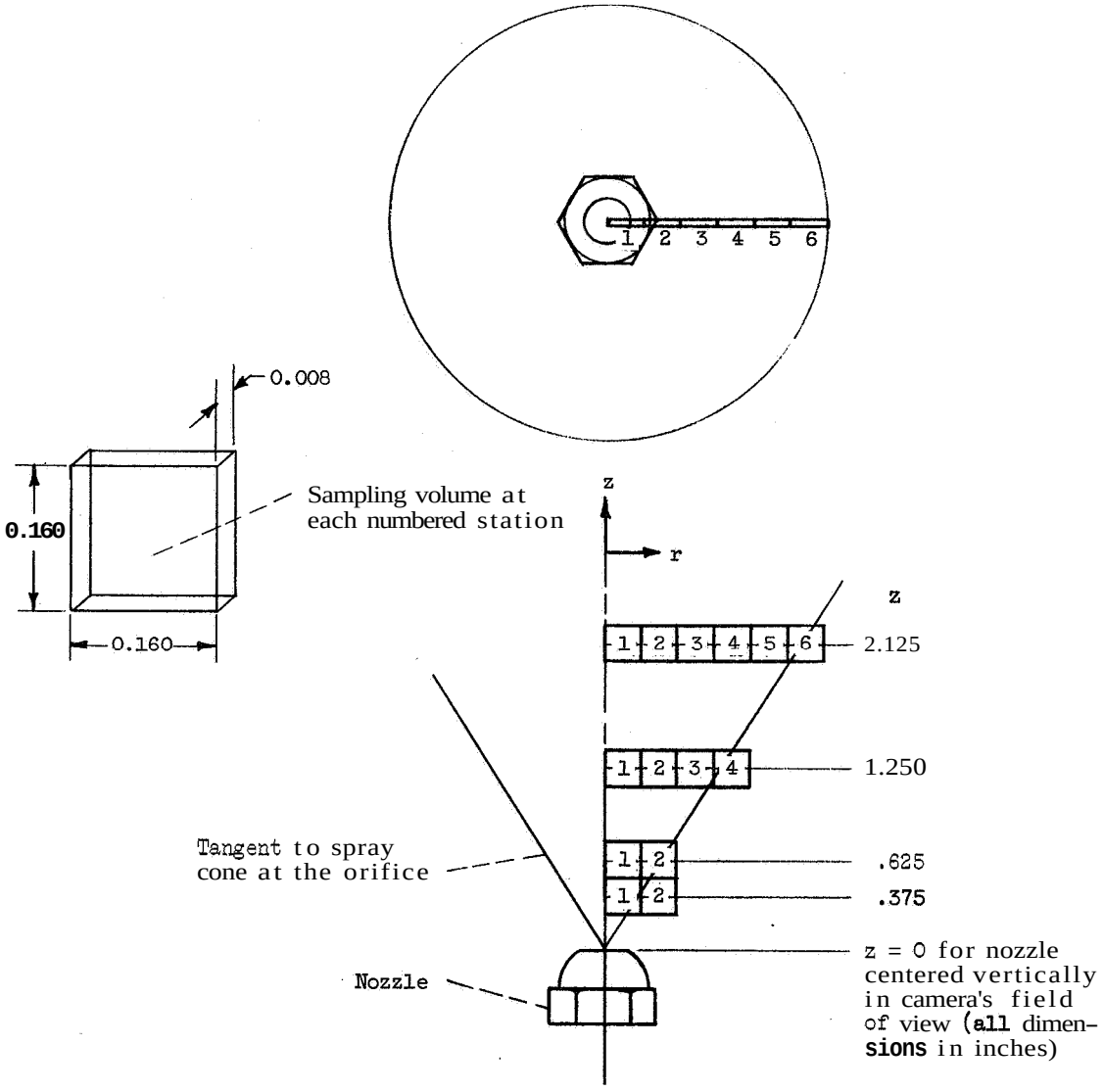

Fig. 23. - Sampling Geometry.

TABLE IX. - SAMPLING CONDITIONS

Δp, psi	Radial station	z, in.	t_I, μs	Total exposures, ϵ
25	1	0.625	13.9	14
	2		18.7	60
	1	1.250	17.6	36
	2		23.0	48
	3		30.6	55
	4		73.9	40
	1	2.125	17.6	48
	2		17.6	60
	3		30.6	72
	4		50.8	72
	5		73.9	40
40	1	0.375	10.4	12
	2		10.2	36
	1	2.125	10.4	36
	2		10.2	36
	3		13.7	48
	4		24.6	60
	5		44.7	72
	6		59.5	20
55	1	0.375	9.5	13
	2		9.6	20

Data were taken in the following manner. The room was darkened and film exposure was determined by the flash sequence once the film holder was opened. Bolaroid 3000 film was used to provide immediate drop photographs which guided the choice of sampling parameters for a particular data set. The axial coordinate nearest the nozzle was selected to roughly approximate the surface of formation, i.e., breakup was nearly complete. Since the light sheet was so thin, any v_θ component of velocity perpendicular to it tended to carry a droplet into or out of the sampling volume between flashes. Therefore, t_I was kept at a minimum consistant with the requirement of image separation for most of the drops. The film processing including the intensification was a very lengthy operation so it was desirable to record as many sets of double-exposure samples on the same film as possible without superposition of images. Roughly equal numbers of drops were photographed at each location by holding the number of films constant and adjusting the number of samples per film. This practice could not be followed at the outer stations since drop density was so low that the number of samples required to accumulate the same total number was prohibitive.

The intensity-time trace for each pair of flashes was monitored visually on the oscilloscope. At least three traces were photographed at each setting and provided the exact values of t_I listed in Table IX. In

the rare instance of a source misfire, the film was discarded and new exposures were made.

Sample photographs are given in Fig. 24, for a range of conditions. The number of samples and interval between exposures vary from picture to picture as noted. It can be seen that the relative concentration of different sizes varies widely with position; and that magnitude and direction of drop velocity differ not only from one size to another, but for similar sizes at the same location.

D. Data Reduction

The raw records consisted of over 200 films each of which had up to 200 pairs of drop images. For the sake of consistency and speed an automated method of data reduction such as the flying spot scanners that were used in previous studies of drop size (Ref. 18 and 19) was desirable. However, in the present study the additional requirements associated with velocity measurement demanded a much more sophisticated analyzer. Pairs of images had to be identified and the distance between image edges along the path of motion had to be measured. Scanners which digitize film according to discrete density levels are available. An appropriate computer program must then be written to search the digital "picture" stored in the computer memory, associate paris, and determine sizes and displacements. Since the scanner was prohibitively expensive, and the generation of a suitable program was,

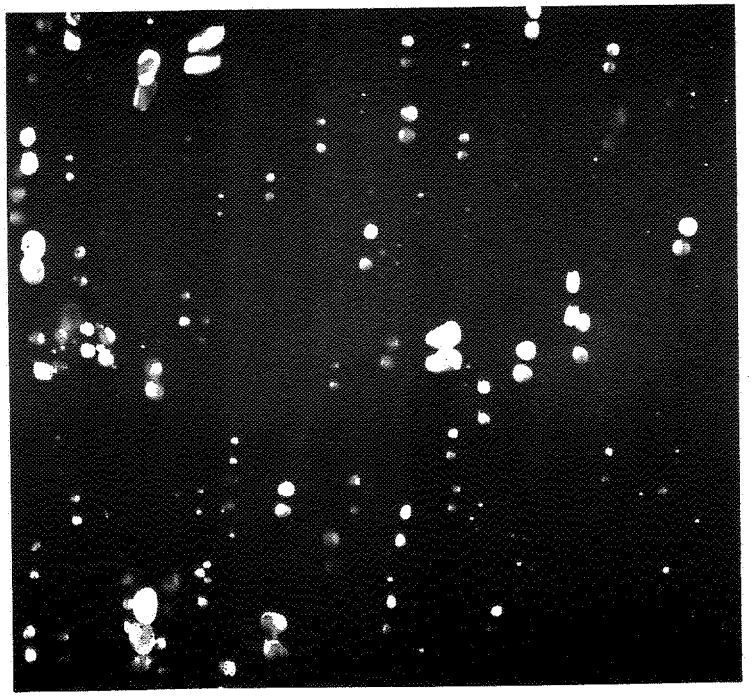

Station 1 1 sample

t_I = 13.9 μs

Station 2 5 samples

t_I = 18.7 μs

Δp = 25 psi z = 0.625 in.

Fig. 24. - Sample double exposure photographs (25×).

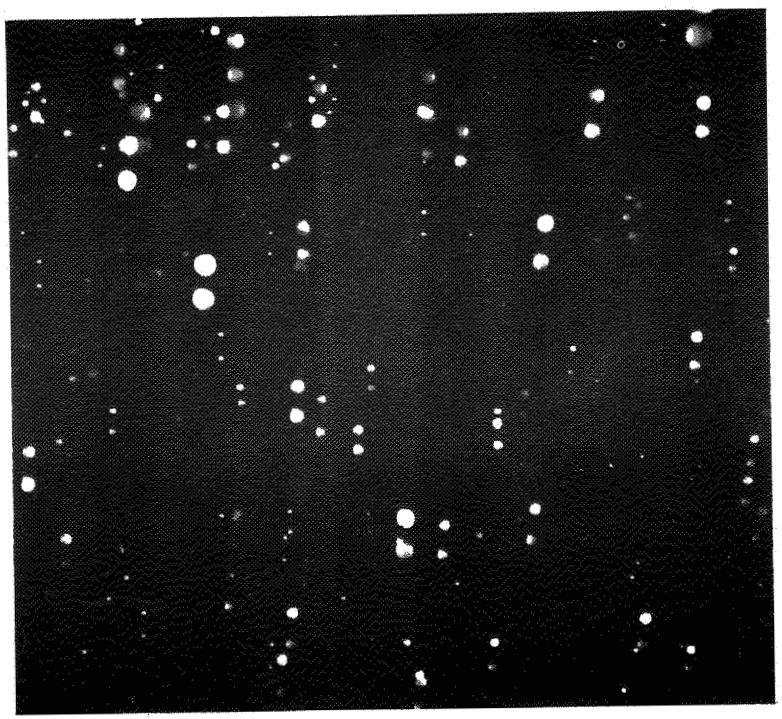

Station 1 3 samples

t_H = 17.6 μs

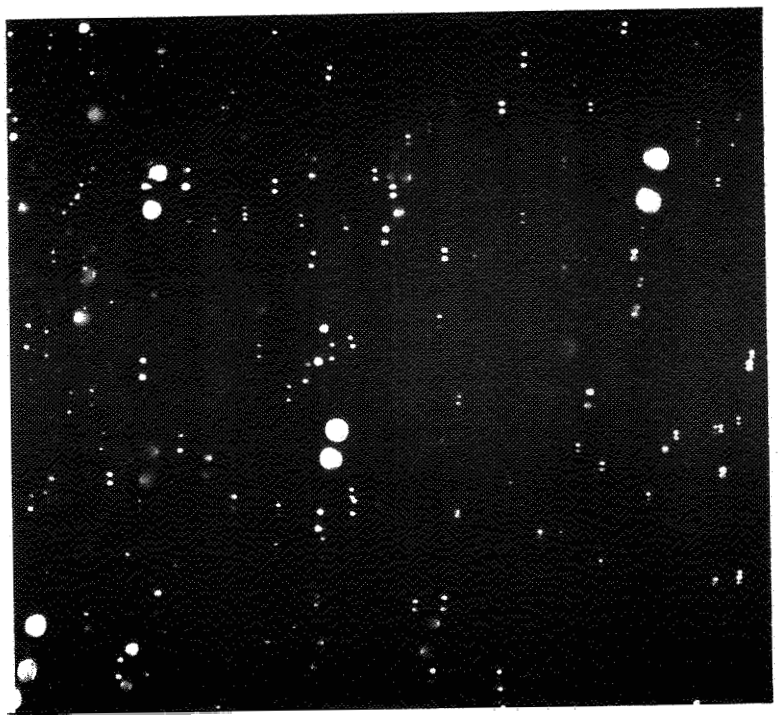

Station 2 4 samples

t_I = 23.0 μs

Δp = 25 psi z = 1.250 in.

Fig. 24. - Continued.

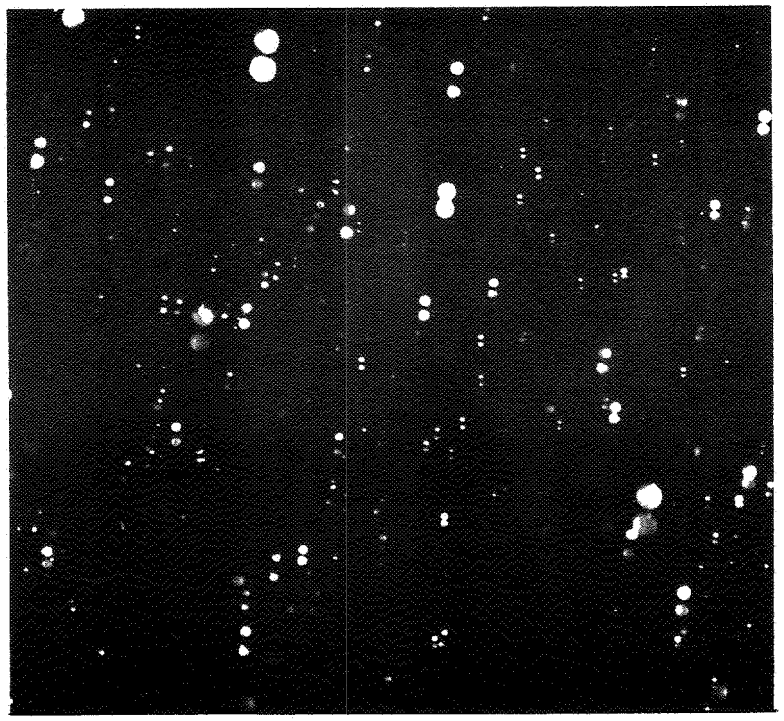

Station 2 5 samples

t_I = 17.6 μs

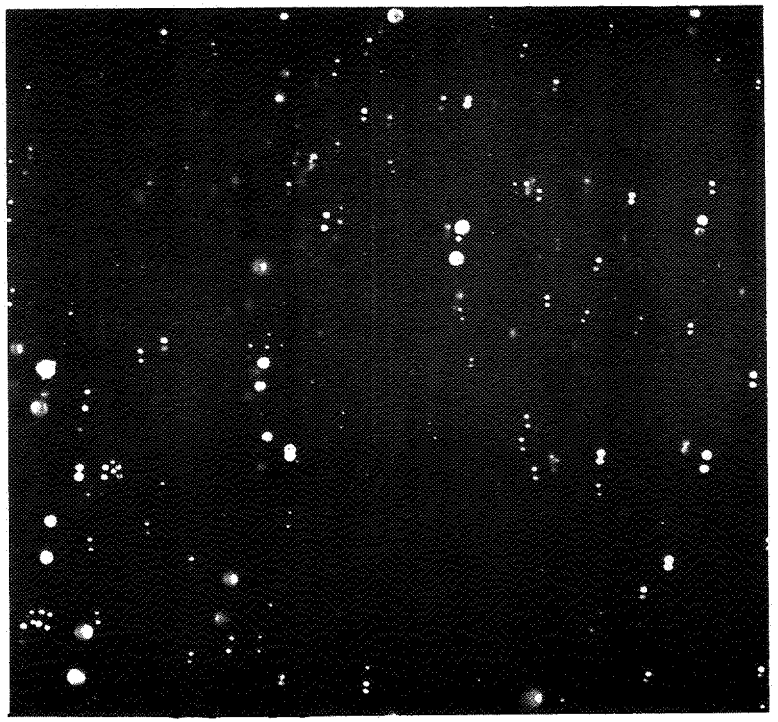

Station 3 6 samples

t_I = 30.6 μs

Δp = 25 psi z = 2.125 in.

Fig. 24. - Concluded.

itself, a major undertaking; the only recourse was to direct, manual measurement.

Microcard readers were used to project the films at additional magnifications of 16.3 to 18.1 times, and measurements were made directly on the screen with transparent scales and protractors. A transparent grid of numbered 1/2 inch squares was placed over the negative before insertion in the reader. One grid square at a time apperaed on the reader screen and usually contained less than 5 or 6 pairs. Figure 25 shows a schematic view of the reader screen with the measured quantities labeled on one droplet pair. Thus, position references were available on each film, and duplicate counts were avoided.

Rather than immediately categorizing sizes or displacements by using specially graduated scales, little additional time was required to record the two measurements to the nearest millimeter on the screen. Thfs gave complete freedom to choose category boundaries later in the analysis. In addition to the two linear measurements, the number of the grid square, the angle φ of the trajectory with the vertical to the nearest 2 degrees, and an image quality indication of 1 or 0 were recorded for each pair. The quality factor gave the measurer a means of differentiating between sharp pairs and those for which measurement was uncertain due to such things as low contrast or poor quality of one member of the pair. A total of more than 32,000 pairs of drop images were measured.

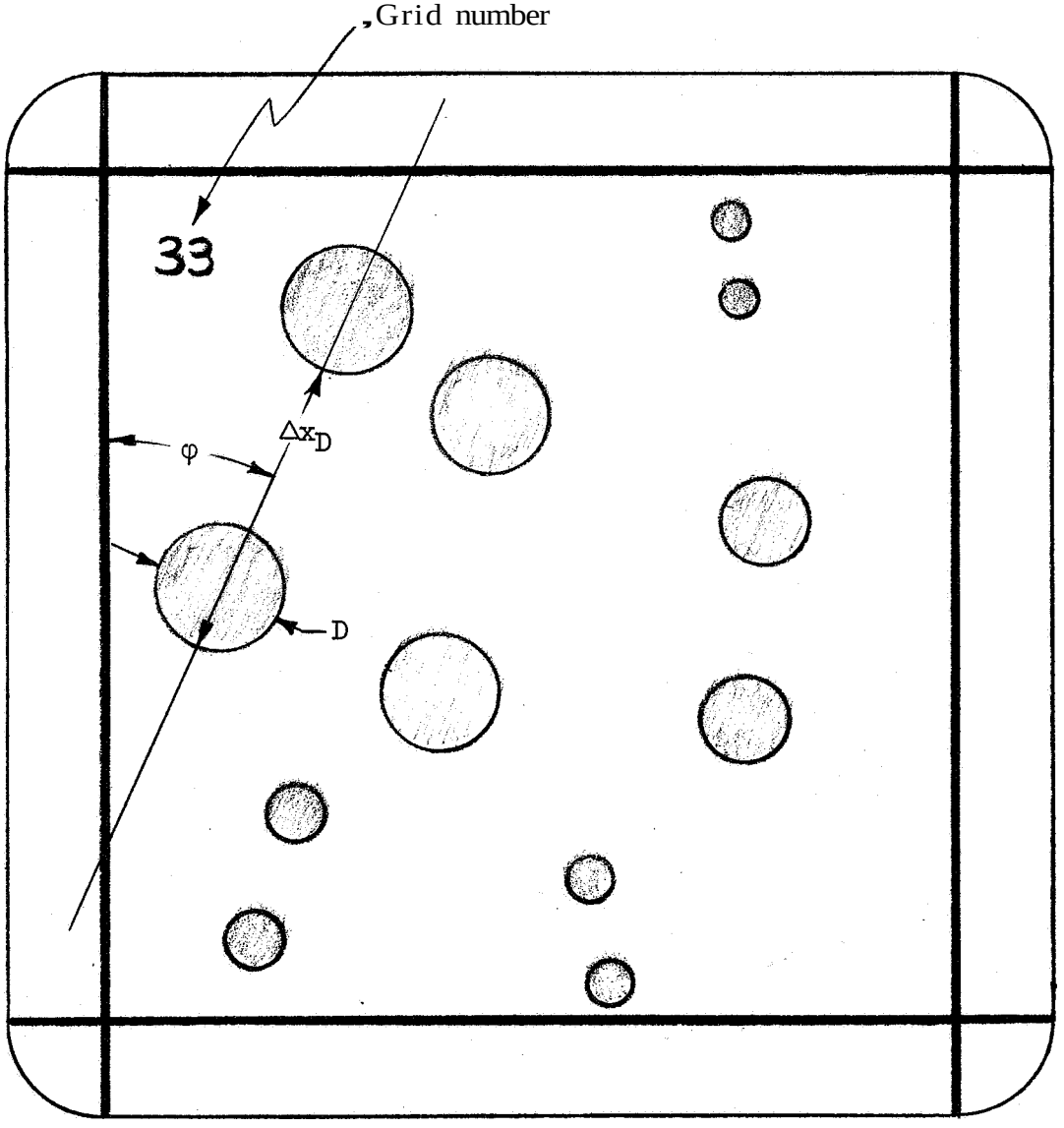

Fig. 25. - Schematic of the Readout Situation.

The data were then transferred to punched cards in a format which contained the film identication, grid location, size, displacement, angle, and quality factor for each drop. These cards were the input data to a program which applied scale factors and sorted the grid areas according to larger film regions. An output card was punched for each drop which had film number, grid area, D, $|\underline{v}|$, v_z, v_r, Φ, film region, and quality. This information was the basic raw data for the estimation of f_B by categorization; and spray profile analysis in terms of various mean quantities obtained by weighted summations.

Chapter IV

ANALYSIS OF THE SIZE-VELOCITY DATA

The size-velocity data which are presented consist of two kinds of spray information. First, the measurements at the shortest downstream distances, which lie near the surface of formation, were made over a small range of injection pressures to provide some insight into the nature of the initial spray density function, f_o. This information is a particular answer to the spray description problem. Second, the data at downstream conditions indicate the propagative behavior which a spray transport theory must be able to reproduce.

Underlying objectives of the data presentation are to show the comprehensive and fundamental qualities of the density function f, and the vital role of drop velocity as a random variable. In addition, the local spatial variations which the data exhibit are emphasized to show why care must be exercised when constructing average quantities to represent an entire spray.

The two ways in which the data are handled parallel the two approaches to the spray propagation problem discussed in Chapter II - characterization in terms of the density function f and reduction to local mean quantities related to mass, momentum and energy. While, in principle, the density function has the advantages of being compact and complete; it is a difficult practical

matter to find a reasonably simple equation to fit the data. Since the spray formation problem remains unsolved, no theoretical guide to the functional form is available; and the behavior of the physical processes which generate f remains obscure. On the other hand, the physical picture in terms of mean quantities is somewhat clearer due to the similarities with traditional gas dynamics. The problem here is that many separate quantities must be specified to provide a complete characterization.

The discussion begins with an outline of the types of operations performed on the data. Next, the overall character of the data is presented with samples of the measurements in their most elementary form. Representations of the general density function f_B and functions derived from it are followed by the complementary picture in terms of mean values. Finally, source terms which appear in the equations of change are given based on the available single drop expressions for the transport rates.

A. Operations Performed on the Data

1. Construction of Density Functions: The density function f_B is estimated by categorizing the size-velocity data and applying an approximate form of Eq. (2.2) to give values of the function at the category means:

$$f_B(\hat{D}_i, \hat{v}_{zj}, \hat{v}_{rk}, \underline{x}') = \frac{n_{ijk}}{V_S \epsilon \, \Delta D_i \, \Delta v_{zj} \, \Delta v_{rk}} \qquad (4.1)$$

where:

n_{ijk} = the number of drops in the i^{th} size, j^{th} axial velocity, and k^{th} radial velocity categories at a position x'

V_S = the size of the sampling volume

ϵ = number of samples at a given condition

$\hat{}$ = indicates the mean value in a category

The category boundaries used increase by a constant multiple so that the fractional change in D or V is a constant. For any drop variable:

$$\Gamma_i = \Gamma_1 m^{i-1} \qquad (4.2)$$

and the geometric mean was used:

$$\hat{\Gamma}_i = (\Gamma_i \Gamma_{i+1})^{1/2} \qquad (4.3)$$

Table X lists the values chosen for m, and the resulting boundaries and means.

Once values for f_B are available any conditional such as $f(D|v_z)$, marginal such as f_S or weighted density function such as f_F can be calculated by performing summations over the categories to approximate the integrals over continuous functions defined in Chapter 11.

A one-dimensional density function f_T may be defined by integrating f_B over a cross section. In cylindrical coordinates with equal radial increments the integral is approximated by a sum over the l radial stations:

TABLE X. - DROP SIZE AND VELOCITY CATEGORY BOUNDARIES AND GEOMETRIC MEANS

Category number	$D(\mu)$ m = 1.31		v_z (in./sec) m = 1.31		v_r (in./sec) m = 1.75	
	Lower limit	Mean	Lower limit	Mean	Lower limit	Mean
1	10.0	11.4	15.0	17.2	-502.6	-380.0
2	13.1	15.0	19.6	22.8	-287.2	-217.1
3	17.2	19.6	25.7	29.5	-164.1	-124.1
4	22.5	25.7	33.7	38.6	-93.8	-70.9
5	29.4	33.7	44.2	50.6	-53.6	-40.5
6	38.6	44.2	57.9	66.2	-30.6	-23.2
7	50.5	57.8	75.8	86.8	-17.5	-13.2
8	66.2	75.8	99.3	113.7	-10.0	10.0
9	86.7	99.3	130.1	148.9	10.0	13.2
10	113.6	130.0	170.4	195.1	17.5	23.2
11	148.8	170.4	223.3	255.5	30.6	40.5
12	195.0	223.2	292.5	334.7	53.6	70.9
13	255.4		383.1	438.5	93.8	124.1
14			501.9	574.5	164.1	217.1
15			657.5	752.5	287.2	380.0
16			861.8	985.8	502.6	
17			1128.3			

$$f_T = \frac{\pi(\Delta r)^2}{V_S \, \Delta D_i \, \Delta v_{zj} \, \Delta v_{rk}} \sum_l \frac{(2l - 1)}{\epsilon_l} n_{ijkl} \qquad (4.4)$$

2. Calculation of Mean Quantities

The mean densities and fluxes of mass, momentum and energy given as weighted integrals over f in Table V may be calculated by summation over the size-velocity categories. They may also be calculated by direct summation over the raw data treating each drop separately. Categorization greatly reduces the number of calculations involved since all drops in a category are considered to have the corresponding mean size and velocity. Both methods were used and the resulting means agreed within a maximum deviation of 10%. The categorized computation usually produced slightly higher values indicating a smoothing influence and heavier weighting by the large categories.

In addition to the physical means from Table V, the related mean diameters from Eqs. *(2.9)* and (2.10); and statistical moments were calculated. Three particular statistical quantities which indicate the form of the density fuhction are the coefficient of variation:

$$\lambda_\Gamma = \frac{\sigma_\Gamma}{\langle \Gamma \rangle} = \frac{(\langle \Gamma^2 \rangle - \langle \Gamma \rangle^2)^{1/2}}{\langle \Gamma \rangle} \qquad (4.5)$$

skewness:

$$\kappa_\Gamma = \frac{\langle \Gamma^3 \rangle - 3\langle \Gamma \rangle \langle \Gamma^2 \rangle + 2\langle \Gamma \rangle^3}{\sigma_\Gamma^3} \qquad (4.6)$$

correlation:

$$\rho_{\Gamma_i \Gamma_j} = \frac{\langle \Gamma_i \Gamma_j \rangle - \langle \Gamma_i \rangle \langle \Gamma_j \rangle}{\sigma_{\Gamma_i} \sigma_{\Gamma_j}} \tag{4.7}$$

These dimensionless quantities which are independent of the absolute magnitudes of the density functions indicate the degree of dispersion about the mean, the degree of asymmetry with respect to the mean, and interdependence of pairs of random variables.* Such moments about the mean are closely related to the peculiar quantities such as $\mathcal{U}$ and $\underline{\underline{\pi}}_S$ appearing in the substantial forms of the spray equations (Eqs. (2.11a) to (2.13a)).

The mean quantities were numerically integrated over the cross section to obtain average values at a given downstream distance. These values correspond to a one-dimensional description of the spray.

3. Spatial Variations and Sample Size

All manipulations are carried out in cylindrical coordinates with the origin at the nozzle orifice. No θ information is available so the treatment is two-dimensional in r and z. For a given z, the data are analyzed at equal radial increments of 0.080 inch beginning at 0.040. These divisions result from dividing each sampling station in half vertically and choosing r at the midpoint of each half (see Fig. 23).

*The ensemble averages in each case may be weighted as defined in Eq. (2.7).

Many of the plots presented in this chapter use the ratio of radial to axial coordinates as the abscissa. This is the tangent of the angle φ, and is approximately equal to φ for the small angles used. Plots of the data versus solid angle or radius alone usually do not superimpose the data to a greater degree. Although the spray approximates a point source in the beginning, the collapsing of the liquid cone and interaction with the gas warp the flow propagation characteristics toward a cylindrical geometry.

The radial component of the mass average velocity is often less than 20% of the axial component* indicating that the radial contributions to z momentum and energy flux terms such as $\rho_s \langle v_z v_r \rangle_M$ and $\rho_s \langle v_z v_r^2 \rangle_M$ are small compared to $\rho_s \langle v_z^2 \rangle_M$ and $\rho_s \langle v_z^3 \rangle_M$. The spray density ρ_s is always a strong function of r and z; and thus, sharply defined axial flux profiles exist.

The spatial resolution attainable is intimately linked with sample size. For a given total number of drops measured at a particular condition, continual reduction in the size of the sample volume considered about a coordinate leads to increasing fluctuations in spray properties from point to point. This situation is

*Exceptions to this occur at combinations of small z, large r, and high Ap where the radial component exceeds 50% of the axial component.

analogous to the breakdown of the continuum treatment of gas dynamics as the density is lowered or the spatial region considered becomes very small. However, in the case of sprays, the number density is always small compared to usual molecular number densities, and the spray density functions must be viewed as representing the ensemble behavior as distinct from local temporal behavior. The same situation exists with respect to the number of size-velocity categories chosen for classification. A given sample size contains a fixed amount of information, and attempts to extract more and more detail eventually lead to a breakdown in the estimation process.*

For the spatial grid chosen, the sample sizes range from approximately 1800 to 100. Means based on summation over the sample gave reasonably smooth results, and density functions presented at a given location using the categories of Table X are limited to bivariate marginals such as $f(D,v_z)$ and $f(D,v_r)$. Thus, the detail achieved represents a useful compromise within the practical restraints on sample size.**

Two sets of calculations, one using all drops regardless of quality factor and the other using only those with a quality factor of 1, show the following results.

---

*The number of samples must become large as $\Delta\Gamma$ becomes small as indicated by Eq. (2.2).

**For a discussion of a binomial model for estimating confidence limits for given sample sizes see Ref. 19.

Quantities such as mean velocities and regression curves which do not depend on the absolute magnitude of the spray density, differ by only a few percent for the two cases. The quantities dependent on ρ_s show the same trends but differ in magnitude by an amount proportional to the fraction of 0 quality drops in the sample (usually 20-30%). An obvious ambiguity exists as to the precise value of the effective sampling volume. This is a shortcoming common to all photographic sampling, and the double-exposure fluorescent technique has not entirely overcome it. Thus, absolute values are subject to some uncertainty but trends and means appear to be reliable. Data which include the entire sample are presented unless otherwise noted.

4. Source Terms

The mean source quantities (Table Vb) are distinguished from the hluxes and densities (Table Va) by their dependence on the transfer rates, $\mathcal{D}$; $\mathcal{A}$ and $\mathcal{T}$. Consequently, they are not directly calculable from the. raw data without the additional specification of the rate dependence on D, v and T_L. The single drop expressions of Chapter I (Eqs. (1.1) to (1.7)) are used to furnish local profiles of vaporization rate, momentum transfer to the gas, and the associated energy transfers for an assummed droplet temperature. Required values of air velocity are inferred from small droplet behavior and attendant uncertainties are discussed.

B. Overall Character of the Data

1. Typical Behavior in the Size-Velocity Plane

The most elementary presentation of bivariate **data** is a direct plot of the raw data in the size-velocity plane. Such a scatter diagram is shown for v_z and D in Fig. 26. Each of the 1400 drops in the sample is represented by a point resulting in much over-plotting. The density of the points in any area of the plane specified by particular ranges of v_z and D is proportional to the frequency of finding drops having those properties at this particular location in the spray. The point density is also an estimate of value of the density function $f(D, v_z)$ for given ranges of the independent variables.

Sheet velocity and the mean values of size* and velocity for this condition are listed. The curve is the calculated mean velocity at a given size: $\langle v_z | D \rangle$. Note that at this location in the densest portion of the newly formed spray, the spread in velocities of similar sized drops is large. Much of the drop population is still so young that not enough time has elapsed for the gaseous environment to greatly change their properties by vaporization or deceleration. Only a moderate depression of the regression curve is observed at the small sizes. The state of the spray, which is far from equilibrium with the

*In the often used notation of Eq. (2.9), $\langle D \rangle = D_{10}$ and $\langle D^3 \rangle^{1/3} = D_{30}$.

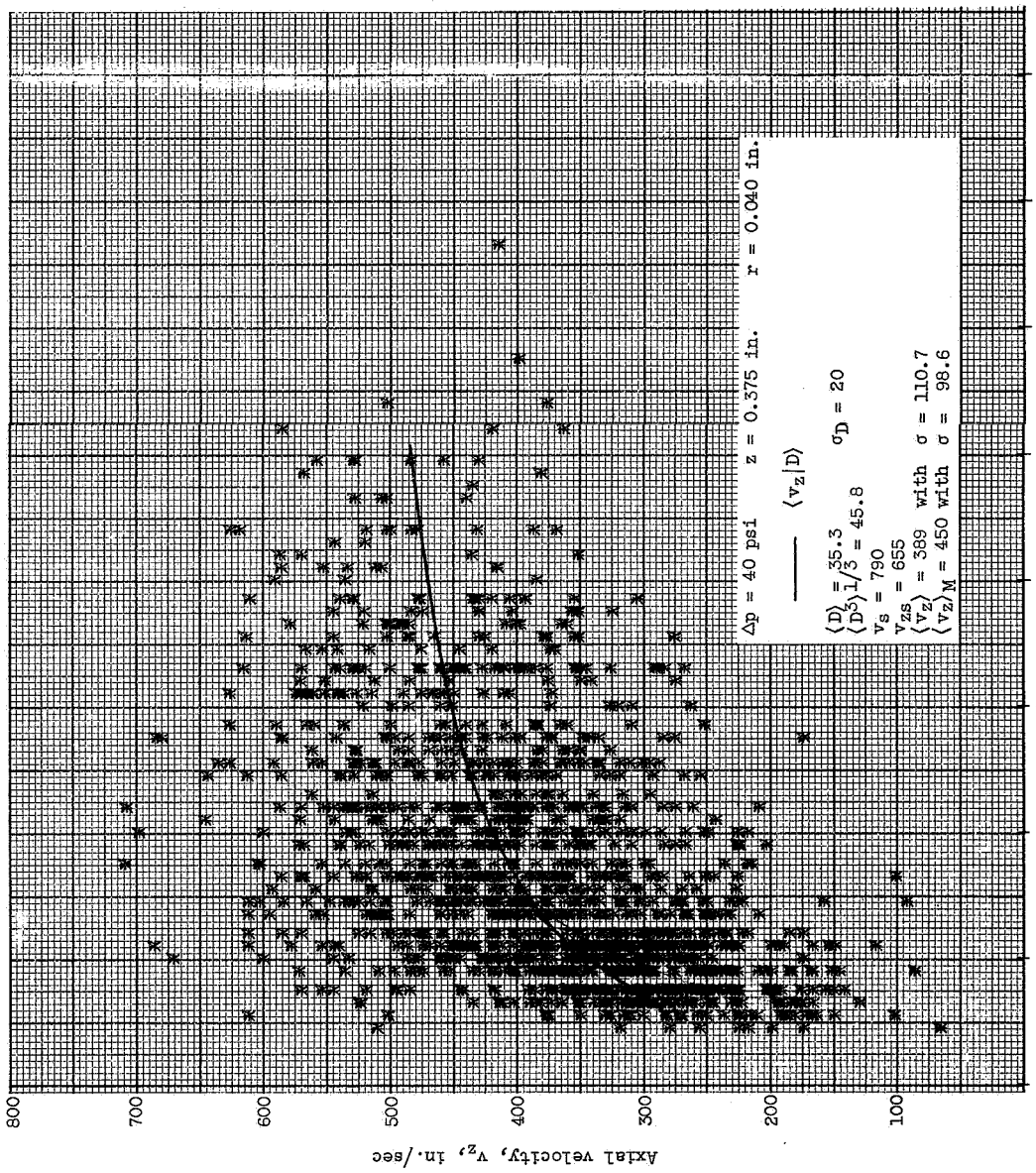

Fig. 26. - Typical v_z - D Scatter Diagram for a Location Near the Axis of a Newly Formed Spray.

gas, is the integrated result of randomly directed droplet births distributed throughout the formation region. Dissipation of kinetic energy occurs in the breakup process as evidenced by fact that the velocities of the large drops are less than sheet velocity.

The corresponding diagram for radial velocity at the same condition is shown in Fig. 27. Drops that are generated inside the hollow liquid sheet crisscross the spray axis with a range of velocities. The mass average velocity is ohly slightly positive as are the expected values of radial velocity which increase slowly with size.

Figures 28 and 29 portray the markedly different behavior observed toward the outer edges of the spray and at downstream positions where the spray is less dense. Under these conditions sufficient time has elapsed for the gas and the drops to strongly interact. The smallest drops which are the most plentiful have nearly come to velocity equilibrium with the gas, while the largest drops which contain a large portion of the spray mass, propagate with small modification. At this radial location, the radial velocities of drops larger than 40μ are predominantly positive with only a few medium-sized offshoots and the very small drops showing inward motion.

The two cases just illustrated by the two pairs of scatter diagrams lie near the opposite ends of the observed spectrum of spray behaivor. A continuous variation exists as a function of position, but the limiting

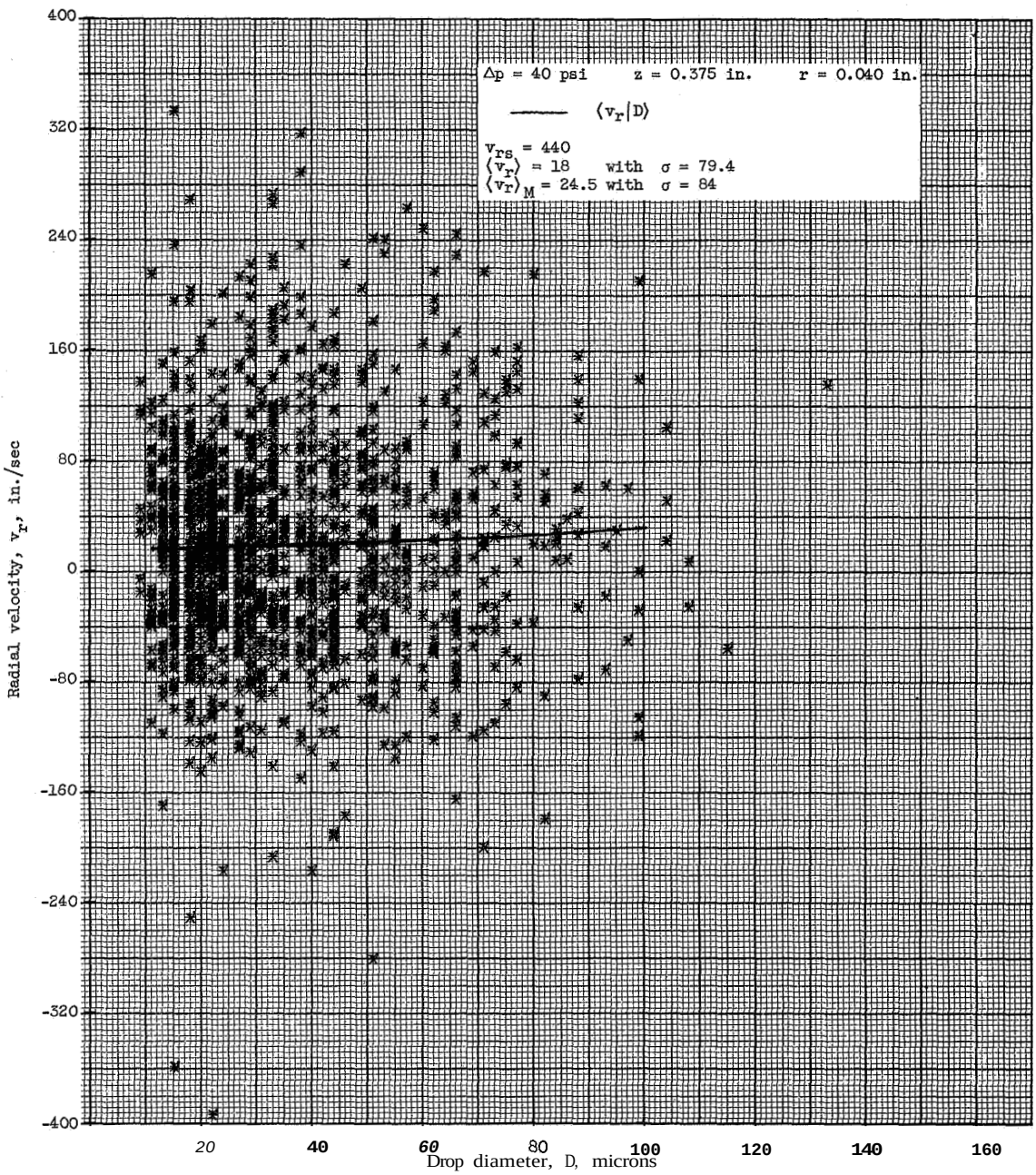

Fig. 27. - Typical v_r - D Scatter Diagram for a Location Near the Axis of a Newly Formed Spray.

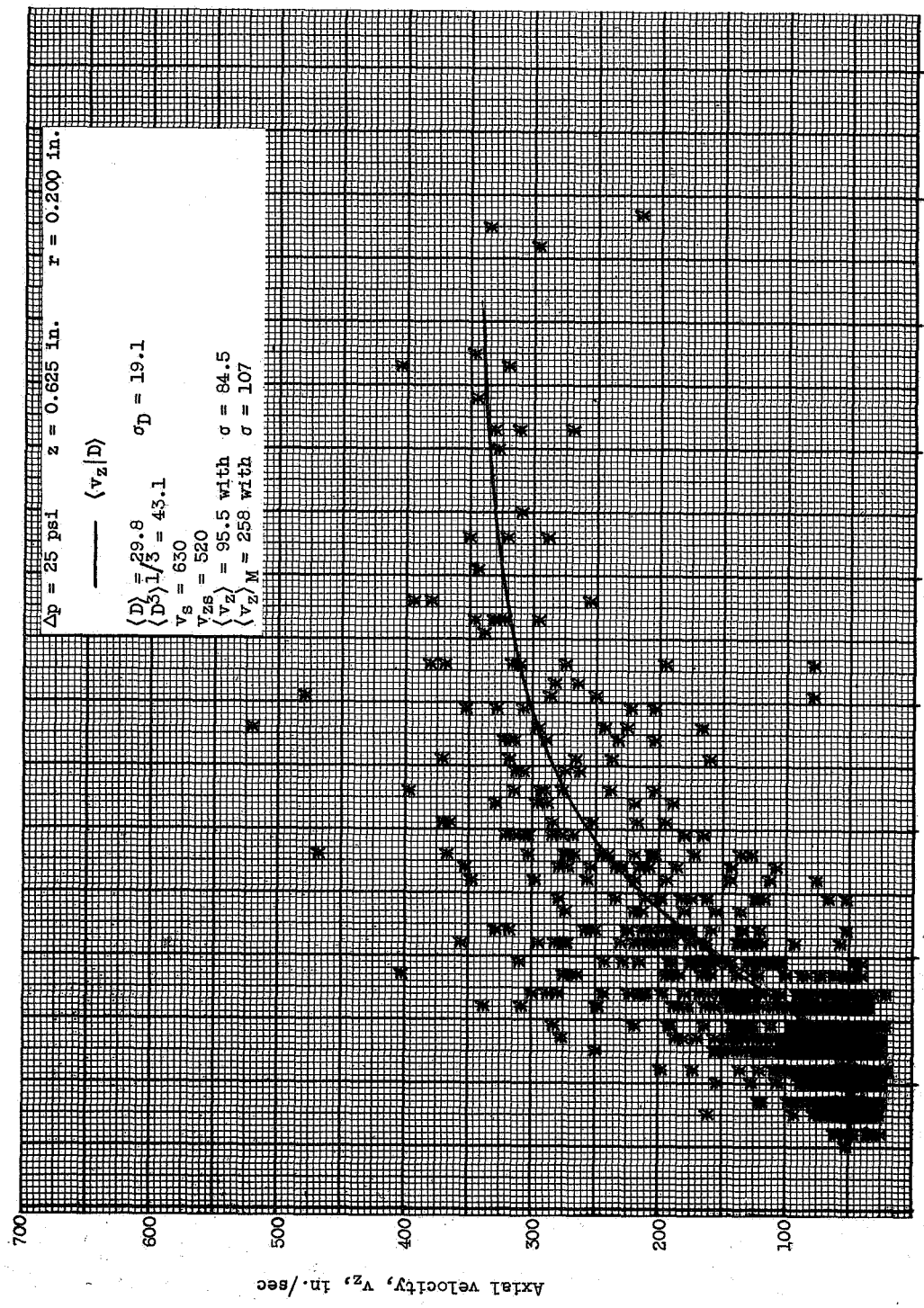

Fig. 28 - Typical v_z - D Scatter Diagram after Strong Interaction of the Spray with the Gaseous Medium.

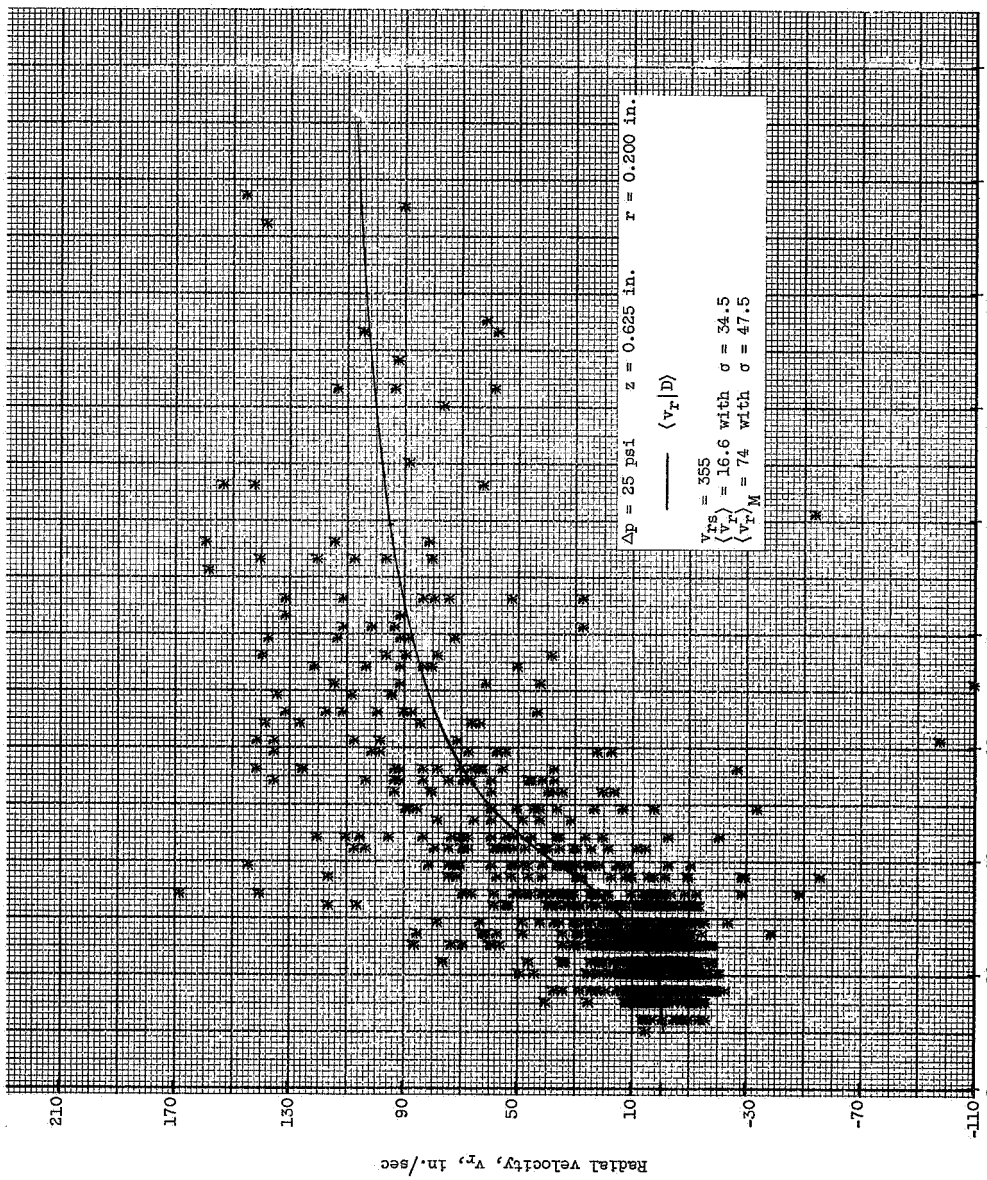

Fig. 29. - Typical v_r - D Scatter Diagram after Strong Interaction of the Spray with the Gaseous Medium.

cases of nearly uniform sizes traveling at either the injection velocity or air velocity are never closely approached.

In general, the allowable ranges of drop variables are, limited in the size-velocity plane as shown schematically in Fig. 30. Two cases are distinguished. The first, where injection velocity is greater than gas velocity, is the condition existing in this investigation while the second is for injection into a higher velocity gas stream. The stability boundaries indicated are of the type obtained for the threshold of aerodynamic breakup (Refs. 20, 21, 22, 36), and are of the form:

$$We_b^a Re^b = C_T \qquad (4.8a)^*$$

or for given liquid and gas properties:

$$D\left|\underline{v} - \underline{u}\right|^n = \text{Constant} \qquad (4.8b)$$

The intersection of the line of constant injection velocity with the stability boundary does not necessarily determine the maximum allowable size since larger drops formed with lower initial velocities are stable. On the other hand, factors such as turbulence conditions in the liquid or the geometry of sheet breakup may determine the scale of the drop formation such that aerodynamic

---

* A common expression (Ref. 22) uses $b = 0$, $a = 1$ and a C_T of 13 to 22 depending on whether the relative velocity is suddenly or gradually applied. Maximum Weber numbers observed in the present investigation were less than 5 indicating that at the locations sampled further aerodynamic breakup was unlikely.

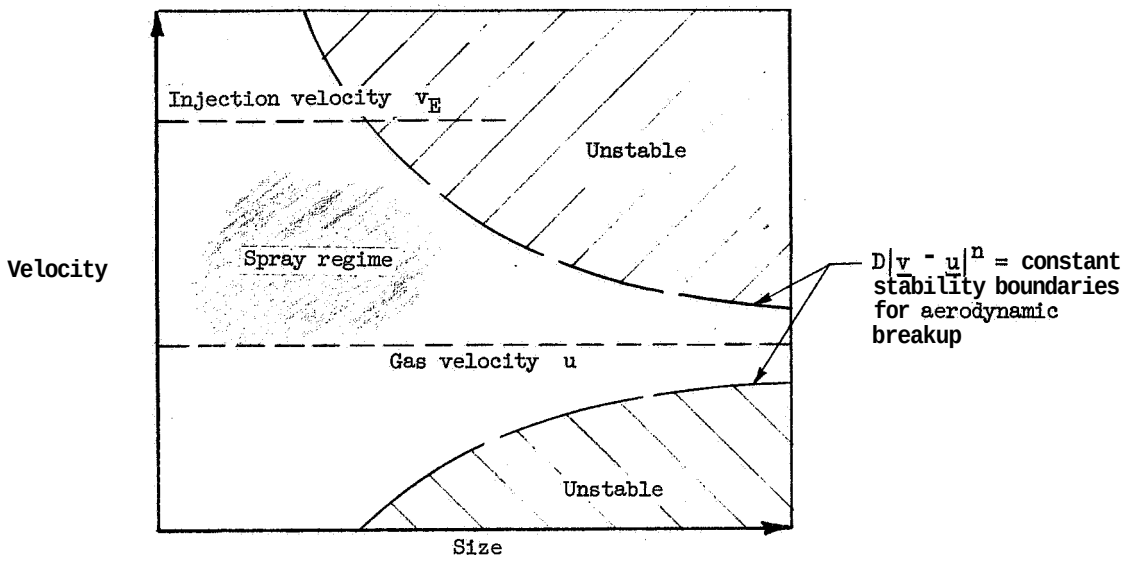

(a) $v_E > u$.

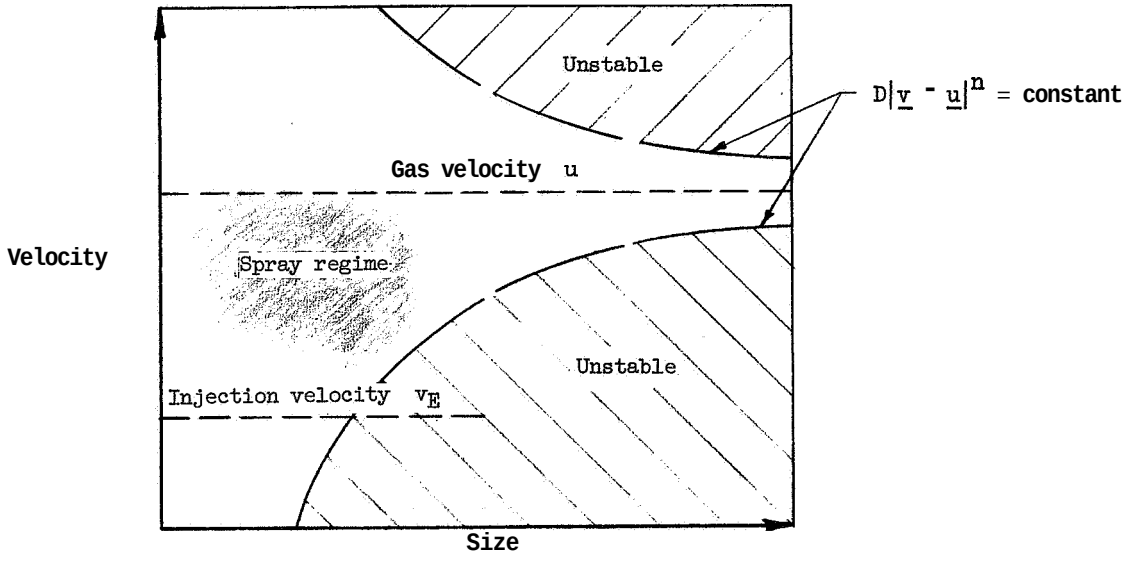

(b) $v_E < u$.

Fig. 30. - Schematic Plots of Allowable Spray Regimes in the Velocity-Size Plane.

stability is a secondary consideration. As the spray propagates, drag shrinks the velocity range toward $\underline{u}$, unless large gradients in gas properties exist with attendant shifts in stability boundaries.

2. Inferred Values of Gas Velocity

The values of $\underline{u}$ inside the spray are dependent on the momentum transferred from the liquid to the gas by drag and also vaporization. As mentioned in Chapter III the mean exhaust fan velocity is very low in the sampling region and represents an approximate lower limit. Under spraying conditions, air is entrained in the flow of drops so that radial and axialprofiles exist (Refs. 68, 69). Assuming that the smallest drops are tracers of the gas motion as indicated by single drop calculations, the drop velocity data should be equivalent to gas velocity information as size approaches zero.

Inspection of Figs. 26 to 29 immediately reveals a problem. There is a spread in the values of drop velocity even at the smallest sizes, and so air velocities estimated from the minimum envelope of the data are not the same as those estimated from the mean value. In the case of Figs. 28 and 29, the difference is not great, but the two values of u_r differ in sign. Since air flows into the spray from the surroundings, a negative u_r seems most reasonable.

For the dense spray conditions (Figs. 26, 27) the difference between the two estimates is larger and the